THE UNIVERSITY
of EDINBURGH

OSTEOPROTEGERIN ANTIBODIES IN THE PATHOGENESIS OF OSTEOPOROSIS

Philip L Riches

A THESIS PRESENTED FOR THE DEGREE OF

DOCTOR OF PHILOSOPHY

UNIVERSITY OF EDINBURGH

JANUARY 2015

Declaration

I have read and understood The University of Edinburgh guidelines on plagiarism and declare that this written dissertation is all my own work except where I indicate otherwise by proper use of quotes and references. This work has been carried out by me, except where specifically acknowledged, and has not been submitted for any other degree or professional qualification.

Philip L Riches

……...……..…….

Abstract

Osteoporosis is a common complication of many autoimmune diseases that is typically attributed to disease specific factors rather than a direct autoimmune process. This thesis arises from the investigation of a patient with severe high bone turnover osteoporosis who was identified as having autoimmune disease but whose osteoporosis deteriorated despite appropriate treatment. This presentation led to the hypothesis that neutralising autoantibodies to the bone protective cytokine osteoprotegerin (OPG) may have developed.

Serum from the index patient, but not healthy controls, was able to immunoprecipitate recombinant OPG protein, demonstrating that OPG had become the target of an autoimmune response. Purified immunoglobulins from the index case were able to inhibit the function of OPG *in vitro*, by suppressing OPG-mediated inhibition of a luciferase reporter cell line. This represents the first description of disease associated with neutralising antibodies to OPG. Whilst the immunoprecipitation assay did identify OPG antibodies in further patients these results were difficult to quantify. A more robust enzyme linked immunosorbent assay for OPG antibodies was developed using OPG as a capture antigen, which allowed the screening of patient cohorts. Presence of OPG antibodies was defined as a titre greater than the mean plus three standard deviations of 101 healthy volunteers. A low prevalence of 14/864 (1.6%) was seen in a general population cohort and no association with bone density or turnover was seen. An association with higher vascular calcification score in this cohort requires replication. A prevalence of 37/315 (11.7%) was seen in an osteoporosis cohort though no association was seen with bone density or response to treatment. In a coeliac cohort OPG antibodies were identified in 14/282 (5.0%) patients and presence of antibody was independently associated with reduced spine bone density. Functional inhibition of OPG was shown *in vitro* in 3/14 (21.4%) of the positive cases. Case finding of osteoporosis in the coeliac cohort was not improved by identification of OPG antibodies. These results are consistent with OPG antibodies being pathological in a small number of patients with osteoporosis but a clinical utility of measuring OPG antibodies has not been established.

Lay Summary of Thesis

Osteoporosis, or thinning of the bones, is a common complication of many autoimmune diseases but is usually thought to be caused by the underlying disease itself. This study describes a patient with autoimmune coeliac and thyroid disease who developed very severe osteoporosis due to a protein in the blood that caused rapid bone breakdown. The protein was an antibody which blocked the function of a key protector of bone called osteoprotegerin. This patient did not respond to treatment of his thyroid and coeliac disease, but instead needed a powerful medicine to reduce bone breakdown. We have developed a test for this antibody and found levels to be raised in some patients attending routine osteoporosis and coeliac disease clinics, though in the general population levels of this protein are low. These results suggest that antibodies to osteoprotegerin might cause osteoporosis in a small number of patients, however it was not possible to show that finding antibodies to OPG will help better identify patients with osteoporosis, or influence their response to treatment with osteoporosis medicines. Further work will be needed before this better understanding of disease can lead to better care of patients.

Contents

Acknowledgments

There are many people to thank for their help and support over the years that this work has taken place. Within the bone group I would like to pay particular tribute to Tamara Gilchrist and Micaela Rios Petrakis for excellent technical support with both the ELISA and functional assays of OPG antibodies. I would like to thank Belinda Stephen, Ken Rose and Assim Asfer who have helped ensure the smooth running of the lab. Omar Albhaga and Rob van'T Hof have been patient and learned pillars of support throughout, and Professor Stuart Ralston has provided inspiration, enthusiasm and insight in equal measure to guide this project. I acknowledge also Professor Alan Wright who supervised my initial studies into the genetics of hyperuricaemia and gout before a chance observation rewrote the title of this thesis, and Professor William Fraser who has given invaluable advice on assay development. I am very grateful to Dr James Wilson and Dr Bente Langdahl who kindly provided patient samples for analysis. Within the Edinburgh Clinical Trials Unit I particularly acknowledge the support of Helen Watters and Debbie Kerr for their help with patient recruitment. I owe particular thanks to Professor Jack Satsangi who made available serum from patients with inflammatory bowel disease as well as Drs Barbara Hauser, Alan Shand, Peter and Helen Gillett and Clive Goddard for their support in recruiting coeliac patients.

This work was made possible by a personal fellowship from the European Calcified Tissue Symposium. I acknowledge also the generous support of the Chief Scientist Office in Scotland, Coeliac UK/Core and the National Osteoporosis Society who have supported the work in the Orkney complex diseases, coeliac and osteoporosis cohorts respectively.

I could not have completed this work however without the amazing support of my wife Emma, and of my children Sophie, Sam and Kate, none of whom can remember a time when I was not working on this project, and to whom I dedicate this thesis.

Papers relating to this work

Riches PL, McRorie E, Fraser WD, Determann C, van't Hof R, Ralston SH. Osteoporosis associated with neutralising autoantibodies to osteoprotegerin. **New England Journal of Medicine** 2009 (361):1459-1465.

Riches PL, Ralston SH. Recent insights into the biology of bone turnover **Journal of the Royal College of Physicians** (Edinburgh), 2010. 40:66-9.

Real A, Gilbert N, Hauser B, Kennedy N, Shand A, Gillett H, Gillett P, Goddard C, Cebolla A, Sousa C, Fraser WD, Satsangi J, Ralston SH, **Riches PL**. Characterisation of osteoprotegerin autoantibodies in coeliac disease. **Calcified Tissue International**. Published online first June 2015 doi:10.1007/s00223-015-0023-4

Hauser B, **Riches PL**, Gilchrist T, Visconti MR, Wilson JF, and Ralston SH. Autoantibodies to osteoprotegerin are associated with increased bone resorption in rheumatoid arthritis. **Annals Rheumatic Diseases** published online first April 2015 doi: 10.1136/annrheumdis-2014-207219

Presentations relating to this work

Riches PL, McRorie E, Ralston SH. Severe high turnover osteoporosis in a young man with autoimmune disease; a novel syndrome? Presentation to **Bone Research Society** 2007. Abstract published in **Journal of Bone and Mineral Research** 2007 (22): Supplement pp 1100-1144.

Riches PL, van't Hof R, McRorie E, Ralston SH. Severe high turnover osteoporosis in a young man with circulating antibodies to osteoprotegerin: a novel syndrome. Presentation to **European Calcified Tissue Symposium** 2008.
Winner of Clinical Case Award. Abstract published in **Calcified Tissue International** 2008 (82): Supplement 1 S42.

Riches PL, Ralston SH. Prevalence of neutralising antibodies to osteoprotegerin in osteoporosis and autoimmune diseases. Presentation to **European Calcified Tissue Symposium** 2010. Abstract OC48 **Bone** 2010 (47): Supplement 1 S49-50.

Riches PL, Gilchrist T, Fraser W, Ralston SH. Detection of autoantibodies to osteoprotegerin in patients with severe idiopathic osteoporosis. Accepted for oral presentati*on to* **European Calcified Tissue Symposium** 2012. Abstract OC31 **Bone** 2012 (50): Supplement 1 S39.

Mattinson A, Hauser B, Gillett H, Gillett P, Goddard C, Kennedy N, Shand A, Ralston SH, Satsangi J, **Riches PL**. PTH-128 The Frax Algorithm is of Limited Utility in Predicting Osteoporosis in Coeliac Disease **Gut** 2013;62:Suppl 1 A263

Hauser B, **Riches PL**, Gilchrist T, Wilson JF, Fraser WD, Ralston SH. Detection of autoantibodies to osteoprotegerin in patients with rheumatoid arthritis and their association with disease activity. Presentation to European Calcified Tissue Symposium 2013 **Bone Abstracts** 2013 Vol 1, pp383.

Piec I, Tang JCY, Washbourne CJ, Greeves J, Jackson S, Ralston SH, **Riches PL**, Fraser WD, Measurement of Autoantibodies Against Osteoprotegerin in Adult Human Serum: Development of a Novel ELISA Assay. Presentation to American Society of Bone and Mineral Research 2014 Abstract SAO443 **Journal of Bone and Mineral Research** 29 (Supplement 1) Available at http://www.asbmr.org/education/2014-abstracts.

Abbreviations

ALP	Alkaline phosphatase
AP-1	Activator protein 1
BCA	Bicinchoninic acid
BMD	Bone mineral density
BMI	Body mass index
BMP	Bone morphogenic protein
BSA	Bovine serum albumin
CT	Computed tomography
CTX	Carboxy-terminal collagen crosslinks
CVD	Cardiovascular disease
DAP12	DNAX activation protein of 12kDa
DEXA	Dual energy X-ray absorptiometry
DKK	Dickkopf
DMP 1	Dentin matrix protein 1
DPD	Deoxypyridinolene
DSH	Dishevilled
ELISA	Enzyme linked immunosorbent assay
ESR1	Estrogen receptor 1
FCR-γ	Fc receptor common γ chain
FCS	Fetal calf serum
FGF	Fibroblast growth factor
FIO	Fibrogenesis imperfecta ossium
FZD	Frizzled
HH	Hedgehog proteins
HLA	Human leukocyte antigen
HRP	Horse radish peroxidase

IBD	Inflammatory bowel disease
IκB	Inhibitor of kappa B
IL	Interleukin
ITAM	Immunoreceptor tyrosine based activation motif
IV	Intra venous
M-CSF	Macrophage colony stimulating factor
mg	Milligram
ml	Millilitre
MMP 9	Matrix metallopeptidase 9
MWU	Mann-Whitney U test
NFATc1	Nuclear factor of activated T-cells, cytoplasmic 1
NFκB	Nuclear factor kappa B
NICE	National Institute for Health and Care Excellence
NOGG	National osteoporosis guidelines group
OPG	Osteoprotegerin
ORCADES	Orkney Complex Diseases Study
OSCAR	Osteoclast associated receptor
pAb	Polyclonal Antibody
PBS	Phosphate buffered saline
PHEX	phosphate regulating gene with homologies to endopeptidases on the X chromosome
PTH	Parathyroid hormone
PVDF	Polyvinyliden difluoride membrane Poly vinyl
RANK	Receptor Activator of Nuclear Factor kappa B beta
RANKL	RANK Ligand
ROC	Receiver operating characteristic
RPM	Revolutions per minute

RU	Relative Units
SC	Subcutaneous
SIGN	Scottish Intercollegiate Guidelines Network
SOST	Sclerostin
TBST	Tris buffered saline with Tween 20
TGF	Transforming growth factor
TMB	Tetramethylbenzidine
TNF	Tumour necrosis factor
TRAP	Tartrate resistant acid phosphatase
TSH	Thyroid stimulating hormone
TTG	Tissue transglutaminase
UK	United Kingdom
US	United States of America
Wnt	Wingless type MMTV integration site family member
µg	Microgram
µl	Microlitre

Chapter 1: Introduction

1.1 Epidemiology of osteoporosis

Osteoporosis is the most common metabolic bone disease in humans and is characterised by low bone mass and micro-architectural deterioration of bone tissue, which leads to enhanced bone fragility and an increased risk of fracture[1]. Osteoporosis is rare under the age of 50 but becomes progressively more common with increasing age, recently estimated in Caucasian populations to affect 11% of men and 35% of women above the age of 80 [2]. Whilst recent estimates of osteoporosis suggest an apparent fall in the age-adjusted prevalence of osteoporosis in Caucasian populations this effect does not outweigh the increased numbers of elderly people with an anticipated increase in the number of people affected by osteoporosis of 32% over the next 20 years. The cause of the apparent fall in age-adjusted prevalence is not clear and does not appear to be explained by increases in body weight, use of bisphosphonate therapies or differences in scanning technologies[2, 3].

The clinical importance of osteoporosis arises from the fact that it is associated with an increased risk of fracture, the risk increasing about 2.6 fold for every standard deviation decline in bone mineral density[4]. The cumulative lifetime risk of a fragility fracture is estimated to be 53% in a 50 year old woman and 21% in a 50 year old man. [5]. Fragility fractures represent a major cause of morbidity and mortality, as well as an economic burden on society as a whole. Following hip fracture mortality is approximately 20% by the end of the first year, with a further 20% of patients requiring long term residential care. For society as a whole the cost of osteoporotic fracture is estimated at $17.9 billion per annum in the US and £4.3 billion per annum in the UK[5, 6]. Whilst a decline in the age-adjusted prevalence of hip fracture in the US appears to parallel the reported fall in hip osteoporosis, once again the absolute numbers of hip fractures are still increasing with no improvement in mortality following fracture observed reflecting the increased numbers of elderly patients with comorbidities in the US population[7].

Osteoporosis can be diagnosed accurately and conveniently by dual energy X-ray absorptiometry (DEXA) scanning. Osteoporosis has been defined by the World Health Organization to exist when levels of bone mineral density (BMD) assessed by DEXA scanning at the spine or hip are equal to or less than 2.5 standard deviations below the mean value observed in a young healthy reference population. There is a consensus on secondary prevention of osteoporotic fracture within the UK, with both the National Institute for Health and Care Excellence (NICE) and the Scottish Intercollegiate Guidelines (SIGN) recommending that post-menopausal women above the age of 50 who have sustained a fragility fracture should be referred for bone density scanning and offered treatment if they are identified as having osteoporosis[8 9].

For primary prevention of osteoporosis there remains considerable debate about which individuals to assess for osteoporosis with DEXA scanning, often made more urgent by limitations in access to scanners. Current NICE guidelines suggest that a fracture risk assessment be performed and an intervention threshold then used to select patients for DEXA scanning referral[10]. The accompanying advice suggests that risk assessment would rarely be required below the age of 50, should be considered in patients with risk factors above the age of 50 and in all women over 65 years, and all men over 75 years of age. No specific intervention threshold is recommended however. In the US the National Osteoporosis Foundation does not suggest any risk assessment be performed prior to requesting DEXA scanning. The populations identified as being at risk of osteoporosis are very similar, though the suggestion is that for all men over 70 years of age, it is already reasonable to perform a DEXA scan[11]. SIGN have recently updated their advice and recommend that fracture risk assessment be performed above the age of 50 in patients with risk factors. Unlike NICE, the SIGN guidance has also suggested a threshold of 10% 10 year fracture risk be adopted pragmatically to determine who should be selected for bone density scanning, and then offered treatment if identified as having osteoporosis. The practical consequences of this advice are currently being worked through. One specific concern is that it will not allow the identification of osteoporosis in younger

patients who have an inherently low risk of fracture, for example those with coeliac disease[12].

1.2 Regulation of bone turnover

1.2.1 Bone modelling and remodelling

Bone modelling is the process by which skeletal mass is shaped, with the formation and resorption of bone occurring on separate bone surfaces[13, 14]. This is of critical importance during bone growth from birth to adulthood, ensuring a mature skeleton of appropriate mass and shape. In adulthood bone modelling occurs at a reduced rate and mediates the adaption of bone to biomechanical loading. Because the bone resorption and formation processes are not coupled this can result in bone loss, for example following immobilisation, or bone gain, seen in the dominant wrist of experienced tennis players[15]. Maintenance of healthy bone depends on a process termed bone remodelling. This involves both resorption of bone by osteoclasts and the laying down of new bone by osteoblasts. This dynamic process allows bone to respond to local micro-damage or changes in biomechanical loading in order to maintain mechanical integrity of the skeleton. Remodelling occurs at discrete sites termed bone remodelling units, with a tightly regulated cycle of resorption and formation that in health maintains bone integrity. In adults between the age of approximately 21 and 45 years bone resorption and bone formation are closely matched leading to little overall change in bone mass or architecture. It is estimated that the entire skeleton is reformed over a period of 10 to 20 years. The bone remodelling cycle is illustrated in Figure 1.

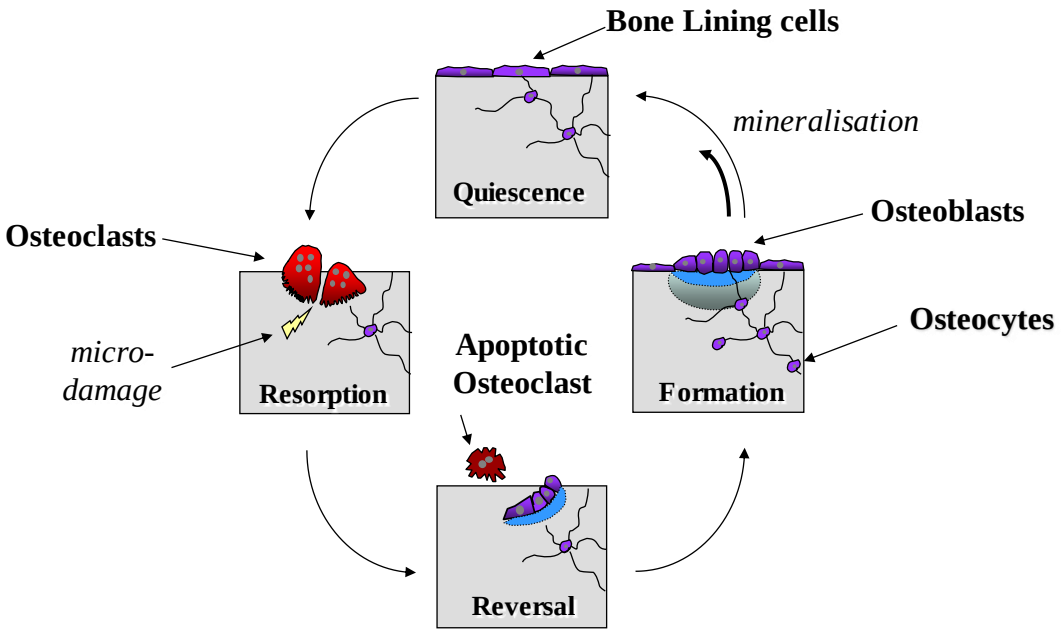

Figure 1. The bone remodelling cycle

Osteoclast precursors are recruited to sites of quiescent bone where they develop into bone resorbing osteoclasts and create a resorption pit. Osteoclasts then undergo apoptosis and the resorption pit is lined by osteoblast cells that synthesise new bone matrix, or osteoid. Over a period of approximately 10 days primary mineralisation of osteoid occurs with the deposition of hydroxyapatite crystals, followed by a slower secondary mineralisation process. Osteoblasts embedded within bone matrix may differentiate into osteocytes, which act as mechanical sensors of bone loading, and are the most abundant cell type in bone. Some osteoblasts differentiate into lining cells which cover the bone surface.

Systemic regulation of bone remodelling is driven by hormones involved in calcium homeostasis, namely parathyroid hormone (PTH), vitamin D and calcitonin, as well as by sex steroids most notably oestrogen. PTH is secreted in response to hypocalcaemia and mediates its effect on bone by binding directly to osteoblasts and bone marrow stromal cells leading to the secretion of macrophage colony stimulating factor (M-CSF) and Receptor Activator of Nuclear Factor kappa B beta ligand (RANKL)[16], indirectly stimulating osteoclast formation and so liberation of calcium from bone. PTH also has important renal effects leading to increased renal

reabsorption of calcium and stimulates 1-α hydroxylase activity leading to formation of active 1, 25 (OH) vitamin D[17]. In turn active 1,25 (OH) vitamin D enhances the absorption of calcium from the gut, and kidneys, as wells as acting as a feedback inhibitor of its own production[18]. Calcitonin binds directly to receptors on osteoclasts leading to inhibition of bone resorption; this pathway has been targeted pharmacologically though its physiological significance remains uncertain[19]. Oestrogen acts as a key bone protective hormone with oestrogen receptors expressed both in osteoclasts and osteoblasts. For example oestrogen signalling in both osteoblasts and osteoclasts has been shown to enhance osteoclast apoptosis mediated by FAS signalling, suggesting a role for prolonged osteoclast survival in post menopausal osteoporosis[20, 21]. In addition oestrogen has emerging indirect effects on bone mediated by lymphocyte production of inflammatory cytokines and expression of RANKL[22].

1.2.2 Determinants of peak bone mass

During early stages of skeletal growth bone formation predominates over resorption until peak bone mass is achieved in early adulthood. Subsequently tight coupling of resorption and formation allows maintenance of bone density in a steady state, but from the third decade on resorption exceeds formation resulting in a gradual reduction in bone density. Adult bone mass is a function of both peak bone mass achieved in young adulthood and subsequent adult bone loss[23].

Genetic factors play a key role in determining peak bone mass with an estimated heritability of between 50 and 80%[24]. Candidate gene studies have suggested a role of estrogen and vitamin D receptor variants whilst acknowledging the significant contribution of body weight, hormonal factors, and physical activity[25, 26]. A recent meta-analysis of genome-wide association studies of bone density confined to premenopausal women confirmed associations within the WNT16 (encoding wingless-type MMTV integration site family, member 16) and ESR1 (encoding Estrogen receptor 1) loci[27]. WNT signalling is seen as an early component of the osteoblastic response to weight bearing exercise in a fashion that is dependent on estrogen receptor signalling, highlighting at least one pathway by which these diverse genetic and environmental signals interact[28], and explaining the benefits that

are seen with increased weight bearing exercise in pre-pubertal children[29]. Most genome-wide association studies performed in osteoporosis have looked at older women and men in whom it is not possible to determine if the genetic associations relate to a deficit in peak bone mass, or subsequent bone loss. Even so the largest meta-analysis performed of these studies to date has identified multiple loci encoding genes implicated in bone formation *in-utero* suggesting that even foetal bone development contributes to bone density in adulthood [30].

1.2.3 Causes of increased bone loss in adulthood

A transient accelerated rate of bone loss is seen in women in the decade following menopause, which is followed by a slower continuous rate of bone loss in subsequent years[31]. Oestrogen deficiency plays an important role in both phases of bone loss with oestrogen replacement leading to significant improvement in bone density[32]. Sex hormones also play a critical role in male osteoporosis however the dominant effect appears to be mediated by oestradiol and the effectiveness and safety of testosterone replacement requires further investigation[33]. Whilst cortical bone, which comprises 80% of the adult skeleton, is preserved in women before menopause, studies using quantitative computed tomography (CT) have been able to discern declines in trabecular bone before menopause, which has been attributed to an independent process of increased oxidative stress associated with ageing[34, 35]. Increased bone resorption correlating with increasing levels of parathyroid hormone with age is also noted in epidemiological studies and is attributed to nutritional or functional deficiency of vitamin D[31].

Lifestyle factors contribute significantly to adult bone mass. Smoking and alcohol excess, both more common in men, contribute to a reduction in trabecular bone mass[36]. Conversely weight bearing exercise has been shown to improve or at least attenuate loss of bone mass in older adults[37].

Diverse medical diseases and treatments have adverse effects on bone health, and can be identified in up to 64% of men and 50% of pre-menopausal women with osteoporosis[38]. Diseases associated with osteoporosis include hypogonadism, hyperthyroidism, hyperparathyroidism, malignancies, gastrointestinal disease and

chronic rheumatic disease[39]. The specific examples of rheumatoid arthritis, coeliac disease and inflammatory bowel disease are discussed in more detail in Section 1.4.2, 1.4.3. and 1.4.4. Drug treatments, notably with corticosteroids, have diverse adverse effects on bone health leading to both worsened bone mineral density and increased fracture risk[40], for example by driving signals of bone resorption in osteoblasts[41] as well as having direct myopathic effects and influencing the risk of falling[42]. Fundamentally in any individual presenting with osteoporosis there are likely to be diverse mechanisms responsible for the development of disease which together have led to a relative imbalance of bone resorption over bone formation

1.3 Cellular regulation of bone turnover

1.3.1 Bone formation

In most parts of the skeleton, both *in-utero* and until skeletal maturity, bone forms within a cartilage template in a process termed endochondral ossification[43]. Alternatively in the flat bones of the skull, bone forms directly in a process termed intramembranous ossification. Cartilage is formed by mesenchymal stem cell derived chondrocytes capable of secreting the various components of the cartilage extracellular matrix, principally collagen type II, aggrecan and hyaluronan[43]. Mature chondrocytes initiate the resorption of the collagen matrix and invasion by capillaries. Further degradation of the cartilage matrix is performed by invading osteoclasts, with mineralisation of the remaining cartilage septa orchestrated by invading osteoblasts resulting in the formation of bone.

Mature bone is formed by mineralisation of an organic matrix secreted by osteoblasts. The organic matrix comprises fibrillar proteins such as collagens type I, III, V and VI, non-fibrillar proteins involved in the formation and mineralisation of the collagen scaffold such as osteopontin, osteocalcin, osteonectin and fibronectin, and finally growth factors such as transforming growth factor-beta(TGF-beta)[44]. The most abundant collagen in bone is type 1 collagen which is normally laid down in an orderly lamellar pattern of alternately orientated fibrils. Mature bone is comprised predominantly (50–70%) of mineral, mostly hydroxyapatite which provides much of the mechanical rigidity and load bearing strength of bone[13].

The adult human skeleton is comprised of 80% dense cortical bone and 20% more porous but metabolically highly active trabecular bone[13]. The relative proportion of each varies between different sites; with cortical bone predominating in the shafts of long bones but trabecular bone predominant in the vertebrae. Both are made up of lamellar bone with mechanical loading thought to mediate the differential development into trabecular or cortical bone. In high bone turnover states, the lamellar pattern of bone is lost leading to functionally weaker woven bone formation. This occurs in disease states such as hyperparathyroidism and Paget's disease of bone[13].

1.3.2 Osteoblasts

Osteoblasts are derived from pluripotent mesenchymal stem cells which have the potential to differentiate into many cell types including adipocytes, myocytes and chondrocytes. The expression of Runx2 is an early marker of mesenchymal stem cells commitment to an osteoblastic lineage, whilst inhibiting the development of adipocytes and chondrocytes[45] with subsequent expression of osterix a marker of increasing osteoblast commitment[46]. Runx2 increases the expression of alkaline phosphatase and osteocalcin, which are markers of osteoblast activity and hence bone formation, though the action of both remains poorly understood. Alkaline phosphatase is responsible for hydrolysing mineralisation inhibitors such as pyrophosphate, and osteocalcin is also thought to promote mineralisation of bone though paradoxically osteocalcin deficient mice have a high bone mass phenotype[13].

A number of factors drive the commitment and maturation of mesenchymal stem cells into mature osteoblasts (Figure 1.2 – adapted from reference [45]). Indian hedgehog (HH) protein is secreted by early and prehypertrophic chondrocytes and is an essential signal in endochondral ossification[47]. HH signalling is mediated at least in part via parathyroid related protein (PTHrP)[48]. Notch signalling appears to inhibit, and bone morphogenic proteins appears to promote the normal differentiation of osteoblasts from Runx2+ve to Osterix and Runx2 double +ve cells[45].

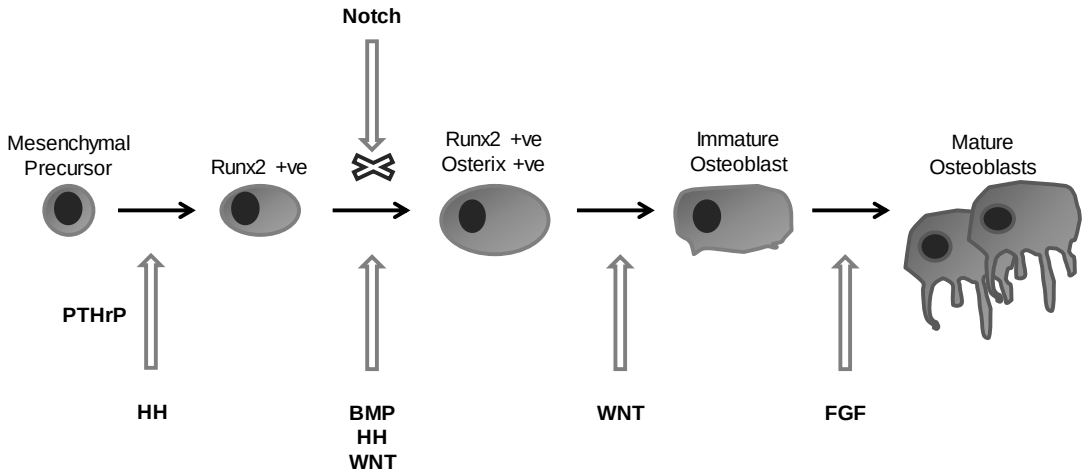

Figure 1.2. Regulatory signals in osteoblast development.
Commitment of mesenchymal precursors to osteoblast development is characterised by expression of Runx2 and subsequently Osterix. Osteoblast differentiation is promoted through signalling by hedgehog proteins (HH) in part mediated by parathyroid related protein (PTHrP), bone morphogenic proteins (BMP) and wingless proteins (WNT). Fibroblast growth factors (FGF) promote the maturation and proliferation of immature osteoblasts. Conversely Notch signalling inhibits Runx2 activity and osteoblast differentiation.

Signalling through the WNT and FGF pathways is important in promoting further osteoblast differentiation, and conversely dexamethasone promotes mesenchymal cell differentiation into adipocytes[49]. WNT signalling is mediated through the Frizzled (FZD) receptor and its co-receptor LRP5 or LRP6 and results in signalling via β-catenin dependent (canonical signalling – Figure 1.3) and independent

pathways[45].

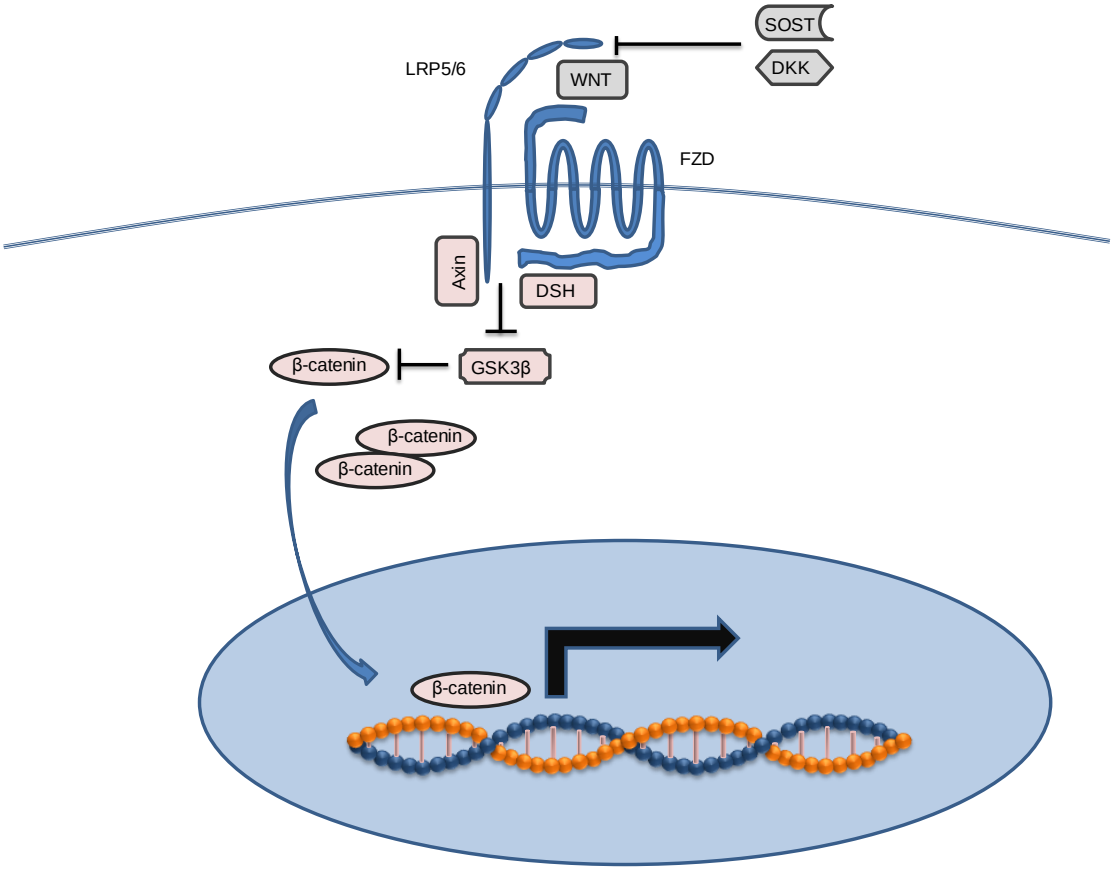

Figure 1.3 Canonical WNT signalling pathway. WNT ligands bind to a co-receptor complex comprising a transmembrane domain of Frizzled receptor (FZD) and either co-receptor LRP5 or LRP6. Dishevilled (DSH) and Axin are recruited intracellularly forming a complex that inhibits GSK3β. The constitutive activity of GSK3β is phosphorylation and hence targeting of β-catenin for proteosomal degradation. Following WNT signalling, there is accumulation of cytoplasmic β-catenin ultimately allowing translocation to the nucleus and enhanced signalling.

Sclerostin, primarily secreted by osteocytes (Section 1.3.4), plays a key role in the maturation and terminal differentiation of osteoblast lineage cells into mature osteoblasts mainly through inhibition of WNT signalling[45], though its effects may also be mediated by suppression of BMP signalling[50]. A key role in bone health has been demonstrated by the study of patients with mutations in components of these pathways. Regulatory mutations in the SOST gene that encodes sclerostin are

associated with an autosomal recessive condition characterised by bony overgrowth of the jaw and skull termed van Buchem disease [51], whereas coding mutations of the SOST gene result in a similar phenotype termed Sclerosteosis[52]. Mutations of LRP5 can cause contrasting phenotypes. A cluster of mutations within LRP5 that result in reduced binding by sclerostin are associated with a high bone mass phenotype due to enhanced WNT signalling[53]. Conversely loss of function mutations in LRP5, have been shown to result in reduced bone density and pseudoglioma due to loss of WNT signalling[54]. Despite the strong evidence of a direct effect in bone of mutations in LRP5 some conflicting reports have been published suggested the effect may be mediated by regulation of serotonin synthesis in the gut, though it has been suggested that this research was methodologically flawed[55, 56].

1.3.3 Osteoclasts and bone resorption

Osteoclasts are multinucleated cells derived from haematopoietic stem cell precursors. A critical early marker of haematopoietic differentiation along a myeloid pathway is PU.1 which is associated with expression of c-fms the receptor for macrophage colony stimulating factor (M-CSF)[57]. PU.1 is also needed for expression of the receptor activator of nuclear factor kappa B (RANK) in response to M-CSF signalling. The expression of the RANK receptor is further upregulated by RANK ligand (RANKL) co-administration[58]. Signalling by M-CSF and RANKL are essential for osteoclast development with deficiency of either factor leading to an osteopetrotic phenotype [59, 60]. Stimulation of osteoclast precursors by RANKL induces the expression of transcription factors such as activator protein 1 (AP1) and nuclear factor of activated T cells, cytoplasmic 1 (NFATc1) leading to the expression of proteins required in the fusion of osteoclast precursors such as dendritic cell-specific transmembrane protein, as well as those required for the resorptive capacity of osteoclasts such as cathepsin K and vacuolar ATPase[61]. Osteoprotegerin (OPG) is a decoy receptor for RANKL that blocks both the maturation and activation of osteoclasts. The regulatory factors involved in osteoclast maturation and activation are summarised in Figure 1.4.

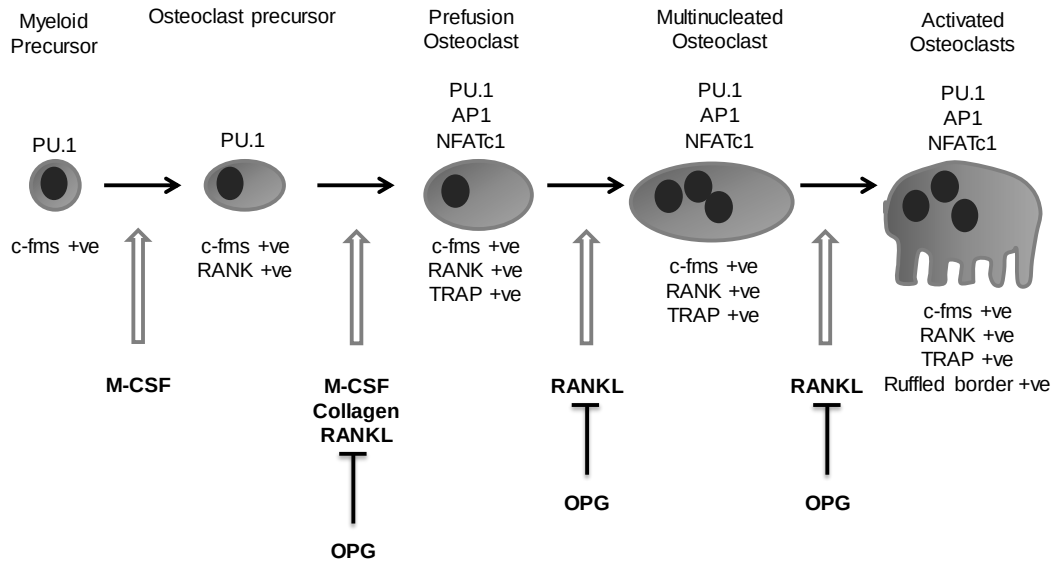

Figure 1.4 Essential signals in the differentiation of osteoclasts.
Expression of the transcription factor PU.1 is an early marker of myeloid commitment by haematopoietic stem cells associated with responsiveness to M-CSF. Signalling by M-CSF induces RANK receptor expression with stimulation by RANKL (co-stimulated by M-CSF and collagen) then driving the expression of osteoclast defining transcription factors AP1 and NFATc1. Osteoclasts are recognised by the expression of tartrate resistant acid phosphatase (TRAP) and by the presence of a ruffled border when activated. OPG, by inhibiting RANKL, blocks the differentiation and activation of osteoclasts.

RANKL stimulation triggers the formation of a RANK/TRAF6 complex which elicits a number of essential downstream signals including the dimeric transcription factors nuclear factor kappaB (NFκB) and AP1 both of which are necessary for effective osteoclastogenesis[62, 63](Figure 1.5). NFκB is made up of homo or heterodimers typically including p50 or p52 subunits and a double deletion of both p50 and p52 subunits is associated with the development of osteopetrosis. Deletion of either subunit alone does not result in osteopetrosis implying overlapping function of the two homologous proteins[64]. Formation of the RANK/TRAF 6 complex leads to phosphorylation of the inhibitor of kappB (IκB) and allows nuclear translocation of NFκB . AP1 comprises a dimer of proteins from the Fos, Jun and activating transcription factor families with deficiency of c-Fos (which forms a heterodimer with c-Jun) resulting in osteopetrosis[65].

A further critical transcription factor downstream of RANK signalling is NFATc1 which has been shown to be both necessary and sufficient for osteoclastogenesis[66]. NFATc1 regulates its own expression and it appears that a complex of AP1 and NFATc1 is required for this autoamplification to occur[66].

In addition to NFκB and AP1 signals it is clear that regulation of the intracellular Ca2+ levels induced by co-stimulation through immunoreceptor tyrosine-based activation motif (ITAM) containing adaptor proteins DNAX activating protein 12 (DAP12) and Fc receptor common γ chain (FcR γ) is also required for the activation of NFATc1[67, 68](Figure 1.5). No ligand has been found for the immunoglobulin-like receptors that associate with DAP12, though M-CSF has been shown to generate a signal through DAP12[69] . Collagen fibres have been shown to signal through the osteoclast associated receptor (OSCAR) which is induced by RANKL and associates with FcR γ[70]. Ultimately NFATc1, in combination with other transcription factors directly drives the expression of osteoclast specific genes such as TRAP, cathepsin K, calcitonin receptor and matrix metallopeptidase 9 (MMP-9)[71].

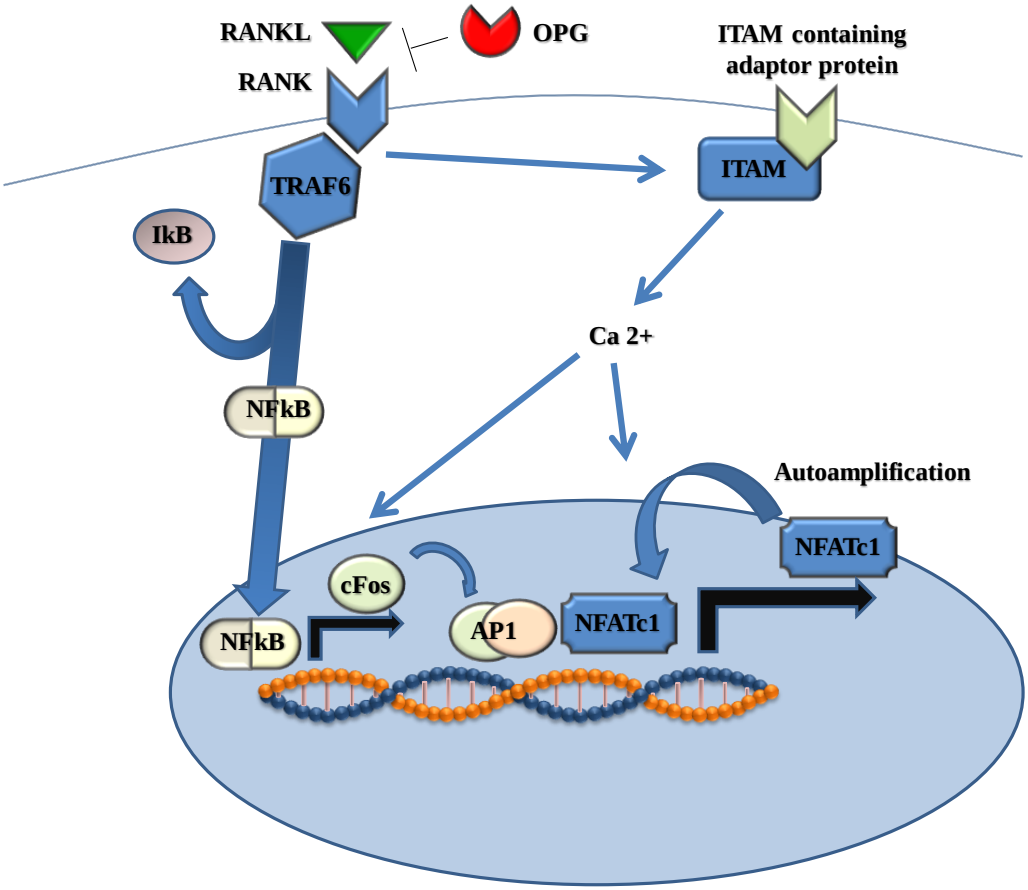

Figure 1.5 Essential signals in osteoclast development. RANKL binding to RANK triggers the formation of a RANK/TRAF 6 complex which leads to the nuclear targeting of NFκB *and the formation of the c-Fos containing transcription factor AP1. Co-stimulation via ITAM containing adaptor proteins provides a second signal mediated by regulation of intracellular calcium levels. In combination, these events drive transcription and autoamplification of the key osteoclast factor NFATc1.*

Osteoclasts are uniquely capable of resorbing mineralised tissues, a process that requires tight binding of osteoclasts to bone and polarisation of the osteoclast cell membrane. The actin cytoskeleton is reorganised to form a ring, which is attached to bone via integrin-based structures called podosomes, sealing off a compartment beneath the cell in which resorption will occur, the 'Howship's lacuna'. Within this

area the osteoclast contains a highly convoluted ruffled border to which acidic vesicles are trafficked and which allows the delivery of the components necessary for bone resorption. The secretion of hydrogen ions by vacuolar proton ATPase transporters can lower the pH within the resorption pit to 4.5 which allows the mineral content of the bone matrix to be dissolved[13]. The organic components of bone matrix are digested by secreted enzymes such as cathepsin K, MMP-9 and tartrate resistant acid phosphatase[13]. An active process of reverse vesicular trafficking targets the degradation products for release on the opposite membrane from the bone surface[72] and incidentally facilitates the measurement of breakdown products (such as N or C telopeptides of type 1 collagen) that can give an indication of bone resorption rate[73]. Impairment of osteoclast function caused by inherited deficiencies of hydrogen ion secretion are the commonest cause of osteopetrosis in humans[74], whilst defects in RANK and RANKL have also been identified in 'osteoclast poor' osteopetrosis[75]. Inherited defects in enzymes such as cathepsin K results in a related osteosclerotic condition pycnodysostosis[74].

Enhanced induction of osteoclasts by autoantibodies targeting citrullinated vimentin have recently been demonstrated in mice in elegant studies by Schett *et al*[76]. This is of direct relevance to rheumatoid arthritis in which anti-citrullinated peptide antibodies are an early marker of disease and correlate directly with bone resorption. It is intriguing to note that osteoclasts express the citrullinating enzyme peptidylarginine deaminase potentially leading to a vicious cycle of immune mediated activation of osteoclasts, in turn leading to the promotion of enhanced autoimmune responses. This work also clearly illustrates that autoantibodies are not only biomarkers of disease but can also directly cause pathology.

1.3.4 Osteocytes and the regulation of bone formation

Osteocytes play a key role in regulating bone mineralisation and remodelling, and function both in an endocrine and paracrine fashion. They are derived from osteoblasts that are buried in bone matrix and are the most abundant cell type within bone. Osteocytes are connected to each other through a remarkably extensive network of dendritic processes which allow the retention of connections to the mineralisation front as well as the bone surface and vasculature[77]. These processes

help osteocytes to function as mechanosensors of bone loading. The mechanisms by which mechanical strain mediates bone formation are not well understood though it has been shown that conditional osteocytic knock down of polycystin 1 (a gene previously established in mechanosensing in renal cilia) results in a failure of the anabolic response to loading[78].

Osteocytes act in a paracrine fashion to regulate both osteoblasts and osteocytes. Sclerostin is a key inhibitor of osteoblast activity and the constitutive expression of sclerostin by osteocytes appears critical to suppress bone formation. Mechanical loading has been shown to dramatically reduce osteocyte expression of sclerostin which in turn promotes new bone formation[79]. Osteocytes have also been recognised to be a key regulator of osteoclasts, with both healthy and apoptotic osteocytes capable of recruiting osteoclasts[77]. Importantly osteocytes are now recognised as the major source of RANKL in the bone microenvironment. This is evidenced by the fact that conditional knock out mice in whom osteocytes did not express RANKL developed a severe osteopetrotic phenotype [80]. This stimulation of osteoclasts is presumed to be mediated by RANKL expressed on the dendritic processes of osteocytes in response to mechanical stress, though whether this is membrane bound or secreted is not currently known. In addition to their influence on osteoblast and osteoclast cells osteocytes have also been shown to directly regulate the perilacunar space with expression of resorptive enzymes such as cathepsin K and TRAP during lactation in mice suggesting that osteocytes are capable of acting in an osteoclast-like fashion[81].

Osteocytes can also act in an endocrine fashion to regulate renal phosphate and calcium handling[77]. As osteocytes mature they change their pattern of gene expression, with reduced expression of alkaline phosphatase and an increase in factors such as FGF23, dentin matrix protein 1 (DMP1) and phosphate regulating gene with homologies to endopeptidases on the X chromosome (PHEX). DMP1 and PHEX are both thought to down regulate FGF23 expression and so maintain renal phosphate reabsorption[77]. Mutations of DMP1 are associated with hypophosphatemic rickets in humans[82], with mutations of PHEX and DMP1 in mice leading to similar

phenotype of osteomalacia with high levels of FGF23[83, 84]. A role for FGF23 in the cardiovascular morbidity associated with renal impairment has also been postulated[85].

1.3.5 Vascular calcification

An association between cardiovascular diseases (CVD) and osteoporosis has long been recognised though it has commonly been assumed that these were simply co-existing but independent conditions of increasing prevalence in older people[86, 87]. Epidemiological studies now indicate that both may share a common pathophysiological basis. For example, a recent twin study showed that the risk of hip fracture was between 2 and 5-fold increased in subjects with various types of CVD as compared with controls, suggesting a shared genetic basis to both conditions. Vascular calcification is a recognised feature of atherosclerosis, and the extent of arterial calcification is generally accepted as a marker of risk for future cardiovascular events[88]. Vascular calcification is typically exacerbated in conditions with increased vascular risk such as diabetes, renal impairment and hyperlipidaemia but osteoporosis is now also recognised as a regulatory influence[89]. This is shown in several studies that have confirmed an independent association between vascular calcification and osteoporosis[90-92].

Mineralisation can occur in any fibrillar extracellular matrix, so long as there is sufficient phosphate to allow formation of hydroxyapatite, and there is inhibition of mineralisation inhibitors, for example the degradation of pyrophosphate usually mediated by alkaline phosphatase[93]. The walls of muscular arteries contain fibres of collagen, and elastin along with abundant vascular smooth muscle cells (VSMC). In calcified arteries it has been shown that VSMCs have an osteoblast like phenotype with increased expression of alkaline phosphatase, diminished expression of mineralisation inhibitors such as matrix Gla protein (MGP) and the ability to support mineralisation in vitro[94, 95]. A great variety of factors have been reported to influence this differentiation including inflammatory cytokines such as TGF-beta, platelet derived growth factors, matrix metalloproteinases, high circulating phosphate and

calcium, as well as dexamethasone, though the relative physiological importance of these factors remains poorly understood[95-98].

Vascular calcification is increasingly understood to be an active process with many parallels to embryonic bone development[99]. For example bone morphogenic protein 2 (BMP) plays a fundamental role in osteoblast differentiation and the formation of bone and cartilage [100, 101], but the same protein is upregulated in the endothelium in response to inflammatory cytokines resulting in vascular calcification and endothelial activation[102]. Perhaps unsurprisingly there are a large number of factors that are involved in both bone metabolism and vascular calcification, though it remains a paradox that too much calcification can occur in the vasculature at the same time as there is too little in the bone[103].

OPG has been suggested as an important common factor in the development of both osteoporosis and vascular calcification, and has been shown to inhibit vascular calcification in experimental models[104,105]. This is supported by evidence from the OPG deficient mouse which is characterised by high bone turnover and fracture as well as extensive vascular calcification [106]. Similarly OPG deficient patients with juvenile Paget's disease who survive into adulthood have been shown to develop extensive vascular calcification[107]. This may be explained by effects on RANKL with elevated levels of RANK and RANKL having been identified in atherosclerotic lesions where they are associated with increased expression of BMP-2 as well as decreased expression of matrix Gla protein (MGP) a key inhibitor of mineralisation[108]. Several investigators have looked for evidence of associations between circulating levels of OPG and/or RANKL, cardiovascular disease and osteoporosis[109-112]. The results of these studies have paradoxically shown an association between high circulating OPG levels and low RANKL levels with vascular calcification. Attempts to rationalise this finding have suggested these factors act in a paracrine rather than endocrine fashion to affect cellular function[113]. An alternative mechanism independent of RANKL has also been suggested. OPG acts as a decoy receptor for TNF related apoptosis inducing ligand (TRAIL) and both

TRAIL and OPG have been identified in atherosclerotic plaques, with TRAIL also shown to enhance the mineralisation of VSMCs *in-vitro*[114].

Many other factors have also been implicated in both bone metabolism and vascular calcification though a full discussion of these factors is beyond the scope of this thesis. Oestrogen has a critical bone protective effect, and has also been shown to protect against vascular calcification, possibly by inhibiting the effects of RANKL on BMP-2 and MGP expression in vascular smooth muscle cells[108]. Vitamin K activates MGP by carboxylation and deficiency of vitamin K has been implicated in both vascular calcification and osteoporosis[115, 116] . Finally PTH and vitamin D exert a permissive effect on vascular calcification by regulating the availability of phosphate and calcium, but have also been shown to have direct effects in the vasculature themselves[117].

1.3.6 Receptor activator of NFκB pathway

The RANK pathway was identified in the late 1990s as the key regulator of osteoclast differentiation and function (see also Section 1.3.3)[118, 119]. The RANK receptor encoded by the TNFRSF11A gene is a member of the tumour necrosis factor (TNF) receptor super family which is expressed on osteoclast precursors and dendritic cells. RANKL encoded by the TNFSF11 gene is a member of the TNF superfamily that is expressed both on the cell membrane and as a soluble ligand (sRANKL) formed by cleavage of RANKL from the cell membrane, and also capable of stimulating RANK[120]. OPG encoded by the gene TNFRSF11B and also a member of the TNF receptor superfamily lacks a transmembrane domain and acts as a decoy receptor for RANKL and was identified as a potent inhibitor of bone resorption by blocking the interaction of RANKL with RANK[121].

The RANK/RANKL/OPG signalling axis is now recognised as a critical pathway in osteoclast differentiation and bone resorption. It is central to the cross talk between osteoclasts and osteoblast lineage cells; as bone marrow stromal cells mature into osteoblasts their expression of RANKL reduces, and secretion of OPG increases, down regulating osteoclast activity[122]. Osteoblasts and mesenchymal-derived

precursors are considered the major source of OPG though this is based primarily on *in vitro* work [123, 124]. As discussed earlier, whilst bone marrow stromal cells can express RANKL, it is now osteocytes that are recognised as the primary source of RANKL *in vivo* and so the key initiators of bone resorption[80] (Figure 1.6)

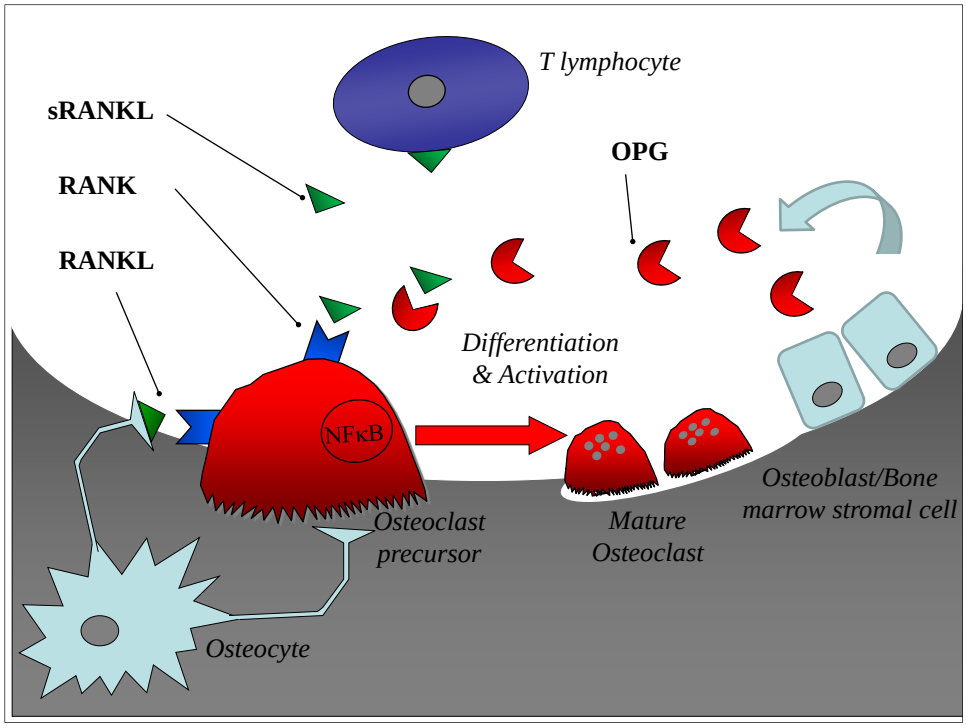

Figure 1.6: Role of the receptor activator of nuclear factor kappa B (RANK) pathway in osteoclast development. RANKL expressed by osteocytes, bone marrow stromal cells or T lymphocytes induces differentiation and activation of osteoclast precursors via RANK and subsequent activation of NFκB. *sRANKL is derived by cleavage from the cell membrane. OPG, a soluble inhibitor of RANKL, inhibits the binding of RANK by RANKL.*

Genetic studies confirm the critical role of RANK/RANKL/OPG in bone homeostasis. Meta-analysis of genome wide association studies into osteoporosis has shown that genetic variation at the TNFSF11, TNFRSF11A and TNFRSF11B loci (encoding RANKL, RANK and OPG respectively) as well as downstream signalling molecules all contribute to variation in bone mineral density[125]. Rare diseases have

also been described in association with mutations in these genes. Complete deficiency of OPG in humans causes "juvenile Paget's disease" which is a rare disease characterised by high bone turnover, bone deformity and multiple fractures [126]. This is confirmed in mouse models where deficiency of OPG also causes severe osteoporosis and multiple fractures [106]. Activating mutations of the TNFRSF11A gene which encodes RANK have been identified as the cause of the rare bone dysplasias, familial expansile osteolysis and expansile skeletal hyperplasia[127, 128]. Conversely deficiency of RANK or RANKL causes osteopetrosis due to defects in osteoclast function[75].

In addition to its role in the regulation of bone, genetic studies in mice have shown that RANK/RANKL signalling also plays a critical role in thymic development, as well as maintaining tolerance to autoreactive T cells[129, 130]. Exploring cross talk between the immune system and bone cells has emerged as a new field of study termed osteoimmunology[131]. RANKL is expressed on both bone marrow stromal cells and lymphocytes[132, 133], thereby representing an intriguing link between bone homeostasis and immune regulation. Activated T cells express RANKL directly and this mediates bone loss and joint destruction that can be blocked by administering recombinant OPG[134]. Similarly in rheumatoid arthritis, blockade of RANKL has been shown to impede the development of bone erosions[135].

T cell expression of RANKL, as well as the osteoclast stimulatory effects of inflammatory cytokines such as tumour necrosis factor α and interferon are likely to contribute to the development of osteoporosis that is seen in many autoimmune conditions[136]. Equally B cells have been shown to produce OPG in response to stimulation of CD40 [137] and by some estimates constitute the major source of OPG within the bone marrow[138]. It is possible that this B cell derived OPG could act as a homeostatic regulator of the osteoclastogenesis that is driven by immune activation, though no role for B cell produced OPG in physiological bone loss has been identified; specifically no exacerbation of ovariectomy induced bone loss was found in B cell deficient mice[139].

Although many factors have been shown to regulate osteoclastogenesis including interleukin-1(IL-1), TGF beta, TNF, IL-6, 1,25 vitamin D3 and parathyroid hormone (PTH), the effects of these agents on osteoclast activity has been shown at least in part to be mediated by alteration of the RANK signalling pathway [140]. For example the importance of oestrogen deficiency to post-menopausal osteoporosis can be partially explained by oestrogen's demonstrated ability to stimulate OPG production by osteoblasts[141].

Investigators have looked for evidence of associations between circulating levels of OPG and/or sRANKL and post-menopausal osteoporosis but paradoxically have found high circulating OPG levels and low sRANKL levels in patients with osteoporosis[142]. Rationalising this difference many authors have emphasized the paracrine rather than endocrine action of these factors on cellular function, or alternatively suggested that this is a compensatory mechanism attempting to restore bone homeostasis. It is important to recognise that OPG and sRANKL are produced by diverse cell types hence the circulating levels may bear little correlation with the bone microenvironment[143-145] and that there exists significant variability within currently available assays for sRANKL[144]. Equally in inflammatory disease a paradoxical association between low sRANKL levels or high circulating OPG levels and osteoporosis has been found[110, 143] again casting doubt on the biological significance of circulating OPG and sRANKL, and demonstrating that despite the key importance of this pathway it cannot be readily exploited to provide a biomarker for osteoporosis.

1.3.7 Osteoprotegerin

OPG is formed as a protein of 401 amino acids containing four tandem cysteine rich domains that have homology to other members of the TNF receptor superfamily and that mediate the binding of RANKL, as well as a C-terminal dimerisation domain [146]. In addition the protein encodes a 21 amino acid N-terminal signal peptide that is cleaved prior to secretion of a final protein of 380 amino acids. OPG has been shown to undergo N-linked glycosylation and cysteine linked dimerization yielding a secreted dimer with a molecular mass of 110kDa, though under reducing conditions OPG runs as a monomer of 55kDa[121] (Figure 1.7).

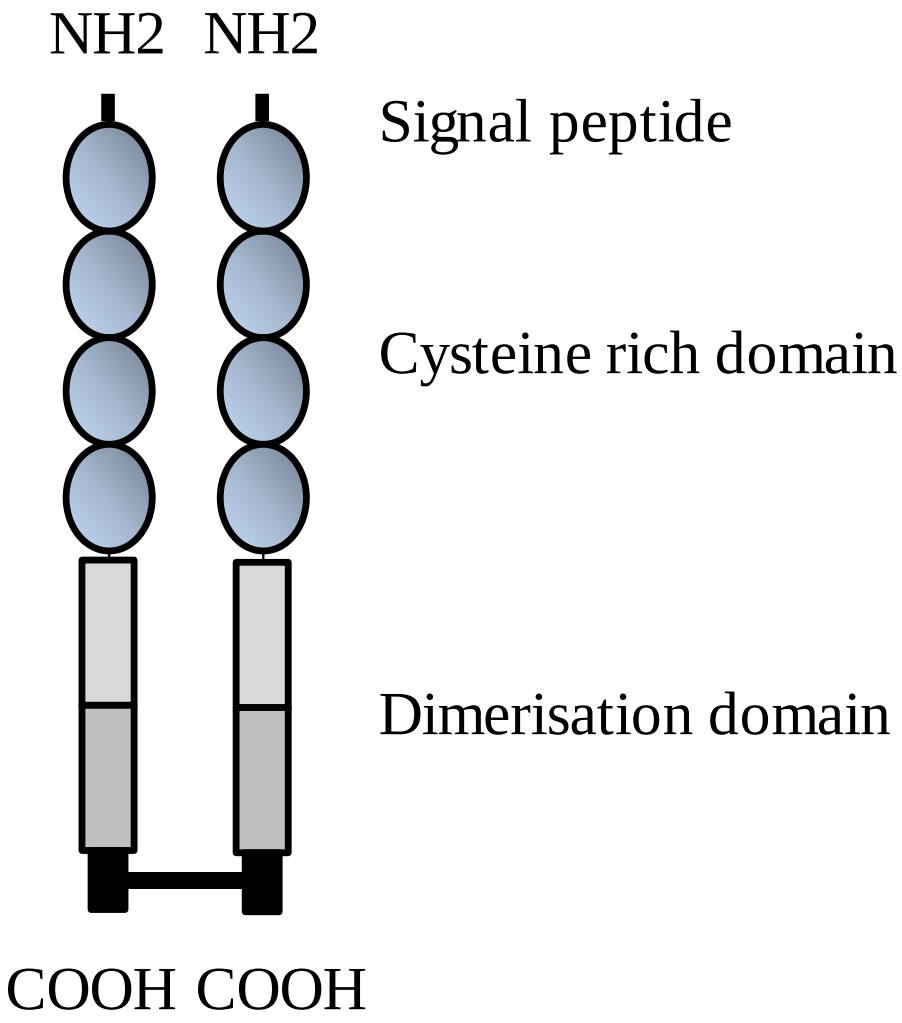

Figure 1.7 Structure of osteoprotegerin

1.4 Complications of autoimmune disease

1.4.1 Osteoporosis in autoimmune disease

Osteoporosis is a recognised complication of autoimmune diseases such as coeliac disease[147], inflammatory bowel disease[148], and inflammatory rheumatic diseases including rheumatoid arthritis[149]. The pathogenesis is complex involving direct effects of local and systemic inflammation, indirect effects mediated through conventional risk factors for osteoporosis, as well as drug treatment effects particularly with corticosteroids. Inflammation has been shown to have a direct effect on bone metabolism mediated by inflammatory cytokines such as IL-6 or TNF,

which are correlated with levels of RANKL or increased RANKL/OPG ratio in rheumatoid arthritis, coeliac disease and inflammatory bowel disease[150, 151]. Indirect effects on bone density may arise from an association of autoimmune disease with smoking and female gender, as well as the potential impact of disease on body mass or mobility[147, 152].

More recently evidence of direct autoimmune stimulation of bone loss has been identified in the work of Schett, who has demonstrated that autoantibodies can recognise antigens expressed by osteoclasts and directly stimulate osteoclast activity both *in-vitro* and *in-vivo*[76].

1.4.2 Rheumatoid arthritis

Rheumatoid arthritis is a systemic inflammatory disorder characterised by polyarticular and deforming arthritis, which is frequently associated with the development of autoantibodies to citrullinated proteins. Anti-citrullinated protein antibodies typically develop in genetically susceptible individuals with exposure to environmental triggers such as smoking or bacterial stimuli[153]. An increased risk of fracture is observed in patients with rheumatoid arthritis after correction for conventional risk factors such as smoking, which is attributed both to complications of the disease and use of corticosteroids[149]. Both local and systemic inflammation result in bone loss with chronic localised inflammation leading to characteristic peri-articular erosions and systemic inflammation also associated with reduced bone mineral density[154, 155]. Effective management of rheumatoid arthritis, particularly with more potent biological therapies, has shown improvements in local bone erosions although systemic osteoporosis remains an issue in rheumatoid arthritis[155, 156].

1.4.3 Coeliac disease

Coeliac disease is one of the most common autoimmune disorders with a prevalence estimated at 1% of the UK population[157]. It is characterised by a gluten sensitive enteropathy and by the development of autoantibodies to transglutaminase. Osteoporosis is the commonest complication affecting 20–50% of newly diagnosed patients[147] with an associated increased relative risk of hip fracture of 1.43 [158].

Reduced bone density in coeliac disease is usually considered a consequence of malabsorption, and a correlation with the severity of villous atrophy has recently been shown[159]. The consequences of malabsorption are diverse with effects on body mass, as well as reduced absorption of vitamin D and calcium. Vitamin D and calcium deficiency in turn cause secondary hyperparathyroidism leading to increased bone turnover. Equally vitamin D deficiency results in muscle weakness and an increased risk of falling[160]. The severity of osteoporosis however correlates poorly with symptoms of disease suggesting that malabsorption alone is not the only factor implicated in reduction of bone density [161].

Despite the high prevalence of coeliac disease and the significant morbidity associated with osteoporosis, there is currently no clear guideline to suggest which patients with coeliac disease should be targeted for bone mineral density scanning either at diagnosis or on follow up.

1.4.4 Thyroid disease

Osteoclasts and osteoblasts are a target of thyroid hormones as well as thyroid stimulating hormone (TSH), with an increase in the turnover of bone associated with thyroid hormone excess, as well as suppression of TSH[162-164]. Untreated hyperthyroidism is associated with lowered bone mineral density and an increased risk of fracture[165]. Even within the normal range higher levels of T3 and T4 hormone have been associated with reduced bone mineral density and increased fracture risk[166]. In the short term there is evidence that treatment of hypothyroidism with thyroxine replacement is associated with a reduction in bone density which suggests it is prudent to use the lowest dose of thyroxine replacement required to suppress thyroid stimulating hormone[167].

1.4.5 Inflammatory Bowel Disease

The inflammatory bowel diseases (IBD) are immune mediated conditions characterised by chronic, relapsing inflammation involving the large bowel (ulcerative colitis) or the entire gastrointestinal tract (Crohns' disease). IBD is commonly complicated by the development of osteoporosis with estimates for the frequency of this complication varying between 17 and 41%[168]. In turn IBD is also

associated with an increased risk of fracture[169]. Conventional risk factors for reduced bone density have been shown to predict lowered bone density in IBD such as reduced body mass index [148], cumulative steroid exposure[170]and smoking[171]. It remains unclear whether disease specific factors such as gut inflammation are also risk factors for the development of osteoporosis[172].

1.4.6 Development of autoantibodies

The fundamental role of the immune system is to discriminate self from non-self and stringent mechanisms are in place to delete or render anergic self-reactive lymphocytes. Despite this, autoimmune diseases are common amongst western populations with pathological auto-reactive antibodies long recognised in conditions as diverse as autoimmune haemolytic anaemia, myasthenia gravis, and neonatal lupus (with antibodies directed against red blood cells, the acetyl-choline cell surface receptor and Ro and La nuclear antigens respectively)[173]. More recently antibodies directed against endogenous cytokines, that are capable of functional inhibition, have been identified as an emerging cause of immunosuppression itself[174].

Extracellular self-antigens typically induce a state of anergy in autoreactive B cells that have escaped clonal deletion in the bone marrow; by contrast sequestered intracellular antigens have been demonstrated to promote autoreactive B cell development[175]. Post translational modification of proteins is an established mechanism in autoimmune disease by which this process of tolerance can be overcome, for example citrullination in rheumatoid arthritis[153]. Environmental factors are thought to contribute to this process, in the example of rheumatoid arthritis smoking and periodontitis are the most compelling [176]. In addition, the genetic makeup of patients who develop autoimmune disease appears to predispose to development of self-reactive immune responses. This can be restricted to specific epitopes by inheritance of human leukocyte antigen alleles as in the ‘shared epitope’ of rheumatoid arthritis[177]. Alternatively an unrestricted tendency to autoimmunity and autoantibody generation may be seen with inherited deficiencies of key regulatory factors as seen in Mendelian disorders of immunodysregulation and polyendocrinopathy[178, 179]. Despite recent advances in understanding, the mechanism of immune tolerance breakdown remains unclear in the majority of cases.

1.5 Identification of autoantibodies

A number of techniques are available for the identification of autoantibodies[173].

1.5.1 Immunofluorescence

Immunofluorescence is a widely used technique in which antibodies that cross react to sections of human tissue or cultured cells are identified by the binding of a secondary fluorescent labelled antibody. Though convenient, the results of this technique may be limited by the quality and availability of substrate as well as the need for an experienced interpreter.

1.5.2 Immunoblotting

A more specific technique for the detection of autoantibodies is thought to be immunoblotting, in which multiple proteins from a tissue or cell culture of interest are first separated out by gel electrophoresis, next transferred onto a membrane and finally probed with serum to identify specific autoreactive antibodies. An advantage of this approach is that the immunoreactive protein spots can be directly cut out and the protein identified, commonly now by mass spectrometry. This technique however may lack sensitivity due to the potential denaturing of the protein of interest prior to interaction with antibody. The technique may also lack specificity due to unanticipated interactions between antibodies and commonly found antigens within cell lysates. In one elegant exploratory paper looking for autoantibodies directed at cell membranes, a large number of intracellular antigens were identified unexpectedly. The authors attribute this to non-specific binding and noted that many of these same antigens have recently been suggested as novel autoantigens by immunoblotting in a diverse range of autoimmune disorders[180].

1.5.3 Enzyme-linked immunosorbent assay

Enzyme-linked immunosorbent assays (ELISA) provide a much more convenient mechanism for the screening of multiple samples for autoantibodies. In this technique a small quantity of protein is bound to a solid surface which is then washed over with serum. Cross-reacting antibodies are then themselves bound by enzyme-linked secondary antibodies allowing for an objective measure of recognition to be made, typically by measurement of a colour change reaction. Although

standardisation of results between assays can be challenging, ELISA tests allow for the analysis of multiple samples with objective results.

1.5.4 Array based technologies

High throughput technologies are emerging that will facilitate the screening of multiple samples against a large numbers of proteins and should ensure both high sensitivity and specificity. These include protein micro-arrays as well as bead based immunoassays. Already such technologies are facilitating the identification of novel autoantibodies[181]

1.6 Aims of the current study

This work arises from the investigation of a patient with severe high bone turnover osteoporosis who was identified as having autoimmune thyroid and coeliac disease but whose osteoporosis deteriorated despite appropriate treatment of these conditions. This presentation led to the hypothesis that neutralising autoantibodies to the bone protective cytokine OPG may have developed in view of the autoimmune diathesis present, as well as the severe high bone turnover state analogous to that seen in patients with inherited deficiency of OPG[182] . This led to the further hypothesis that autoantibodies to OPG may play a pathogenic role in other patients with osteoporosis, in particular those with concomitant autoimmune disease. This study has aimed to test these hypotheses with the following specific goals;

- Establish if immunoglobulins isolated from the index patient are capable of recognising OPG in-vitro
- Establish if identified OPG autoantibodies are functional ie capable of inhibiting OPG activity in-vitro
- Develop an assay for OPG autoantibodies to facilitate the screening of patient cohorts, as well as building/accessing biobanks of serum from suitable patient groups
- Establish if the presence of OPG autoantibodies within different cohorts of patients is associated with reduced bone mineral density, and if so whether this is independent of conventional risk factors for osteoporosis. As a

secondary study the potential impact of OPG autoantibodies on vascular calcification has been investigated.

To summarise the structure of the thesis, characteristics of the index patient himself as well as the results of preliminary assays developed to detect and assess functionality of OPG antibodies in serum are presented in Chapter 3. A variety of approaches to measuring and assessing functionality of OPG antibodies were considered and are described within Chapter 2: Materials and Methods. A particular focus of this work has been to develop a high throughput assay for OPG antibodies in order to allow the screening of distinct patient cohorts for the presence of OPG autoantibodies. The reproducibility of the immunoprecipitation and ELISA assays used to identify OPG autoantibodies is discussed in Chapter 4, as well as the influence of serum factors on the performance of the ELISA. The characteristics of patients with OPG antibodies identified in a general population study (the Orkney complex diseases cohort -ORCADES) are presented in Chapter 5. Cohorts of patients attending the osteoporosis service and coeliac patients attending the gastroenterology department have been recruited over the course of the study and the results of screening these cohorts, as well as an established cohort of inflammatory bowel disease patients, are presented in Chapters 6 and 7. Whilst the main focus has been to establish whether the presence of OPG antibodies is associated with reduced bone mineral density, the possible clinical utility of measuring OPG antibodies in these disease cohorts is also explored.

Chapter 2: Materials and Methods

Within this section the protocols that were developed to identify and characterise antibodies to OPG are described in detail. The source of the reagents used is listed alphabetically in Appendix A1. Apparatus used is detailed in Appendix A2 and the constituents of the solutions used are listed in Appendix A3. The results of preliminary experiments developing an ELISA assay for OPG antibodies are presented in this section; this includes details of a prototype indirect ELISA which was not taken forward, as well as iterations of a direct ELISA the results of which are presented in subsequent sections. Exploratory studies using a number of different cell lines to demonstrate functional activity of OPG antibodies which were not taken forward are described separately in Appendix A4.

2.1 Immunoprecipitation assay for osteoprotegerin antibodies

The ability of serum from the index patient to recognise OPG was first demonstrated using a modification of a standard immunoprecipitation assay. The principals of the assay are shown in Figure 2. 1.

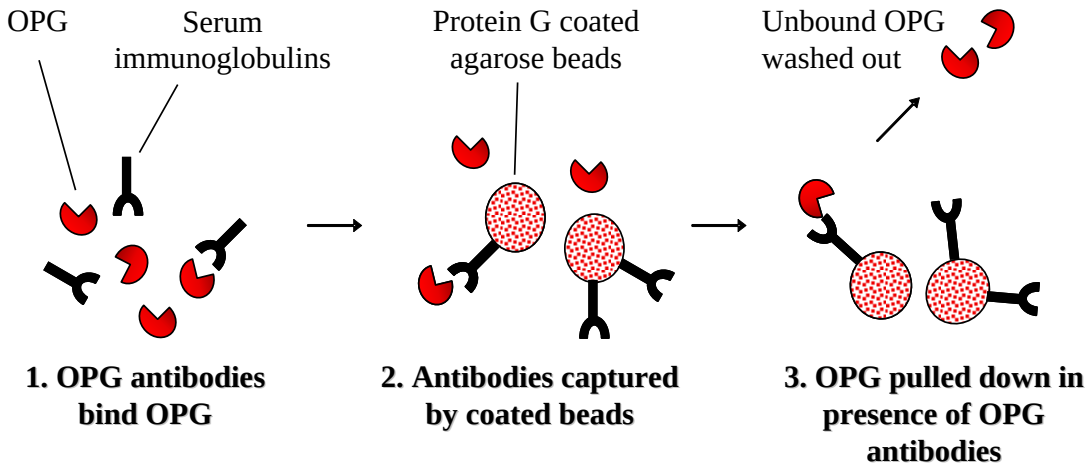

Figure 2.1 Immunoprecipitation assay for OPG antibodies

Recombinant OPG is added to patient serum, allowing immune complexes to form in the presence of OPG antibodies (1). Serum immunoglobulins are pulled down by addition of excess protein G coated agarose beads (2). Unbound OPG is washed out in patients without OPG antibodies by sequential washes, but retained in the presence of OPG antibodies (3). Retained OPG is subsequently demonstrated by Western blot using a commercial anti-OPG antibody.

2.1.1 Immunoprecipitation assay

A working solution of recombinant homo-dimeric full length OPG (R&D systems) was made in 5% bovine serum albumin (BSA) to minimise non-specific binding. The stock solution of OPG was typically made at a concentration of 25ug/ml with a working solution made up by adding 7.5µlof OPG stock to 3ml of 5% BSA. In the final protocol, 2µl of serum was added to 200µl of OPG working solution (ie a 1 in 100 dilution of serum in a solution containing 12.5ng OPG). These samples were incubated for 1 hour at 37º C whilst being shaken vigorously. Meantime protein G coated agarose beads (Calbiochem) were pre-incubated with 5% BSA. Typically 390µl of agarose beads was added to 2.61ml of 5% BSA and mixed end over end for at least 10 minutes), with 230µl of this solution added to each treatment Eppendorf. Eppendorf tubes were centrifuged at 1400rpm for 3 minutes and 200µl of supernatant removed to leave 30µl of beads per tube.

Immunoprecipitation of immune complexes was performed by adding 200µl of serum/OPG solution to each treatment eppendorf, resuspending the beads by briefly vortexing and incubating for 1 hour at 37º C. Beads were resuspended periodically by further brief vortexing. Subsequently each eppendorf was spun at 14000rpm for 1 minute and the supernatant removed. The samples were resuspended in 200µl of warm phosphate buffered saline (PBS), with this wash step repeated five times to remove unbound OPG. Finally the bead pellet was resuspended in 30µl of sample loading buffer (Appendix 3.1) and incubated at 90º C for 5 minutes.

Following brief centrifugation, the supernatant was either frozen for later analysis or analysed immediately by gel electrophoreses and Western blot.

2.1.2 Gel electrophoresis

Gel electrophoresis was performed using CriterionTM XT BioRad (12% Bis-Tris) pre-cast gels, which were placed into a vertical electrophoresis tank filled with electrophoresis running buffer (Appendix 3.1). Samples from the immunoprecipitation assay were already made up in sample loading buffer (Appendix 2.1) to a final volume less than 50µl. All samples were heated at 90°C for 5 minutes and loaded carefully into the well. A Kaleidoscope pre-stained standard and a Magic Marker XP western

standard were used to identify molecular weights. Gels were run at constant voltage of 200V for 45 minutes.

2.1.3 Electrophoretic transfer

This procedure allows the recovery of proteins from the polyacrylamide gel to a solid protein-binding membrane. The gel was removed from the pre-cast gel cassette and immersed into transfer buffer (Appendix 3.1) for 5 minutes. Meanwhile, a polyvinyliden difluoride membrane (PVDF membrane - Hybond™-P) was cut to the size of polyacrylamide gel, immersed in 100% methanol and then allowed to equilibrate in transfer buffer for 5 minutes. A blotting sandwich was prepared with the following successive layers: pre-soaked extra thick blot paper, membrane, polyacrylamide gel and pre-soaked extra thick blot paper. The sandwich was orientated to ensure that the negatively charged proteins were moved out of the polyacrylamide gel and transferred across to the membrane. The transfer was carried out using a Biometra transfer machine at a constant current of 90mA for 1 hour 20 minutes.

2.1.4 Immunostaining and antibody detection

The PVDF membrane was incubated at room temperature for 1 hour in blocking solution of 5% (w/v) bovine serum albumin in TBST (Appendix 3.1) to ensure blocking of non-specific binding sites. Once completed, the membrane was washed in TBST for 30 minutes, while changing the buffer every 10 minutes. Membranes were incubated overnight at 4°C with continuous agitation, with a primary monoclonal antibody to OPG (Abcam) at a concentration of 1:2000 in 5% BSA in TBST. The membrane was washed three times in TBST for 15 minutes and incubated with an anti-mouse secondary antibody at a concentration of 1:5000 in 5% w/v dried non-fat milk in TBST for 1 hour at room temperature. Membranes were again washed three times with TBST. To visualise immunoreactivity, the Pierce SuperSignal® West Dura Extended Duration chemiluminescent detection system was used and the signal was detected on a Syngene Genegnome Bio Imaging System. The intensities of the bands were quantified using the GeneSnap software from Syngene.

Membranes were stripped of bound antibodies by incubation in stripping buffer (Appendix 3.2) for 5 minutes at 50°C. Equal loading of the samples was assessed by probing the blot with peroxidase conjugated goat anti-human antibody (Jackson) at a 1/5000 dilution in 5% BSA for 1 hour. Immunolabelled bands were again detected using Pierce Supersignal chemiluminescence detection system.

2.2. Assays of functional inhibition by OPG antibodies

A number of cellular models were investigated to see if they might be able to demonstrate functional inhibition of OPG by the patient's serum. A potential high throughput functional assay of OPG antibodies was investigated using the AlphaLISA bead-based protocol (Perkin Elmer). This is a proximity assay of protein interactions, in which a signal is emitted when coupled beads are brought together by linked protein pairs, in this case recombinant OPG and RANKL. Relatively weak enhancement of background signalling was observed however with increasing concentrations of OPG and RANKL, as well as an inconsistent dose response despite trials of a number of blocking buffers. In view of the high cost of the reagents this was not pursued (further details in Appendix A4.1).

The generation of osteoclast like multi-nucleated cells from RAW264.7 cells has been reported in response to RANKL stimulation[183]. These cells have been reported to express tartrate resistant acid phosphatase (TRAP) which can readily be measured by direct staining of the osteoclast cells or potentially by analysis of the culture supernatant, and this assay had promise as a more physiological assay of OPG function. No expression of TRAP in RANKL stimulated RAW cells was detected in preliminary experiments exploring this assay and in view of the assay complexity this approach was not pursued (further details in Appendix A4.3). RAW264.7 cells expressing the secreted alkaline phosphatase (SEAP) gene under the transcriptional control of an NFκB response element (IML-120 Imgenex) were obtained, but these were found to be unresponsive to RANKL (further details in Appendix A4.3).

Finally human embryonic kidney 293 cells (HEK 293) stably transfected with a NFκB luciferase reporter construct (Panomics RC0014) were examined. Although

these cells are thought to be embryonic kidney cell in origin, they were shown to respond to RANKL in a dose-dependent fashion (Figure 2.2).

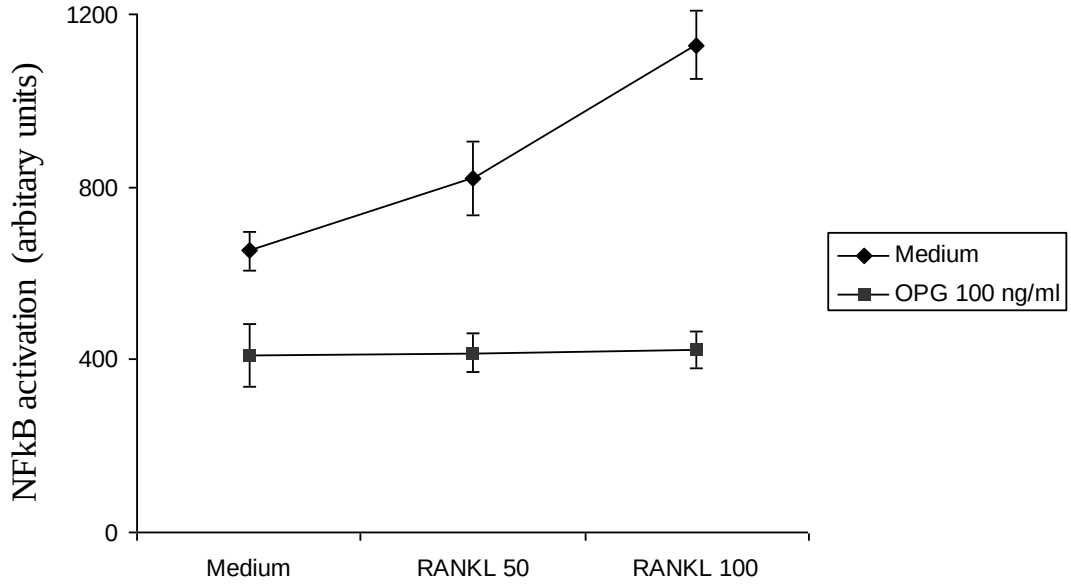

Figure 2.2 Dose response to RANKL in HEK293 NFκB *luciferase cells.*
A linear dose response to 50ng/ml or 100ng/ml RANKL was demonstrated (diamonds – Medium) with suppression of signalling demonstrated by addition of OPG 100ng/ml (squares – OPG100ng/ml). Results shown are means ± standard deviations of triplicate experiments.

Based on these experiments 100ng/ml RANKL is expected to give robust activation of reporter gene expression. Importantly this effect is abrogated by the addition of equimolar human recombinant OPG providing a direct measure of OPG function. Based on these results, an assay demonstrating functional inhibition of OPG by immunoglobulins from our index patient was developed (principles shown in Figure 2.3).

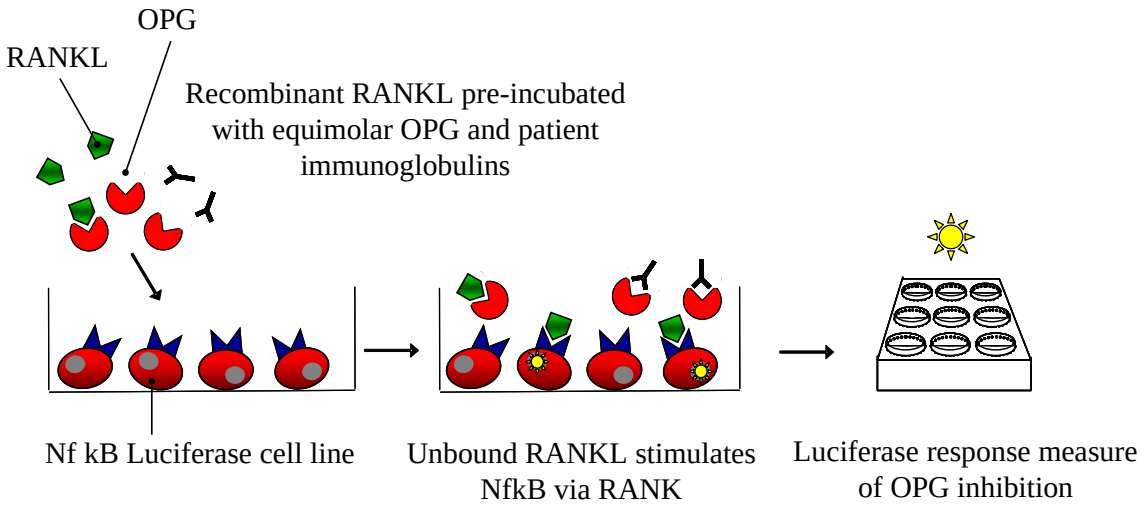

Figure 2.3 Functional assay for osteoprotegerin antibodies
First recombinant OPG is incubated with immunoglobulins purified from the patients' sample. This with equimolar RANKL was added to a cell line stably transfected with an NFκB luciferase response element which had been shown to respond to RANKL in a dose dependent manner. The luciferase response measured gives a measure of the functional inhibition of OPG.

2.2.1 Purification of immunoglobulins

Two techniques were utilised to purify immunoglobulins from serum samples. The first used protein G coated agarose beads (Pierce Protein G spin columns) to pull down serum immunoglobulins, the second utilised a proprietary filtration gel which depletes non-immunoglobulin components of serum (Melon™ Gel IgG Spin Purification Kit).

For both systems, all steps of the immunoglobulin purification were performed at room temperature, with buffers also equilibrated to room temperature. All centrifugation steps were performed on a micro-centrifuge set to 5,000g (8,000rpm) for 1 minute.

After an initial spin to remove storage solution, Protein G spin columns were equilibrated by addition of 400µl binding buffer (Pierce Protein G IgG Binding Buffer 21019) and brief mixing. Columns were centrifuged again and the flow

through discarded. This step was repeated once. 250µl of serum sample was mixed with an equal volume of binding buffer and added to the column for a 10 minute incubation at room temperature with end over end mixing. After centrifugation the columns were washed three times by adding 400µl binding buffer and centrifugation. For collection of the purified immunoglobulins, the spin columns were placed in collection tubes containing 40µl of neutralisation buffer (1M Tris ph 7.5-9). 400µl of IgG Elution buffer (Pierce IgG Elution Buffer 21004) was added to each column, mixed gently then centrifuged with the collected solution making the first elution fraction. Second and third elution fractions were collected in the same fashion. The protein content of the elution fractions was estimated using standard protein concentration assay (Section 2.2.2). Spin columns were regenerated by adding 400µl elution buffer and centrifuging for 1 minute. This step repeated three times. Resin then washed several times in storage solution and stored at 4˚C. Columns could be used up to 10 times without significant loss in binding capacity.

This protocol generated approximately 6mg/ml purified immunoglobulins from the positive control though lower levels of antibody were typically seen with other patient or volunteer samples. Overnight mixing of serum samples in the spin columns showed enhanced protein retention with the immunoglobulin yield increasing from 2.21mg/ml to 5.05mg/ml facilitating equivalent immunoglobulin treatment in the functional studies.

For the melon gel purification, the bottle containing the purification support was swirled to obtain an even suspension before 500µl aliquots of the gel were dispensed into spin columns using a cut pipette tip. Spin columns were placed in micro centrifuge tubes and an initial spin performed to remove storage solution. Two washes were then performed using 300µl of purification buffer with brief centrifugation for 10 seconds and discarding of the flow-through. A bottom cap was then placed on the columns. 50µl of serum sample was added to 450µl of melon gel purification buffer and added to the column. A top cap was placed on the column prior to incubation for 5 minutes at room temperature with end-over-end mixing. The bottom cap was removed from the column, and the top cap loosened prior to re-inserting the spin column in the

collection tube. The purified sample was then collected after a final spin for 1 minute. The antibody was then either used directly or stored and the used Gel Support discarded.

2.2.2 Measuring protein concentration

The protein concentration was determined using the bicinchoninic acid (BCA) Pierce protein assay. A standard curve was generated using supplied standard concentrations of bovine BSA (1,000ug/µl to 5ug/µl). In a fresh 96-well plate, 10µl of each concentration standard and protein samples (1:10 and 1:20 diluted in water) were plated in duplicate. 200µl of copper (II)-sulfate (diluted 1:50 with BCA) were added in each well and incubated for 10 minutes at 37ºC. The absorbance was measured at 562nm on a plate reader and the protein concentration in each sample was calculated from the BSA standard curve.

2.2.3 NFκB Reporter Assay

HEK 293 cells stably transfected with an NFκB luciferase reporter (Panomics RC0014) were maintained in d-minimum essential solution (d-MEM) with 1% Penicillin/Streptomycin/Glutamine and 10% Foetal calf serum (FCS). Cells were harvested once a confluent layer of cells was seen. Incubation with 1/500 agromycin was performed every five cycles to maintain purity of cells.
Prior to assay, the medium was removed and cells rinsed with 10ml of warm PBS. Cells were suspended by trypsinisation (2ml trypsin added to adherent cells). Total volume made up to 10ml of supplemented d-MEM then liberated cells were spun down and made up to 3ml supplemented d-MEM. Cells counted in modified Neubauer cell counter and resuspended to give final concentration of 500,000 cells/ml (ie in order to give 50,000 cells/well with addition of 100µl of cells to each well of a 96-well plate. Cells were plated out overnight and prior to assay serum starved in 100µl of d-MEM with 2% cytokine free tissue culture medium (TCH solution –MP Biomedicals) for 2 hours

All assays were performed in sextuplet in 96-well black-out plates to minimise transference of signal. Sufficient treatments for all cells was made up at 10 times concentration for administration in final volume of 10µl serum deplete d-MEM per

well. A pre-incubation was performed of the patient serum (final concentration 1/40 dilution) with human recombinant OPG (final concentration 100 to 400ng/ml) in a water bath at 37˚C with shaker on for 20 minutes. Subsequently human recombinant RANKL (final concentration 100ng/ml) was added to each sample for a further 20 minutes, again in the water bath at 37˚C.

10µl of each treatment was added directly to cells and incubated for minimum of 3 hours (optimum approximately 7 hours) at 37˚C. 10µl alamar blue was added with treatment to assess cell viability.

During cell stimulation, Steady Glo reagent (Promega) was equilibrated to room temperature. To minimise use of reagents, 50µl sample was typically removed before addition of 50µl Steady Glo reagent. Cells were left for 5 minutes to lyse then read immediately on plate reader. To correct for cell viability, the luciferase reading was divided by the alamar blue reading for final result.

2.3 Enzyme linked immunosorbent assay

In view of difficulties in quantifying the immunoprecipitation assay, a high throughput ELISA for OPG antibodies was developed. Two fundamental approaches were assessed: an indirect assay in which serum OPG antibodies compete with the signal from labelled anti OPG antibodies, and a direct assay in which OPG antibodies recognising membrane bound OPG are labelled.

2.3.1 Indirect ELISA for OPG antibodies

An indirect ELISA-based assay for OPG antibodies was developed using the principals shown in Figure 2.4. In preliminary experiments, a rabbit biotinylated polyclonal antibody to human OPG (AbCam, Ab18068) was used at a concentration of 2.5ng/well to compete with antibodies to OPG found in patient serum.

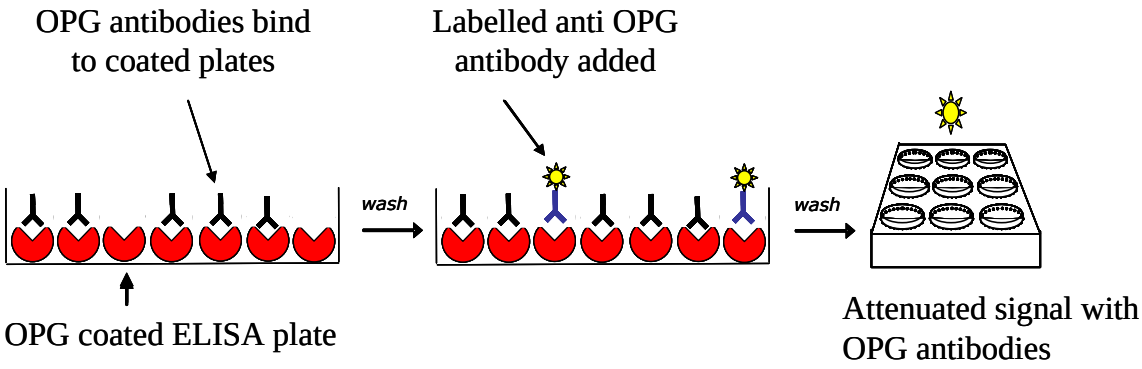

Figure 2.4 Principals of indirect ELISA for OPG antibodies
Recombinant human OPG adsorbed to the base of 96-well plates is used as a capture antigen. OPG antibodies found in serum would be expected to bind to OPG in proportion to their serum concentration. A labelled secondary antibody against OPG was used to measure the levels of unbound OPG and hence give an indirect measure of serum levels of OPG antibodies

A standard curve was created by addition of a murine monoclonal anti human OPG (Abcam, Ab140491) at a concentration of to 1,600 ng/well. Results of a preliminary experiment are shown in Figure 2.5. Serum from the index patient was shown to substantially compete with the labelled antibody, reducing the colour that developed in these wells when streptavidin linked horse radish peroxidase was added. Since the level of absorbance seen with addition of serum fell below the limit of the standard curve it was not possible to attempt any quantification of patient serum OPG antibody concentration in this experiment.

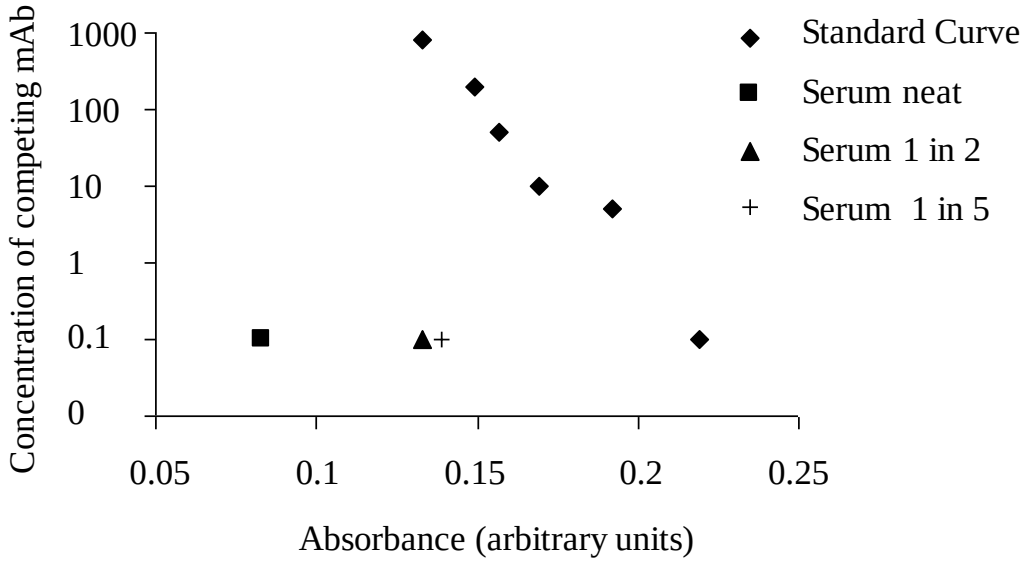

Figure 2.5 Preliminary competitive ELISA experiment
The principal of the assay is confirmed with decreasing level of signal seen with increasing concentration of the competing monoclonal antibody (mAb, standard curve ♦) though complete suppression of the signal could not be achieved despite greatly increasing the concentration (note logarithmic scale for concentration of competing mAb). A greater suppression of signal is seen with addition of patient serum than with the highest concentration of murine anti-human OPG.

A number of further experiments were performed in an attempt to optimise this assay, varying both the concentration of OPG (to optimise the number of binding sites) and the concentration of the labelled polyclonal anti-OPG antibody (to optimise competition for OPG). Results of a dose ranging experiment are shown (Table 2.1). In this experiment, concentrations of plated OPG between 5ng/well to 20ng/well were used, as well as concentrations of labelled anti-OPG antibody from 0.1ng/ml to 5ng/ml.

	OPG conc/well (ng)			
PAb conc/well (ng)	**20**	**15**	**10**	**5**
0	0.23	0.21	0.20	0.21
0.1	0.25	0.24	0.23	0.21
0.2	0.27	0.26	0.26	0.24
0.4	0.34	0.32	0.31	0.27
0.8	0.48	0.45	0.44	0.34
1.6	0.68	0.66	0.64	0.48
5.0	1.43	**1.35**	0.90	0.61

Table 2.1 Dose ranging experiment demonstrating reduced levels of signal with decreasing concentrations of OPG used as a capture antigen, as well as increasing levels of signal with increasing labelled polycloncal antibody to OPG (pAb)

Only a relatively modest increase in signal is seen when increasing from 15 to 20ng/well of OPG so for ongoing experiments 15ng/well OPG was selected. A relatively high background signal is seen even in the absence of specific labelled polyclonal antibody. A variety of blocking buffers were assessed but were not able to reduce the background signal seen (data not shown).

Finally an unlabelled rabbit polyclonal antibody to OPG (Abcam, ab9986), 2.5 to 1,280ng/well) was used for the standard curve to negate the possibility that the epitope specificity of the monoclonal antibody rendered it impossible to completely suppress the signal from the labelled polyclonal antibody. This antibody was able to suppress signal at relatively low concentrations, though once again complete suppression of signal could not be achieved (Figure 2.6).

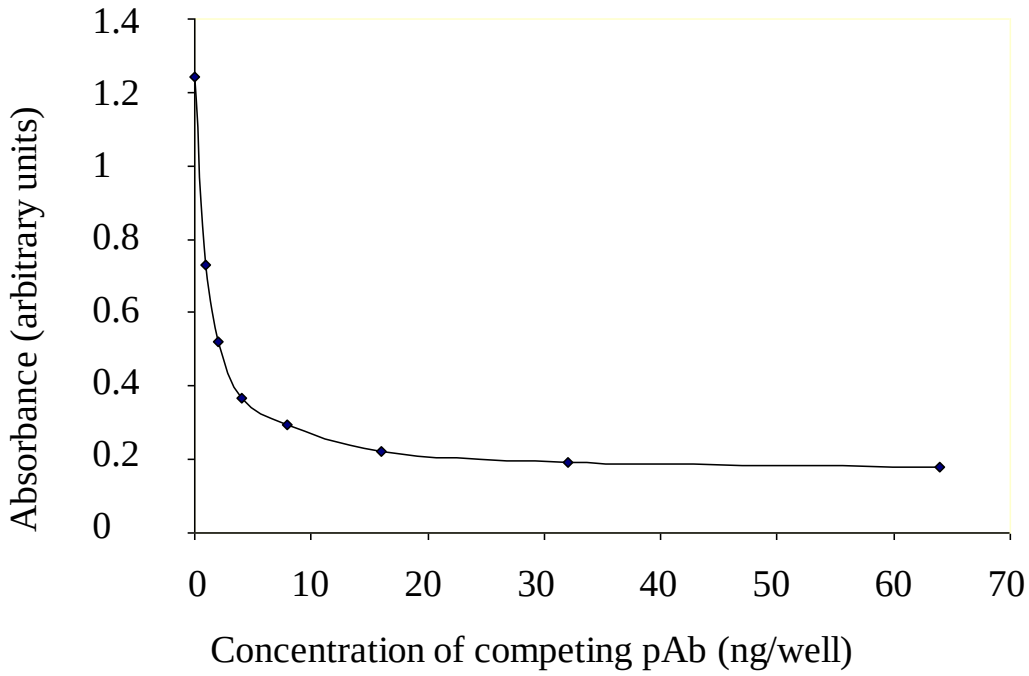

Figure 2.6 Inhibition by polyclonal OPG antibody

Based on these experiments the optimised protocol comprised 15ng OPG per well plated out overnight and then blocked in 1% BSA. Serum was added at a dilution of 1:2.5 and incubated for 1 hour at 37˚C. A standard curve was created using serial dilutions of the polyclonal antibody to OPG. Biotinylated polyclonal antibody to OPG was added at a concentration of 0.1ng/ml to each well and this was incubated for 1 hour at 37˚C. Following a further wash, optical density was read after addition of substrate. Results are shown in Figure 2.7. A reduction in absorbance is seen with addition of the serum from our index patient that is greater than that seen with a negative control, providing proof of principal. The absolute fall in signal intensity seen is relatively modest suggesting it would be very difficult to use this assay to identify further positive serum samples. Consequently a direct ELISA assay was developed.

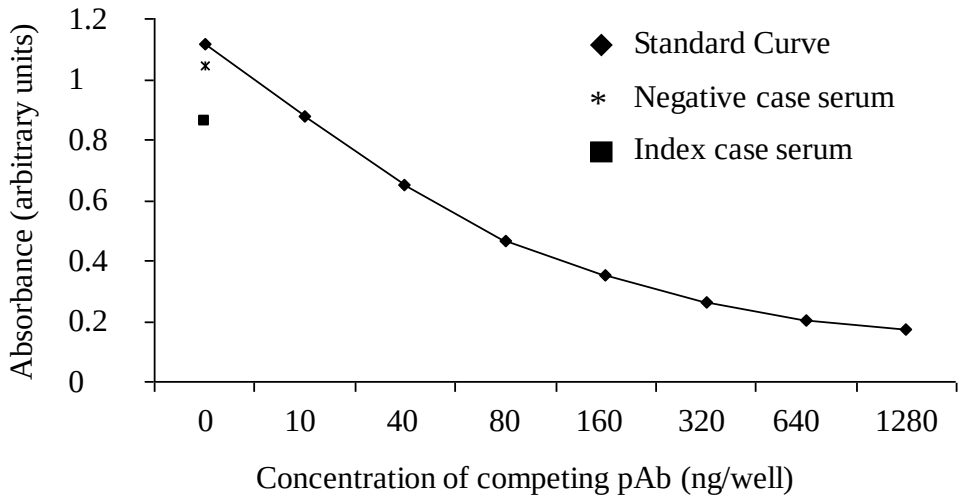

Figure 2.7 Suppression of signal seen with increasing concentration of competing polyclonal antibody to OPG. The sample from our index patient showing suppression of signal but a relatively modest suppression of signal intensity by 1/3 suggests that the dynamic range of the assay is likely to be insufficient to demonstrate suppression effects in patients with lower levels of OPG antibody.

2.3.2 Principals of a direct ELISA for OPG autoantibodies

A direct capture ELISA for antibodies to OPG was developed by modification of the indirect ELISA protocol. Once again recombinant OPG was used to coat an ELISA plate, but this time patient serum samples were added directly, with the addition of labelled anti-human immunoglobulin G giving a direct measure of the presence of autoantibodies. The same polyclonal rabbit antibody to OPG (Abcam, ab9986) was used to create a standard curve, taking advantage of a cross reactivity of the labelled anti-human IgG with rabbit antibodies. The principals of a direct capture ELISA for OPG antibodies is shown in Figure 2.8.

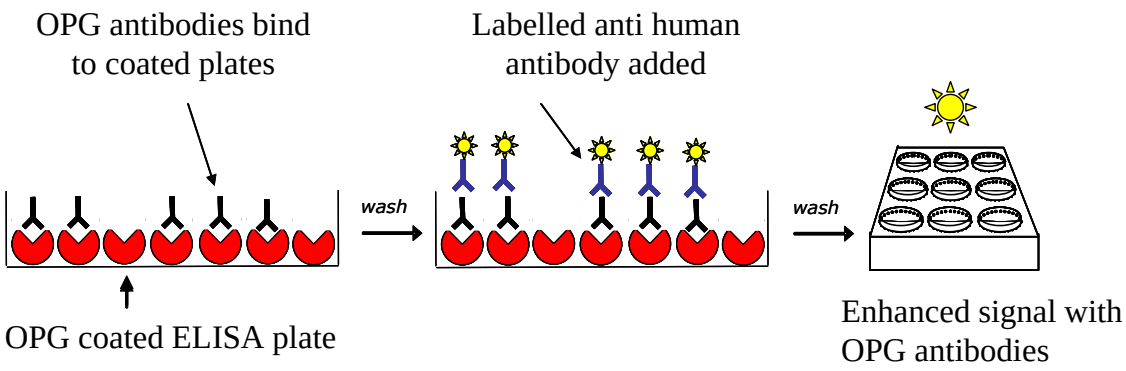

Figure 2.8 Principals of direct ELISA for OPG antibodies
Recombinant human OPG adsorbed to the base of 96-well plates is used as a capture antigen. OPG antibodies found in serum would be expected to bind to OPG in proportion to their serum concentration. A labelled secondary antibody against human immunoglobulin directly measures the quantity of OPG antibodies.

In a dose ranging experiment, OPG concentrations between 1 and 15ng/well were utilised to coat the plate, and serum was added in doubling dilutions from 1 in 40, to 1 in 640 (see Table 2.2). Unsurprisingly a dose response is seen both with increasing concentration of OPG and with increasing concentration of serum.

Serum dilution	OPG concentration used to coat plate (ng/well)				
	1.0	**2.5**	**5.0**	**10**	**15**
Negative control					
1 in 40	1.055	0.973	0.931	0.993	1.009
1 in 80	0.680	0.711	0.683	0.731	0.723
1 in 160	0.634	0.597	0.621	0.610	0.622
1 in 320	0.442	0.452	0.446	0.452	0.489
1 in 640	0.363	0.353	0.331	0.349	**0.369**
Positive control					
1 in 40	1.507	1.859	2.060	2.240	2.264
1 in 80	1.185	1.406	1.735	1.971	2.008
1 in 160	0.963	1.121	1.507	1.695	1.914
1 in 320	0.621	0.833	1.087	1.287	1.495
1 in 640	0.459	0.524	0.725	0.908	**1.029**

Table 2.2 Optimisation of conditions for direct OPG ELISA
Plate reader absorbance values (arbitrary units) are shown with increasing concentration of OPG used to coat ELISA plates both for a sample known to be negative for OPG (Negative control) and serum from the index case (Positive control). Effects of serial dilutions of both samples was also explored to identify conditions that would optimally discriminate positive from negative samples.

Relatively high background signal is seen with the negative control, which was attenuated with increasing dilution of serum, whilst maintaining a similar ratio of positive to control signal at all dilutions. Attenuation of the signal seen with the positive control is seen with increasing dilutions however (Table 2.3). On the basis of these experiments a final dilution of 1 in 1,000 was typically used to prevent non-specific binding from giving falsely high absorbance readings.

	Serum sample and dilution					
	Negative control			Positive control		
	1: 640	**1: 1,280**	**1: 2,560**	**1: 640**	**1: 1,280**	**1: 2,560**
Repetition 1	0.151	0.115	0.074	2.070	1.574	0.943
Repetition 2	0.161	0.113	0.076	2.104	1.530	0.896
Mean	**0.156**	**0.114**	**0.075**	**2.087**	**1.552**	**0.920**
Standard deviation	0.007	0.001	0.001	0.024	0.031	0.033

Table 2.3 Effect of serum dilution on direct OPG ELISA
Plate reader absorbance values (arbitrary units) are shown with varying dilutions of a sample known to be negative for OPG antibodies(negative control), as well as serum from the index case (positive control). Results of duplicate experiments are shown.

An inherent difficulty with this approach is that no human antibody to OPG is commercially available, and so the primary antibody used to generate a standard curve is necessarily from a different species than that in the assayed samples (ie a commercial polyclonal antibody raised in rabbit to OPG was used to form a standard curve initially). As a result there will be an inherent difference in the affinity of the labelled secondary antibody for the primary antibody in the assayed samples compared to the standard curve. This potentially introduces error both within assays, for example at differing concentrations of sample, and between assays, for example if the affinity of the reaction is differentially affected by environmental factors.

Initially this was accepted as an unavoidable hazard and a first iteration of the ELISA using a rabbit polyclonal antibody to derive a standard curve was used (referred to throughout thesis as ELISA I – protocol given in Section 2.3.4). Results from a number of populations are reported with this assay. Subsequently a generous donation of serum from the index patient meant that there was sufficient serum to use to derive a standard curve in all the assays that we intended to run, thereby avoiding this problem altogether. From this point on serial dilutions of index patient serum

were used to create a standard curve, with an arbitrary value of 100 units assigned to the absorbance reading obtained by a sample of serum from the index patient. This iteration of the assay is referred to as ELISA II (protocol given in Section 2.3.6). Both protocols utilise similar conditions to coat the plates, assay samples and measure levels of antibody however in ELISA I a normal range for the assay was derived from a small cohort of healthy volunteers within the department, and for ELISA II a larger cohort of healthy volunteers taken from the ORCADES population was used to derive a normal range (standardization of assays described in detail in Section 2.3.3 and Section 2.3.5).

2.3.3 Standardisation of ELISA I

A linear standard curve was produced using serial dilutions from 5 to 500pg/µl of a rabbit polyclonal antibody to OPG (Figure 2.9). This allows a quantification of the signal obtained for assayed samples, which since they were typically measured at a 1/1000 dilution yielded final antibody concentrations measured in ng/µl. A signal that is close to the background signal is seen with the negative control and approximately ten fold increases in signal with the positive control suggesting that this assay would have a sufficient dynamic range to allow population screening.

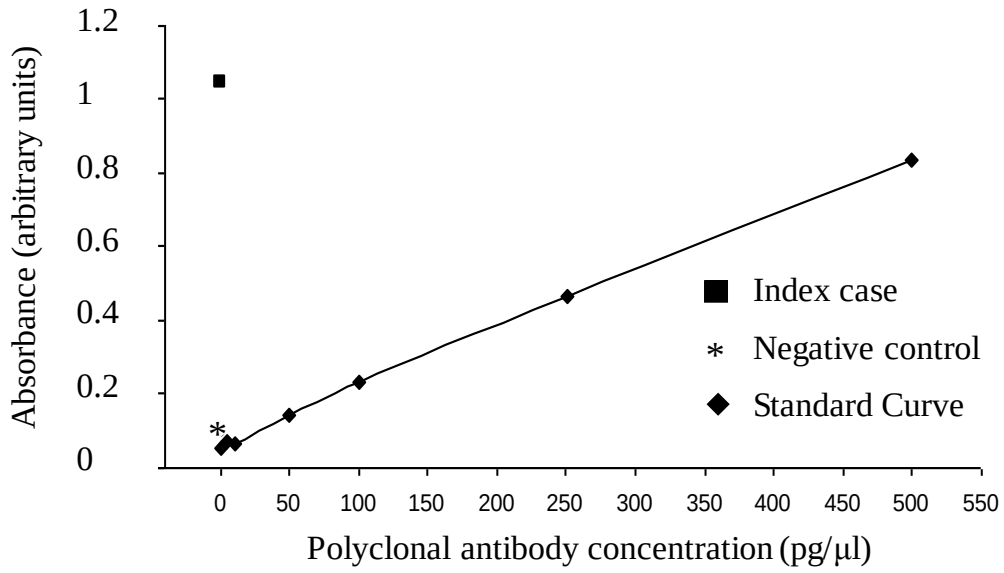

Figure 2.9 Indicative standard curve for direct OPG antibody ELISA I illustrating also the value of serum from index case (black square) and a sample from healthy volunteer (asterix). Standard curve for the assay was derived from increasing concentrations of rabbit polyclonal antibody to OPG between 5 and 500ng/µl. Plate reader absorbance is close to background for sample negative for OPG antibodies, with enhanced signal seen with serum from index case.

Whilst a linear standard curve was originally fitted to the data a plateau effect was observed that was non-linear. The plate reader software included a spline analysis function to determine concentration more accurately in this situation. A sample standard curve including standard deviations for each reading and showing spline and linear curve fits is shown (Figure 2.10).

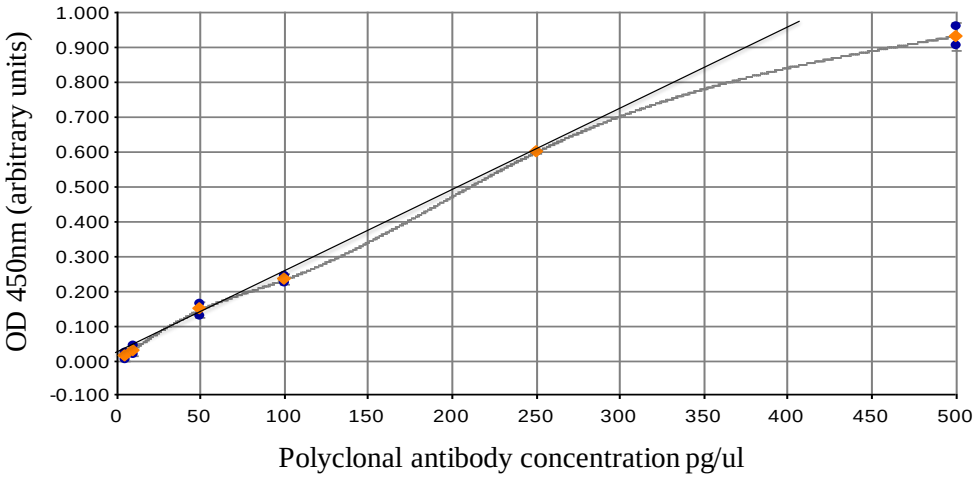

Figure 2.10 Standard curve of ELISA 1 showing spline and linear fit

In order to generate a normal range and so allow categorisation of the presence of raised titres of OPG antibody, serum was obtained from 20 healthy volunteers of known normal bone density working within the department of medical physics, or the Institute of Genetics &Molecular Medicine. Volunteers were of average age 48 (±7), average BMI 23.75 (±5) and 14/20 female (70%). The distribution of OPG antibodies within the healthy volunteer cohort is illustrated in Figure 2.11. Mean OPG antibody titre was 19.39 ng/µl (±23.94). A threshold was chosen of mean plus 3 standard deviations equivalent to 91.21 ng/µl which lies above the 100th percentile and would therefore be anticipated to exclude the vast majority of negative samples.

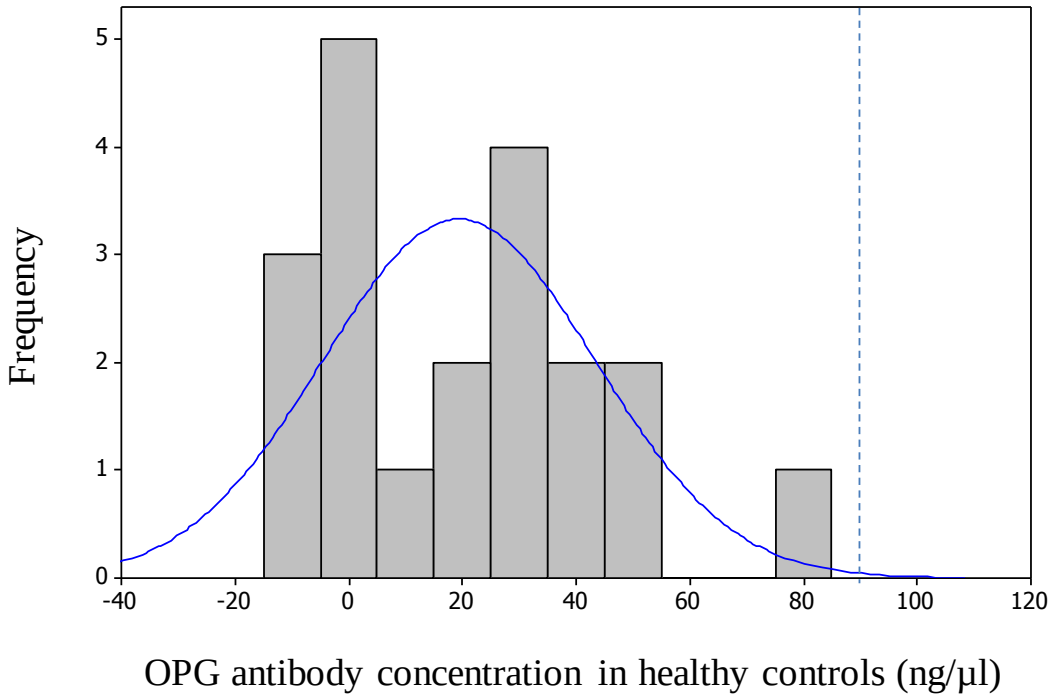

Figure 2.11 Frequency distribution of OPG antibodies in 20 healthy volunteers with normal bone density using ELISA I. Dotted line represents the threshold used to describe positive OPG antibodies derived from the mean plus three standard deviations (91 ng/µl).

2.3.4 Protocol for ELISA I

In subsequent results sections where this iteration of the assay are used (with a standard curve based on commercial-labelled OPG antibody) the assay is referred to as ELISA I, with this protocol now described in detail. Human recombinant OPG (R&D Systems) was reconstituted to prepare an OPG stock solution of 100ug/ml by adding 250µl of 0.2um filtered PBS to 25ug lyophilised powder. Reconstituted OPG was stored in the same vial at 4^{o}C for later use. OPG stock (100 ng/µl) was diluted to 0.3ng/µl using 16µl stock + 5,319µl of coating buffer per plate. Coating buffer (Sigma) is prepared by dissolving 1 capsule in 100ml distilled water.

50µl aliquots of the diluted OPG solution were added to all wells of a Costar high-binding micro-titre plate (Corning), giving a final total of 15ng OPG per well. The

plate was sealed with a plate sealer and incubated at 4°C for approximately 24 hours (±1 hour).

The plate was washed seven times in TBST wash buffer (Appendix 3.3) and dried thoroughly. Plate was blocked by addition of 300µl of 1% BSA blocking buffer (1g BSA in 100ml TBST) to each well, and incubated at 24°C for 2 hours. After incubation, the plate was washed seven times and dried thoroughly.

To create a standard curve, a non-biotinylated polyclonal rabbit antibody to OPG was used (Abcam ab9986) from a stock solution at 500ng/µl. Briefly 3 µl of stock was added to 7,797µl of buffer giving a concentration of 192pg/ µl with doubling dilutions used down to 3pg/µl. 50µl of sample was added to each well to give a standard curve of 9.6ng down to 0.15ng per well.

Serum was obtained from the index case and unselected patients after giving informed consent. Positive control serum from the index case was used at a dilution of 1 in 6,000, negative control serum and serum under investigation was used at a dilution of 1 in 2,000. Dilutions were prepared in a standard micro-titre plate and used at a final volume of 50µl added to each plate. The well contents were mixed by gently tapping the plate for approximately 1 minute. The plate was then re-covered and incubated at 37°C for 1.5 hours.

After incubation, the plate was washed eight times and dried thoroughly. Secondary peroxidase conjugated anti-human detection antibody (Jackson) was diluted 1:40,000 and added at a volume of 100µl per well. The plate was re-covered and incubated at 24°C for 1.5 hours.

Colour development: After incubation, the plate was washed eight times and dried. To each test well of the plate 100µl of tetramethylbenzidine (TMB) substrate solution (Sigma) was added and the plate was incubated at 24°C for 20 minutes to permit colour development (plate was covered with foil to protect from direct light). 100µl of TMB stop solution (KPL) was then added to each well of the plate. Optical density for

samples in all wells was measured at 450nm within 30 minutes of adding the stop solution. An automated spline analysis (using plate reader software) was used to determine the sample concentrations.

2.3.5 Standardisation of ELISA II

As discussed in 2.3.2, and following a generous donation of serum, serial dilutions of serum from the index patient were used to generate the standard curve for the ELISA. A value of 100 relative units (RU) was adopted for serum from the index patient. A sample standard curve generated by the plate reader is shown in Figure 2.12. There is saturation of signal with increasing concentration of positive control serum, with a logistic curve chosen to best fit the standard curve. Positive samples that fell on the non-linear part of the curve were re-analysed after dilution.

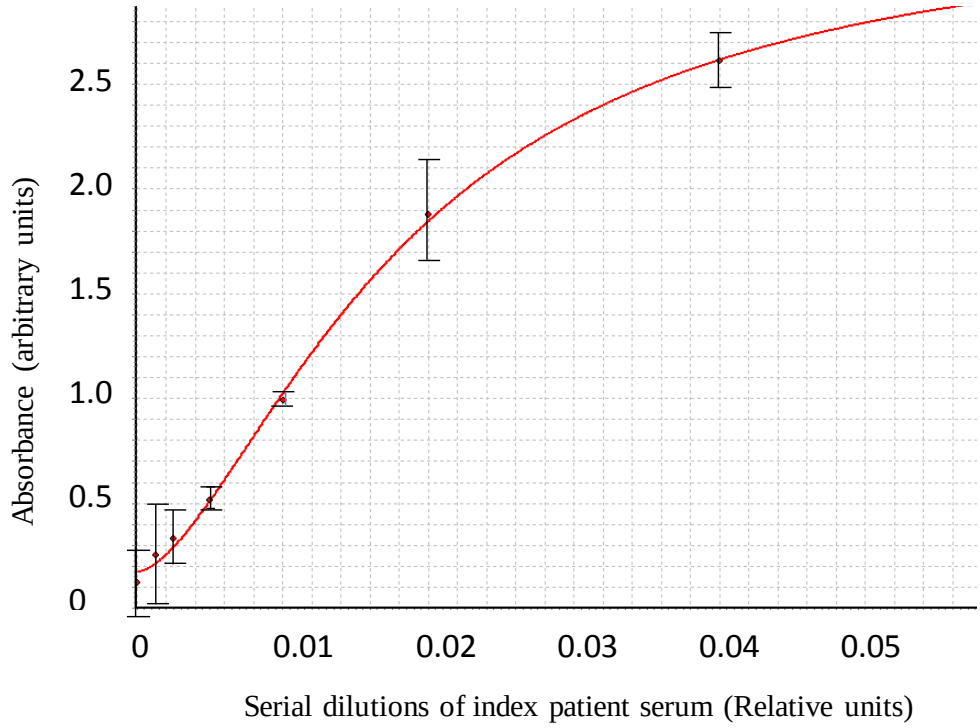

Figure 2.12 Standard curve utilising serial dilutions of index case serum. An arbitrary value of 100 units is assigned to neat serum such that the starting dilution of 1/2500 is assigned a value of 0.04, from which doubling dilutions were derived to generate a standard curve. Samples are assayed at 1/1000 dilution but final concentrations are expressed for the value of a neat sample..

Typically readings for patient samples generated results that were greater than the lowest dilutions of the standard curve using index serum, suggesting that non-specific serum effects were still influencing readings in healthy patients. 101 samples from healthy volunteers taken from the ORCADES cohort and with known normal bone mineral density were used to generate a reference range for the ELISA II assay. The mean reading obtained was 3.45 RU (±3.62) with a threshold of 14.31 RU adopted of the mean of healthy volunteers plus three standard deviations which would be expected to exclude the vast majority of negative samples. Since the results from these volunteers did not follow a strictly normal distribution (Figure 2.13) this threshold corresponded to a 98th percentile for healthy volunteers. In view of the arbitrary nature of this threshold, all analyses were also repeated using the absolute titre of OPG antibody.

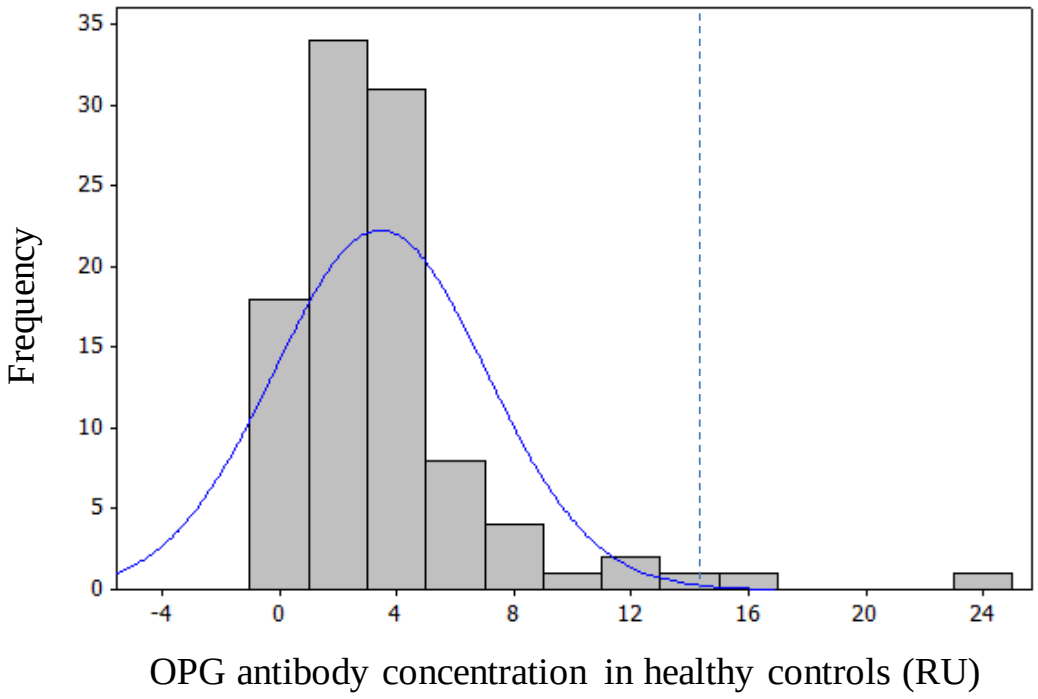

Figure 2.13 Frequency distribution of OPG antibodies in healthy volunteers with normal bone density measured using ELISA II. Dotted line represents the threshold used to describe positive OPG antibodies

2.3.6 Protocol for ELISA II

The second iteration of the direct ELISA assay using positive control serum to provide a standard curve is referred to as ELISA II. In a minor modification to the protocol the plates were not dried after coating with OPG lest this influence protein integrity. As before, human recombinant OPG (R&D Systems) was reconstituted to prepare an OPG stock solution of 100µg/ml by adding 250µl of 0.2um filtered PBS to 25ug lyophilised powder. Reconstituted OPG was stored in the same vial at 4^{o}C for later use. OPG stock (100ng/µl) was diluted to 1ng/µl using 99µl stock + 9801µl of coating buffer per plate. Coating buffer (Sigma) is prepared by dissolving 1 capsule in 100ml distilled water.

100µl of diluted OPG is added to all wells of a Costar high-binding micro-titre plate (Corning), giving a final total of 100ng OPG per well. The plate was sealed with a plate sealer and incubated at 4^{o}C for approximately 24 hours (±1 hour). Subsequently the wells are washed twice with 200µl/well of wash buffer for 5 minutes.

200µl/well of 3% BSA blocking buffer is then added to each well for 1 hour at room temperature (3g of BSA added to 100ml of PBS). In this time a standard curve of positive control serum is prepared from a fresh aliquot of the index serum This is diluted 1 in 100 in binding buffer, with further dilutions taken to give 300µl of the positive control at dilutions of 1/2,500, 1/5,000, 1/10,000, 1/20,000, 1/25,000 and 1/50,000. An arbitrary value of 100 units was assigned to neat positive serum, yielding a standard curve from 0.04 down to 0.002 units. Samples falling below the lower limit of the standard curve are assigned 0 for further analysis. Samples to be analysed were diluted 1/1000 in binding buffer (typically 2µl of the sample is added to 198µl of binding buffer, with a second dilution step of 30µl added to 270µl of binding buffer).

Blocking solution is removed from each well and the samples added at a volume of 100µl/well, and incubated for 1 hour at room temperature. After incubation, the plate was washed five times with 200µl/well of wash buffer. Secondary peroxidase conjugated anti-human detection antibody (Jackson) was diluted 1:20,000 and added

at a volume of 100µl per well. The plate was re-covered and incubated at room temperature for 1 hour.

Colour development: after incubation, the plate was washed five times. To each test well of the plate, 100µl of TMB substrate solution (Sigma) was added and the plate was incubated at 24^{o}C for 30 minutes to permit colour development (plate was covered with foil to protect from direct light). 100µl of TMB stop solution (KPL) was then added to each well of the plate. Optical density for samples in all wells was measured at 450nm within 30 minutes of adding the stop solution, with a reference wavelength of 640nm. An automated four parameter analysis (using plate reader software) was used to determine the sample concentrations.

2.4 Commercial assays of OPG and RANKL

Commercial ELISA assays for both free (Biomedica) and total (Biovendor) RANKL as well as OPG (Biomedica) were purchased and utilised according to manufacturers' instructions. Unless otherwise stated all reaction steps were carried out at room temperature

2.4.1 Human Ampli-sRANKL ELISA (free RANKL)

A commercial ELISA assay for total free sRANKL was used according to manufacturer's instructions (Biomedica BI-20452). Standards and control were reconstituted by adding 700µl of deionised water to each and leaving for at least 15 minutes. All reagents and samples (undiluted) were brought to room temperature prior to assay. Wash buffer was prepared by adding 50ml of the supplied stock Washbuffer to 950ml distilled water and this was stored at room temperature until required. 100µl of the standards and the control were pipetted in duplicate into respective wells. Additionally, 100µl of the serum samples to be tested was added to the respective wells. For the duplicate sample, 10µl of the same serum samples were added to the desired wells and in these wells 90µl of wash buffer had already been added to dilute the samples.

To each well (including the blank), 100µl of solution AB (green cap) was added and the plates swirled gently to mix. Plates were sealed tightly and incubated overnight with vigorous shaking.

After incubation, wells were aspirated and washed five times with 300µl of wash buffer. Remaining wash buffer was removed by tapping onto paper towels after the last wash.

200µl CONJ solution (Amber cap) was added into each well, the plates were sealed tightly and incubated for 1 hour (no shaking). After incubation plates were washed five times. Amplifier A and B were squeezed into clean troughs, then 100µl Amplifier A (Blue cap) was added to each well. Subsequently, 100µl Amplifier B (Red cap) was added to each well and the plate incubated for 25 min (no shaking).

At this point the pink/red colour had developed substantially and so the plate was read quickly at 490nm. The highest standard had an optical density value of approximately 2.0 and the blank a value of less than 0.2. Therefore, the reaction was stopped by addition of 50µl STOP solution (White cap) to each well. The absorbance at 490nm, with reference of 630nm was then immediately measured.

2.4.2 Human sRANKL ELISA (total RANKL)

A commercial ELISA assay for total human sRANKL was used according to the manufacturer's instructions (Biovendor RD193004200R). The master standard and the high and low quality controls were reconstituted with dilution buffer using the volumes stated on the Certificate of Analysis just prior to assay. These were left for 15 minutes with gentle shaking.

The following standards were prepared using the reconstituted master standard. Serum samples were diluted by adding 2.5µl sample to 247.5µl of dilution buffer. 100µl of Standards, Controls, Dilution buffer (Blank) and Samples were pipetted (in duplicate) into the appropriate wells. Due to low volumes for serum samples only 90µl was used per well. Plate was incubated at 2–8 ^{o}C overnight with shaking at

approximately 300 rpm. Biotin labelled antibody was brought to room temperature overnight

Wash solution was diluted by adding 100ml of concentrate to 900ml of distilled water, using 350µl of this wash solution the wells of the plates were washed five times. After the final wash, plates were tapped onto paper towels to dry.

100µl of biotin labelled antibody was added to each well and the plates incubated for 1 hour with shaking (300rpm). Wells were washed five times, then 100µl of Streptavidin-horse radish peroxidase (HRP) Conjugate was added to each well. The plates were incubated for 1 hour with shaking. Wells were again washed five times then 100µl of Substrate solution was added to each well. The plate was covered with foil to protect from light and incubated for 25 minutes.

The colour development was stopped by addition of 100µl of stop solution. Subsequently, the absorbance at 450nm was determined (with a reference of 630nm). The blank OD 450 value was subtracted from 450nm readings as was the reading at 630 nm (subtracted from the 450nm value).

2.4.3 Human OPG ELISA

A commercial assay for human OPG was utilised according to manufacturer's instructions (Biomedica, BI-20403). The master standard and the high and low quality controls were reconstituted with dilution buffer using the volume stated on the Certificate of Analysis, just prior to assay. These were left for 15 minutes with gentle shaking (without allowing to foam).

Assay standards were prepared as below: the prepared standards and the reconstituted high and low controls were further diluted three fold with dilution buffer (100µl standard and 200µl of dilution buffer). Serum samples were similarly diluted three fold (100µl sample and 200µl of dilution buffer). 100µl of the diluted Standards, Controls, Dilution buffer (Blank) and Samples (in duplicate) were

pipetted into the appropriate wells. Plates were incubated for 1 hour with shaking at approximately 300 rpm.

Wash solution was diluted by adding 100ml of concentrate to 900ml of distilled water. Subsequently, the wells were washed three times with 350µl of the prepared wash solution. After the final wash plates were inverted onto paper towels to dry. 100µl of Biotin labelled Ab was added to each well and the plates incubated for 1 hour with shaking (300rpm). Wells were washed three times then 100µl of Streptavidin-HRP Conjugate was added to each well and the plates incubated for 30 minutes with shaking. Wells were washed three times then 100µl substrate solution was added to each well. The plates were covered with foil to protect from light and incubated for 10 minutes. Colour development was then stopped by the addition of 100µl of stop solution. The absorbance at 450nm (with a reference of 630nm) was determined. After subtracting the blanks absorbance values from the 450nm values, the 630nm reading was also subtracted from that at 450nm.

2.5 Assessment of vascular calcification on lateral image DEXA

DEXA scanning was performed using a Hologic QDR4500 densitometer. Whilst CT scanning is the gold standard for assessing vascular calcification a simple scoring system based on the lateral lumbar spine image obtained at DEXA scanning has been shown to have reasonable agreement with CT, and offers great advantages in terms of safety and convenience[184].

A simple semi-quantitative 8-point scoring system has been derived based on assessments of the anterior and posterior aortic wall on the lateral image DEXA of lumbar vertebrae (L1–L4), with each wall scored between 0 to 4 (Figure 2.14). High correlation was found between this score and a more detailed 24 point score ($r=0.98$, $p<0.0001$) and the latter score was in turn shown to have a sensitivity of between 56% and 71%, and specificity between 80% and 63% when compared to varying thresholds of CT determined aortic calcification[184]. The 24-point score is also calculated based on the extent of calcification observed adjacent to the lumbar vertebra, but in this system a score of 0–3 is given for each vertebra depending

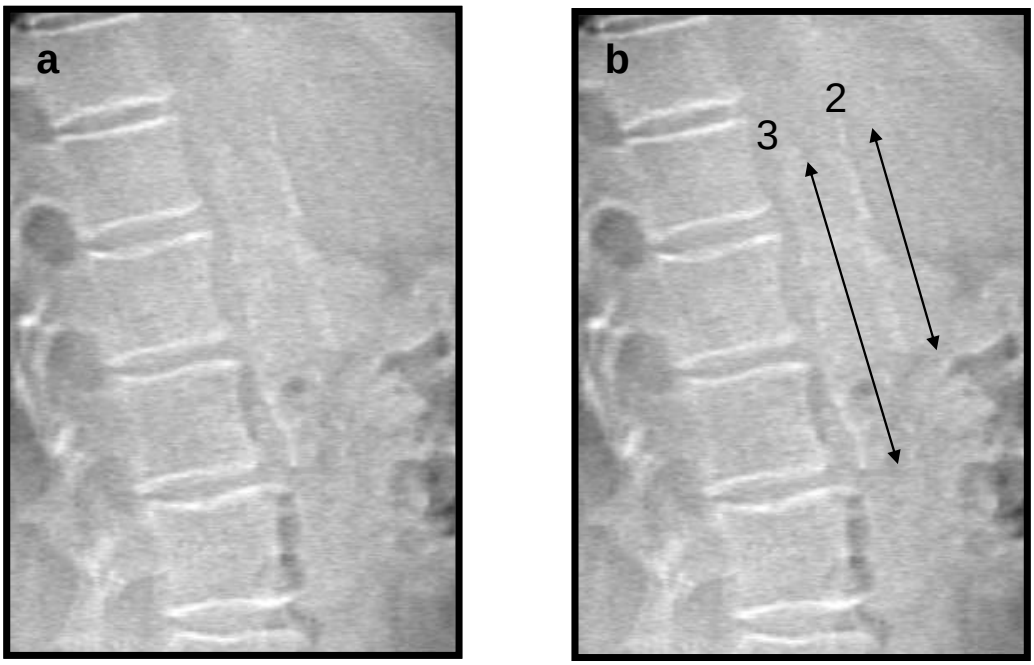

Figure 2.14 Vascular calcification scoring of lateral image DEXA scan
A score of 0 is given if there is no calcification, 1 if the extent of calcification is equal to or less than the height of one vertebra, 2 if calcification is greater than one vertebra but equal to or less than the height of two vertebrae and so on. (a)Sample image from ORCADES showing extensive vascular calcification. (b)In this example the anterior aortic wall scores 2 and posterior wall 3 giving a total score of 5.

on whether there is no calcification (0), calcification involves less than 1/3 of the vertebral height (1), calcification involves between 1/3 and 2/3 of the vertebral height (2) and calcification involving more than 2/3 of the vertebral height (3). Both anterior and posterior aortic walls are scored to give a maximum possible score of 24. Vascular calcification was assessed in patients from a general population cohort who had undergone DEXA scanning as part of the ORCADES study (described in detail in Section 2.3.3) using this method.

Similarly a semi-quantitative technique has been described to detect prevalent vertebral fractures using lateral imaging DEXA with good inter-observer reliability[185]

2.6 Study populations

A number of different populations were studied in the course of this thesis and the details of how each has been derived are listed here. A summary of the characteristics available for analysis in each cohort is given in table 2.4.

Characteristic	ORCADES	Coeliac	OP	IBD
Age	✓	✓	✓	✓
Gender	✓	✓	✓	✓
Height	✓	✓	✓	✓
Weight	✓	✓	✓	✓
Spine BMD T-score	✓	✓	✓	✓
Spine BMD Z-score	✓	✓	✓	✓
Hip BMD T-score	✓	✓	✓	✓
Hip BMD Z-score	✓	✓	✓	✓
Medication history (Bisphosphonate, Ca/D, Steroids	✓	✓	✓	✓
Co-morbidities	✓	✓	✓	✓
Current smoker	✓	✓	✓	✓
Alcohol (units/week)	✓	✓	✓	✓
Serum ALP, Ca			✓	
Additional disease specific factors		Age of onset TTG levels Pathology grading		Age of onset Crohn's disease/ Ulcerative colitis Pathology grading

Table 2.4 Characteristics available to study in each cohort

2.6.1 ORCADES cohort

The Orkney Complex Disease (ORCADES) study is a population-based study for health research, designed to identify genetic risk factors for complex diseases (Orkney Research Ethics Committee approval - 27/02/2004). Exceptionally high recruitment has yielded a cohort of 2000 healthy volunteers whose grandparents originated from the Orkney Islands (from a total population of 12000). The study is cross-sectional in nature. The average age is 53 years (range 18–100 years), and approximately 42% are male. Up to 200 different traits have been measured in each individual. Bone mineral density assessed by DEXA is available in 1,578 patients. Data are also available on subjects' medical and surgical history, medication, family history, diet, smoking, alcohol, physical activity, angina, claudication, lung symptoms and socio-economic status. All participants are flagged at Information Statistics Division (NHS Scotland) for deaths and hospital admissions allowing prospective analysis of the value of biomarkers in predicting major health events. A bank of stored plasma, serum and whole blood was made available by Dr James Wilson. I played no part in the recruitment of these patients, though assisted in the cataloguing of the approximately 2000 samples.

2.6.2 Osteoporosis Cohort

All patients attending the osteoporosis service at the Western General Hospital in Edinburgh, including the index case, were invited to contribute a blood sample to support ongoing research. Appropriate approval from the local research ethics committee (reference 04/S1102/41) was in place to recruit patients attending the clinic, though an amendment was agreed to allow direct recruitment of patients that had previously attended the department in addition. BMD measurements were performed in line with routine clinical care. At time of DEXA scanning detailed information on risk factors for osteoporosis was recorded including patient demographics, body mass index (BMI), lifestyle factors and calcium intake (a copy of the questionnaire is given in Appendix A5).

2.6.3 Coeliac and Inflammatory Bowel Disease Cohorts

A cohort of patients with coeliac disease was recruited over the course of this study with approval of local research ethics committee (reference 10/S1402/33). All

patients attending coeliac disease clinics across Lothian were invited to give serum samples. BMD measurements were performed in line with routine clinical care. At time of DEXA scanning detailed information on risk factors for osteoporosis was recorded including patient demographics, BMI, lifestyle factors and calcium intake. Specific permission has been obtained for ongoing surveillance of these patients for complications obtained by record linkage. The Inflammatory Bowel Disease cohort samples had been collected already under the supervision of Professor Jack Satsangi from patients attending gastroenterology clinics in NHS Lothian. Results from this cohort have been previously published, with extensive phenotype data obtained by case note review[148].

2.7 Statistical Analysis

Two-tailed independent student t-tests were applied for between group comparisons of normally distributed data. Results are displayed as mean ± standard deviation (SD). A Mann Whitney U test (MWU) was applied when the variables were not normally distributed, with results given as median (interquartile range IQR). Comparison of proportions was performed using the Chi-square test of independence, or Fishers Exact test for categorical variables where expected values in any cell of the contingency table are less than 5, with results displayed as frequency (percentages). Linear regression modelling was performed to identify significant predictors of bone density at the spine and the hip, with model variables entered either as categorical variables such as sex, or continuous variables such as age, weight, height or OPG antibody concentration. Regression diagnostics were performed in minitab with the distribution of response variables and residuals of the models visually inspected, and tested for normality using the Anderson-Darling test. Histograms of model variables were visually inspected to identify outliers and assess for normality. Correlation testing for non-normally distributed data was performed using Spearman's rank test on SPSS. All p-values of <0.05 were considered significant.

Statistical analysis was performed using Minitab version 16 (Minitab Inc., Pennsylvania, US) or the Statistical Package for Social Services version 19 (SPSS IBM Corp, NY State, US).

Chapter 3: Severe osteoporosis due to neutralising autoantibodies to Osteoprotegerin

3.1 Abstract

3.1.1 Background

Osteoporosis is a recognized complication of coeliac disease which is generally considered to be secondary to malabsorption of calcium, vitamin D and other nutrients. This study describes the occurrence of severe osteoporosis in a patient with coeliac disease who had developed neutralising antibodies to OPG.

3.1.2 Patient, Methods and Results

A 40 year old man presented with severe osteoporosis with a BMD T score at the lumbar spine of -6.6; a low trauma fracture of the clavicle and raised biochemical markers of bone turnover about 20 times the normal range. Investigations revealed evidence of coeliac disease and primary hypothyroidism but other causes of osteoporosis were excluded. He was advised on a gluten-free diet, and prescribed calcium and vitamin D supplements as well as thyroxine replacement, but the osteoporosis progressed with further bone loss and the development of fragility fractures of the spine and humerus. Good compliance with his gluten free diet was confirmed on a repeat duodenal biopsy. On further investigation, autoantibodies to OPG were detected in the patient's serum by an immunoprecipitation assay and the immunoglobulin fraction from patient's serum blocked the inhibitory effect of OPG on RANK signalling *in vitro*. No evidence of OPG autoantibodies was found in 10 controls or 14 patients with hypothyroidism but autoantibodies to OPG were detected in 3/15 unselected patients with coeliac disease.

3.1.3 Conclusion

These studies demonstrate the presence of neutralising autoantibodies to OPG in a patient with high bone turnover osteoporosis, and raise the possibility that OPG antibodies may contribute to the development of osteoporosis in coeliac disease.

3.2 Case report

A 40-year-old Caucasian man, previously in good health, presented with a low trauma fracture of the left clavicle sustained in a trial of strength with his 13-year-old son. He had no previous history of fracture despite having played rugby during his 20s and 30s. DEXA performed using a Hologic QDR4500 densitometer detected low levels of BMD with a T score of –6.6 at the spine (L1–L4) and –2.9 at the femoral neck. Routine investigations showed an elevated total alkaline phosphatase (ALP) (2610U/L; normal 25-120U/L), an elevated serum phosphate (2.36mmol/L; normal 0.8–1.4mmol/L) but normal serum calcium, albumin, urea and electrolytes, liver function tests and full blood count. Isoenzyme studies showed that the raised ALP was of bony origin. Serum PTH was low (8ng/L; normal 10–65ng/L), and serum 25(OH)D was 33nmol/L (normal 25–150nmol/L). A short synacthen test was normal. He was screened for primary hypothyroidism since he had experienced cold intolerance and lack of energy over the 12 months prior to presentation. Serum free thyroxine was <5pmol/L (normal 10–20), TSH was raised (>65 mU/L; normal 2-5mU/L) and anti-thyroid peroxidase antibodies were detected (243u/ml; normal 0–82u/ml). Tests for TSH receptor blocking antibodies[186] were negative. Serum testosterone and gonadotrophins were normal. He was commenced on L-thyroxine 100mcg daily, but ALP levels increased further to 3595U/L and hypercalcaemia developed (2.8mmol/L; normal 2.1–2.6mmol/L). At this point serum PTH and 1,25(OH)2D3 were undetectable and urinary calcium/creatinine ratio was elevated (4.78; normal <0.5) consistent with a resorptive mechanism of hypercalcaemia[187]. The hypercalcaemia resolved with intravenous rehydration. A transiliac bone biopsy was performed without tetracycline pre-labelling. This showed high bone turnover and woven bone (Figure 3.1a); the extent of osteoid seams was increased but thickness was normal (Figure 3.1b). Investigations were performed to exclude occult malignancy including bone marrow biopsy, CT scan of chest, abdomen and pelvis and measurements of serum PTH-related protein but the results were normal. A radionuclide bone scan showed a generalised increase in tracer uptake but no focal lesions (Figure 3.1c). Titres of transglutaminase IgA antibodies were raised (101u/L; normal 5-30u/L) and occult coeliac disease was confirmed by small bowel biopsy.

Treatment was commenced with a gluten-free diet, ergocalciferol 10,000 units daily and calcium supplements (1g/day). This decreased ALP to about 1,000U/L over

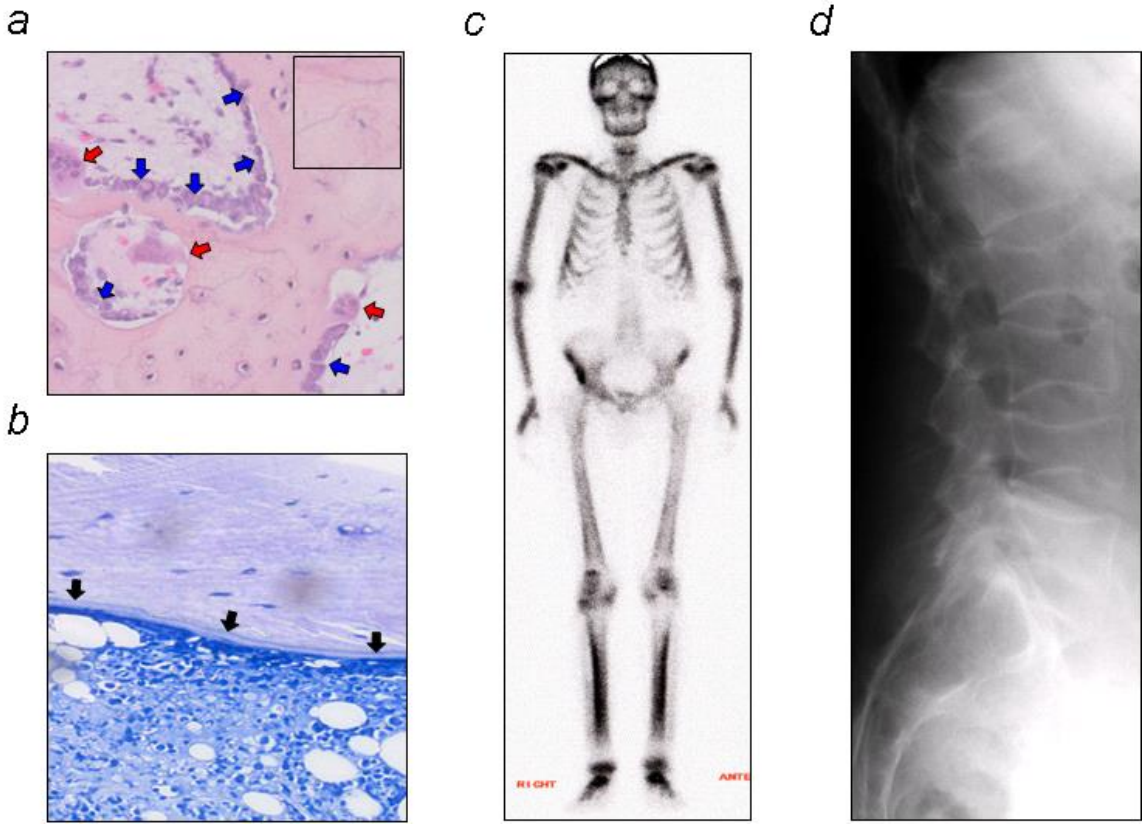

Figure 3.1 Clinical and histological features of the patient
Panel a. Photomicrograph of transiliac bone specimen stained with haematoxylin and eosin showing the increase in osteoclast numbers (red arrows) and osteoblast numbers (blue arrows). Woven bone is present throughout the biopsy as evidenced by the irregular cement lines. The inset shows a higher power view, illustrating the irregular cement lines. Panel b. Photomicrograph of transiliac bone specimen stained with toluidine blue illustrating increased extent of osteoid seams of normal thickness. Panel c. Radionuclide bone scan showing generalised increase in tracer uptake, but no focal lesions. Panel d. Radiograph of the lumbar spine showing osteopenia and multiple vertebral compression fractures

a period of 6 months, but the osteoporosis deteriorated with an 8% decrease in spine BMD to a T-score of -7.1 (Figure 3.2a). He suffered a low trauma fracture of the left humerus and 6cm height loss due to multiple vertebral fractures (Figure 3.1d) despite

the fact that repeat duodenal biopsy showed normalisation of bowel histology and serum 25(OH)D3 levels were normal (68nmol/L). Serum OPG was measured by ELISA (Biomedica, Oxford Biosystems, Oxford UK) on two occasions approximately 4 weeks apart and levels were 0.78 and 0.47pmol/L respectively (normal 0.14–130). Serum total RANKL levels measured by ELISA (Apotech, Epalinges, Switzerland) at the same time points were 0.152 and 0.143nmol/L respectively (normal 0–10).
Urinary deoxypyridinoline(DPD)/creatinine values were measured at this point and were about 20 times above the upper limit of normal (93nmol/mmol creatinine; normal 2.3–5.4). Alkaline phosphatase normalised following treatment with a gluten-free diet, calcium and vitamin D, but urinary DPD remained grossly elevated.

3.3 Differential diagnosis

A number of potential diagnoses were considered. An inherited form of osteoporosis was excluded by the late onset of the disease and the fact that the patient had never previously sustained a fracture despite leading an active lifestyle, for example regularly playing rugby whilst in his 20s. Osteoporosis and osteomalacia are known complications of coeliac disease due to malabsorption and the effects of calcium and vitamin D deficiency[161, 188]. The severity of the osteoporosis and dramatic elevation in bone turnover observed in this patient is out of keeping with that usually observed in coeliac disease however [161, 188, 189], and the patient's failure to respond to a gluten-free diet, and calcium and vitamin D supplements, argued strongly against coeliac disease as the primary cause of the bone disease. Whilst extensive seams of osteoid were observed on his bone biopsy these were of normal thickness, unlike the thickened osteoid seams expected in osteomalacia. It would be most unusual for a patient with osteomalacia to develop hypercalcaemia, and again the patient failed to respond to effective therapy for osteomalacia.

Fibrogenesis imperfecta ossium (FIO) was also considered since it presents in adulthood with fragility fractures and a mineralisation defect[190]. The clinical features in our patient were quite distinct from those described in FIO however, which is characterised by trabecular thickening on radiographs, accumulation of thick osteoid

on bone biopsy and a poor response to treatment. It was difficult to reconcile the development of autoimmune hypothyroidism with his high bone turnover state since increased TSH would be expected to suppress bone turnover[164]. We therefore speculated that the patient might have developed inhibitory antibodies to the TSH receptor. We looked for evidence of such antibodies using the methods of Minich *et al*[186] but these results were negative.

The severity of the bone disease and clinical deterioration despite treatment of the coeliac disease and supplementation with calcium and vitamin D was matched only by the remarkable recovery that occurred in response to treatment with the potent inhibitor of osteoclastic bone resorption, zoledronic acid. These observations underscored the importance of elevated bone turnover as the primary cause for this patient's osteoporosis and would be compatible with an acquired defect of OPG. This coincided with the development of autoantibodies against thyroid peroxidase and tissue transglutaminase.

The high turnover osteoporosis, elevation in ALP and fragility fractures were consistent with the reported phenotype seen in mice with targeted inactivation of the gene encoding OPG [106] and in humans with juvenile Paget's disease who have inactivating mutations in OPG [126, 182]. Further studies were therefore initiated to determine the cause of the increase in bone turnover focusing on the possibility that he might have developed neutralising antibodies to OPG, in view of the high bone turnover and autoimmune diathesis.

3.4 Identification of OPG autoantibodies

The patient's serum immunoprecipitated OPG, reflected by appearance of a strong band at 55Kd on the Western blot (Figure 3.2 **a** and **b**, arrows lane 2). Sera from 10 healthy controls and 14 patients with primary hypothyroidism yielded negative results (representative blot shown Figure 3.2 panel **a**), but 3/15 samples from patients with coeliac disease yielded positive results, albeit with lower intensity than the index case (Figure 3.2 panel **b**, lanes 10-12). Equal loading of the samples was confirmed by probing the same blots for total immunoglobulin (lower half of each panel, labelled anti human IgG). The immunoprecipitation assay was repeated in the presence of gliadin, but this had no effect on the ability of the index patient's serum

to immunoprecipitate OPG suggesting that the OPG autoantibodies did not cross react with gliadin.

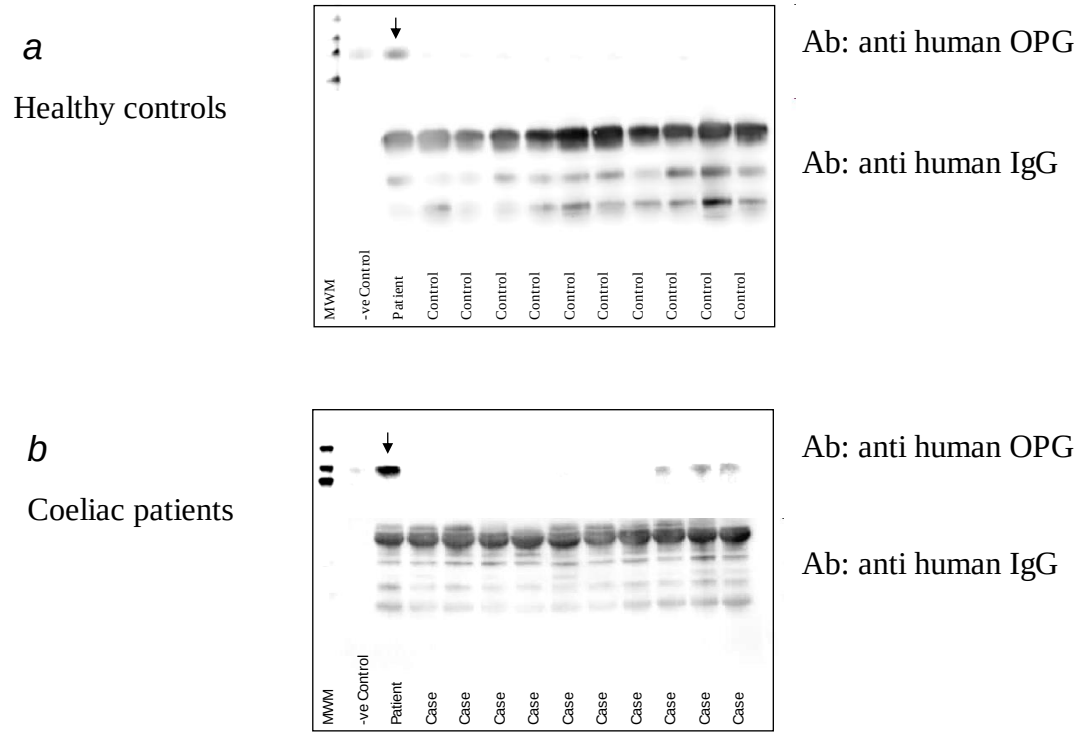

Figure 3.2 Identification of OPG antibodies by immunoprecipitation
Figure 3.2a The top panel shows the presence of autoantibodies directed against OPG in the patient's serum (lane 2- arrow), reflected by the detection of a strong ~55 Kd band on western blot by an anti-OPG antibody following immunoprecipitation. Lane 1 shows a negative control. Samples from healthy controls (lanes 3-10) showed no evidence of OPG antibodies. Figure 3.2b again shows a robust ~55Kd band recognised by anti-OPG antibody following immunoprecipitation by patient serum (lane 2). In addition 3/15 samples from patients with coeliac disease also showed the 55Kd band consistent with anti-OPG antibodies (lanes 9–12). In each case the lower panel is stained for immunoglobulin and confirms equal loading of the gel. The result shown is representative of three independent experiments. Molecular weight markers of 80, 60 and 50kDa are shown (lane MWM).

3.5 Functional inhibition of OPG by patient immunoglobulins

The ability of immunoglobulins purified from the index patient's serum to overcome the activity of OPG was next assessed in a cellular assay. Immunoglobulins were purified on protein G spin columns to avoid any non-specific serum effects on the cells and a final dilution of 1 in 40 used (Methods 2.2.1). Functional inhibition of RANKL signalling by OPG was demonstrated in a HEK293 cell line stably expressing a NFκB luciferase reporter (protocol described in detail in Methods 2.2.3) (Figure 3.3).

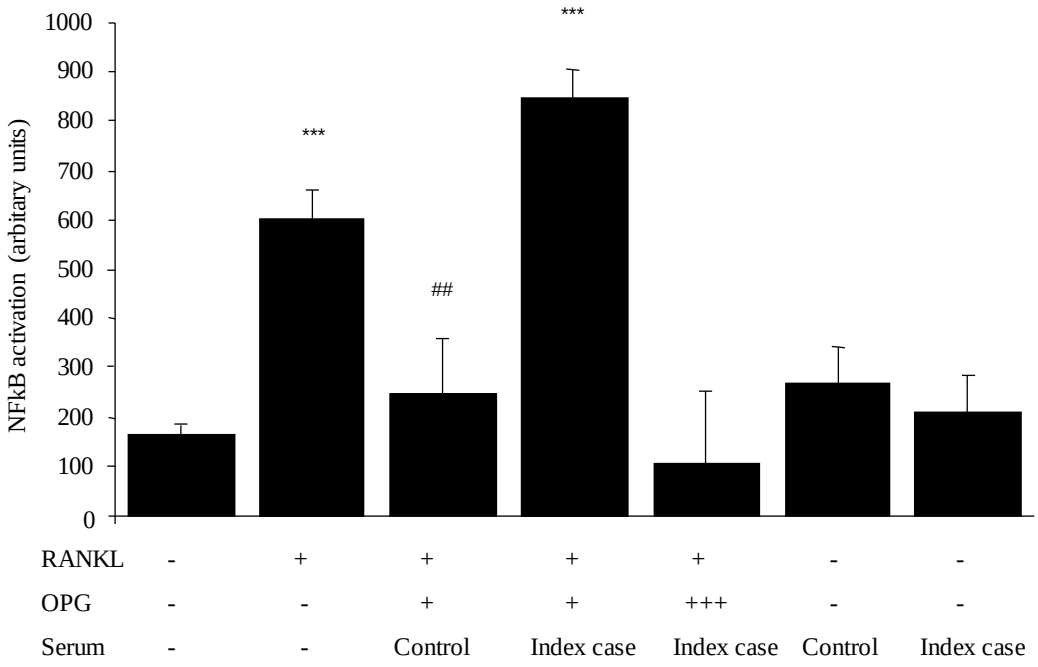

Figure 3.3 Functional inhibition of OPG by patient serum
Patient serum, but not control serum abrogates the inhibitory effect of 100ng/mL OPG on RANKL stimulated NFκB *activation in HEK293 cells. Addition of 400ng/mL OPG (indicated +++) overcame the inhibition. *** p<0.001 from vehicle; ## p<0.01 from RANKL and from RANKL+ OPG + patient serum. The result is representative of three independent experiments.*

The addition of RANKL to the cell line at a concentration of 100ng/ml caused robust activation of reporter gene expression. This was inhibited by human recombinant

OPG at a concentration of 100ng/ml in the presence of the immunoglobulin fraction from control serum, but in the presence of immunoglobulins purified from the index case's serum, the inhibitory effect of OPG was lost. Addition of OPG at a higher concentration (400ng/ml) overcame the inhibition. Addition of immunoglobulin fractions from the patient and a control in the absence of RANKL had no significant effect on reporter gene expression.

3.6 Progress of index case

Following his bone biopsy which confirmed severe high bone turnover osteoporosis he was treated with three monthly infusions of zoledronic acid which normalised his markers of bone turnover (Figure 3.4). Following the first infusion, serum calcium decreased to 1.91mmol/L and this was accompanied by an elevation in PTH to 163 ng/L and 1,25(OH)2D3 to 992pmol/L(normal 15–150pmol/L). No symptoms of hypocalcaemia were reported. Subsequently, serum calcium, PTH, 1,25(OH)2D3, ALP and urinary DPD/creatinine ratio returned to normal. When he was reviewed 42 months after the original presentation, no further clinical fractures had occurred; his height had remained stable and there was no evidence of progression of the vertebral fractures; the spine BMD T-score had increased to –1.7, the femoral neck T-score to –0.8 (Figure 3.4a) and levels of ALP and urinary DPD were normal (Figure 3.4b).

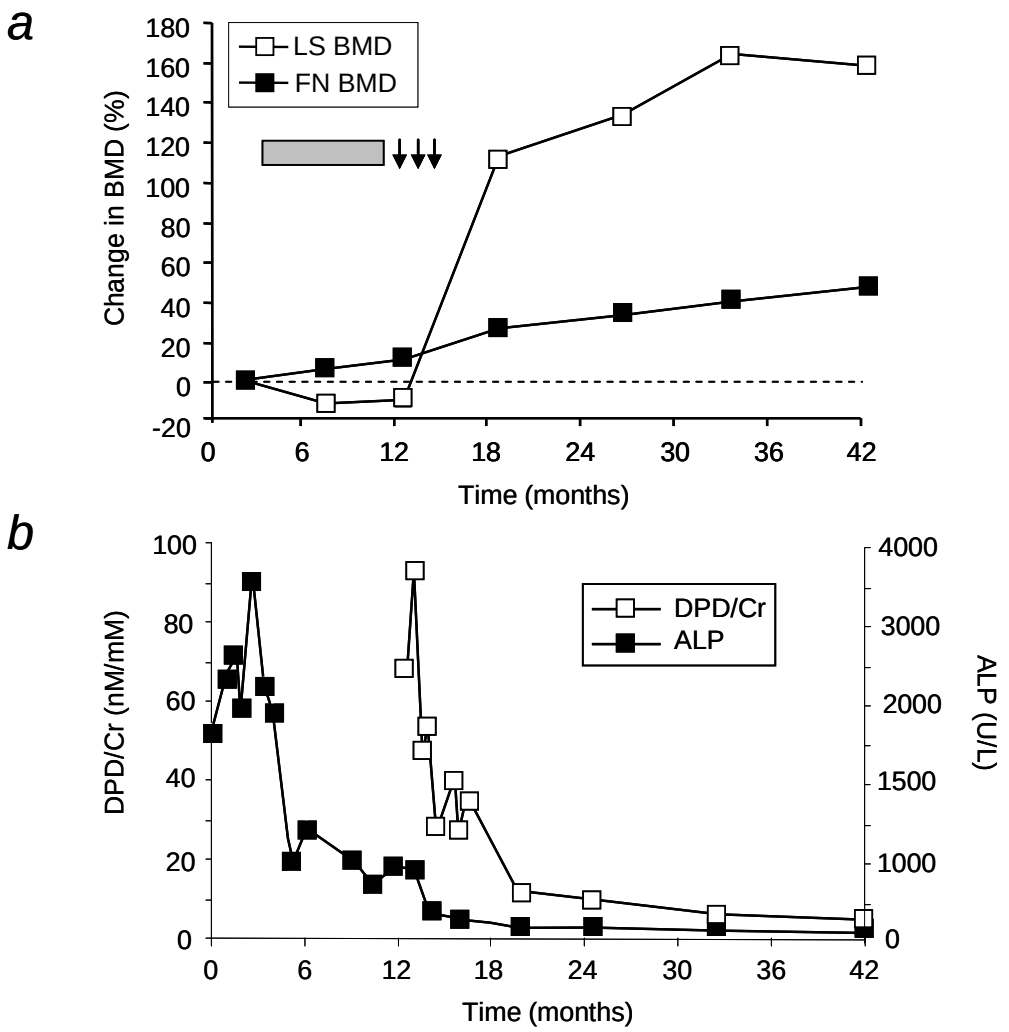

Figure 3.4. Bone density, biochemical markers and response to treatment
Panel a) Lumbar spine and femoral neck BMD at presentation and in response to treatment. Lumbar spine BMD (LS-BMD) decreased by about 8% despite an extended period of treatment with a gluten-free diet, calcium and vitamin D (grey bar), but BMD progressively increased at both the spine and femoral neck (FN-BMD) following treatment with zoledronic acid (arrows). Panel b) Urinary DPD and ALP levels at presentation and in response to treatment. Serum ALP levels decreased from over 3000U/L to about100 U/L

The index patient has remained under regular follow up since his initial presentation. He has kept in good health overall with no further fractures. Bone turnover has remained well controlled with no recurrence of hypercalcaemia. Two years after his

presentation, a minor rise in ALP was noted associated with non-specific symptoms of arthralgia and malaise for which he received an infusion of 5mg zoledronate (Aclasta) that was effective in alleviating symptoms and restoring normal ALP. At this time he was also screened for the presence of vascular calcification with a CT scan of chest/abdomen/pelvis which revealed mild calcification in the carotid, abdominal and iliac arteries. After a further 2 years he once again developed minor elevation of ALP and on this occasion in view of the mechanism of his disease, as well as the known association of OPG deficiency with vascular calcification, the decision was made to switch his treatment to subcutaneous denosumab (Prolia). This is a monoclonal antibody blocking RANKL and was given in the usual osteoporosis treatment regime of 60mg every 6 months for a period of 2.5 years. Over this time he developed modest elevation of ALP and symptoms of arthralgia and malaise that responded only temporarily to denosumab injections. At his most recent attendance the decision was taken to treat with intravenous zoledronate (Aclasta) once again (Figure 3.5).

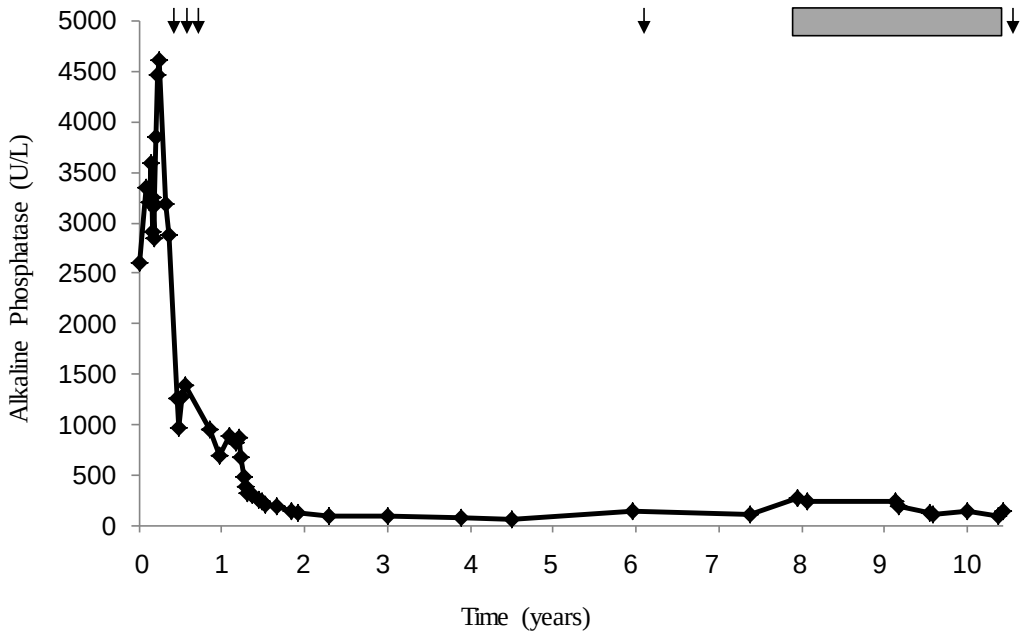

Figure 3.5 ALP levels in index case from presentation to most recent attendance. Treatment pulses of iv zoledronate indicated by vertical arrows, 6 monthly subcutaneous denosumab indicated by grey box.

The remarkable improvement that was seen in BMD has been maintained over the last five years of follow up (Figure 3.6). An ELISA assay for OPG antibodies has been developed (full details of the protocol in Section 2.3.5: ELISA II) and using this assay in frozen serum samples from a variety of time points it is interesting to note that high levels of antibody are maintained throughout this time. Indeed the highest level is seen on the most recently obtained sample.

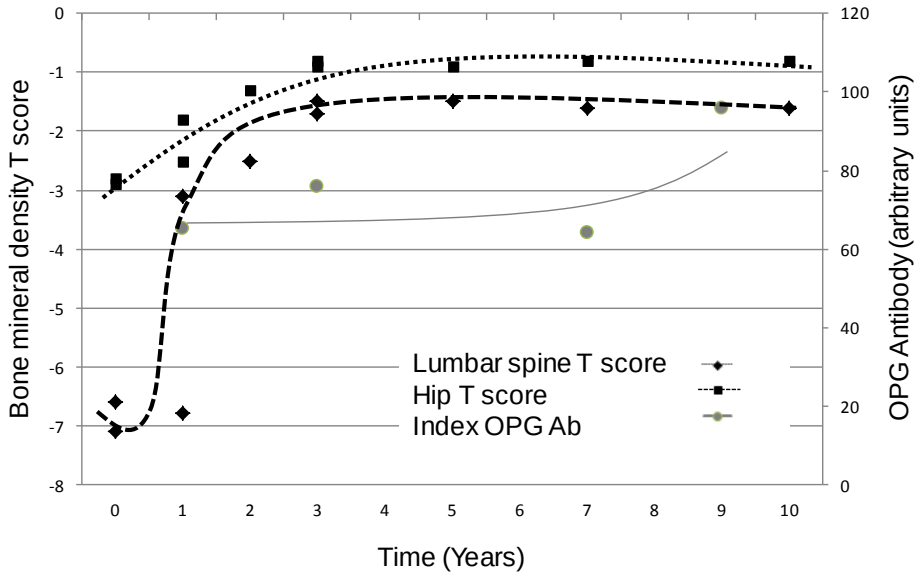

Figure 3.6 Time course of bone density up to present day. Lumbar spine bone density T scores are marked with black squares (▪), Hip bone density T scores with black diamonds (♦) and levels of OPG antibody by ELISA (right hand scale in arbitrary units) in grey circle (●).

3.7 Summary and Discussion

The patient described here presented in adulthood with severe, high turnover osteoporosis associated with subclinical coeliac disease and autoimmune hypothyroidism. The patient had circulating antibodies to OPG and immunoglobulins purified from the patient's serum, but not control sera, abolished the inhibitory effect of OPG on RANKL-induced NFκB signalling *in vitro*, consistent with the presence of neutralising antibodies to OPG. No evidence of circulating antibodies to OPG was found in sera from 10 healthy controls and 14 patients with autoimmune hypothyroidism, but antibodies were detected in 3 out of 15 patients with coeliac disease.

This is the first report of a bone disease occurring in association with the spontaneous development of antibodies to OPG. Whilst one patient has been described in whom treatment with a recombinant immunoglobulin Fc region-OPG construct led to the development of autoantibodies to the fusion protein, this did not result in a clinical illness [191]. The mechanism by which OPG antibodies developed in the patient described here remains unclear, but autoantibodies to other circulating proteins have been reported to develop in patients with autoimmune disease [192] which is also the case here.

The patient described is unusual in many respects. His osteoporosis was extreme with bone density T score falling to a nadir of -7.1 in the spine and multiple vertebral fractures resulting in height loss of 6cm. Very high bone turnover was confirmed both on bone biopsy and in marked elevation of calcium, alkaline phosphatase and urinary deoxypyridinoline. Unlike many patients with coeliac disease there was no improvement in his bone density with a gluten-free diet and calcium and vitamin D replacement, yet his response to treatment with the anti-resorptive zoledronate (Aclasta) was astonishing. This raises the possibility that the identification of OPG antibodies in other coeliac patients might justify a more aggressive approach to the management of osteoporosis in these patients.

Another lesson is in the very high level of OPG antibody observed in the most recent sample assayed from the index patient. Whilst it is possible that the delay in processing the stored samples may have led to sample degradation, these samples were all stored at -80˚C and it would normally be assumed that antibodies are stable in such conditions. This demonstrates at least that for some patients antibody persists even after treatment of associated autoimmune conditions. In turn, the persistence of OPG antibodies in the index case raises a number of cautions in interpreting the clinical significance of OPG antibodies. Firstly the response to treatment in the index case occurred despite persistently high OPG antibody levels. This does suggest that care must be taken in interpreting the association of BMD with presence of OPG antibodies in patients that have received anti-resorptive therapies. Such difficulties

are likely to make it more difficult to demonstrate an association between bone density and OPG antibodies in patients who have received treatment. This will be of most relevance in an osteoporosis cohort, though could attenuate associations seen in the coeliac populations too. It emphasises the importance of building a prospective cohort of patients in order to properly assess the evolution of bone disease associated with OPG antibodies.

The immunoprecipitation assay also demonstrated the presence of anti-OPG antibodies in 3/15 coeliac patients studied. Whilst these observations raised the possibility that OPG antibodies might contribute to the pathogenesis of osteoporosis in coeliac disease more generally, the observations should be interpreted with caution since BMD is a complex trait which is influenced by many genetic and environmental factors. Overall these findings justify further research to determine if OPG antibodies are associated with the development or severity of osteoporosis in patients with autoimmune disease or in ‘idiopathic’ osteoporosis, and in turn whether this insight into the mechanism of disease might influence response to treatment.

Chapter 4: Performance of assays for OPG antibodies

4.1 Abstract

4.1.1 Introduction

Neutralising antibodies to OPG have recently been identified using an immunoprecipitation assay and subsequently an ELISA. The suitability of these assays for population screening has not been characterised.

4.1.2 Materials and Methods

The immunoprecipitation assay uses the patient serum itself to precipitate recombinant OPG, with the protein then visualised by chemiluminescence on a Western blot (see Materials and Methods Section 2.1). An ELISA was developed using membrane bound OPG as a capture antigen. Two protocols were established the first using a commercial antibody to OPG to provide a standard curve (ELISA I - Section 2.3.3), and the second using serial dilutions of serum from the index case to derive a standard curve (ELISA II – Section 2.3.5). Full details of the patient populations screened are given in Section 2.6.

4.1.3 Results

A coefficient of variation of 50% was observed using the immunoprecipitation assay. An ELISA for OPG antibodies showed improved convenience of use, though still significant variation. ELISA I had an intra-assay variability of 11.1% and inter-assay variability of 30.4% in a cohort of 600 patients. ELISA II showed similar performance with an intra-assay variability of 12.9% and inter-assay variability of 21.8% in a cohort of 192 patients. Circulating OPG and RANKL do not affect the assay though repeated freeze thaw cycles do reduce assay reproducibility.

4.1.4 Conclusion

The immunoprecipitation assay was not suitable for population screening. The ELISA showed improved reproducibility and convenience. Whilst there remains variability particularly in inter-assay reproducibility, this appears less of an issue in positive samples.

4.2 Reproducibility of immunoprecipitation assay

OPG antibodies were first identified using an immunoprecipitation assay in which the test serum itself immunoprecipitates recombinant OPG from solution, and then a commercial anti-OPG antibody is used to label any precipitated protein on a Western blot. Using this approach, serum from patients with coeliac disease (n=46), multiple sclerosis (n=20), rheumatoid arthritis (n=10), thyroid disease (n=14) and severe osteoporosis (n=10) were screened for the presence of OPG antibodies (representative western blots shown in Figure 4.1).

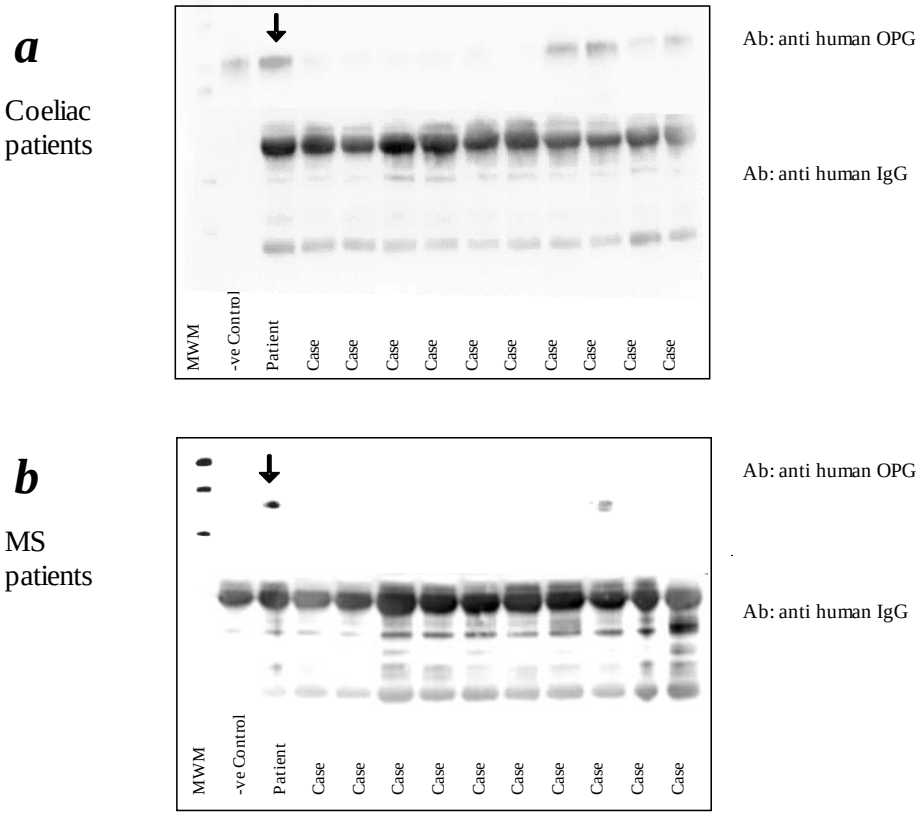

Figure 4.1 Identification of OPG antibodies by immunoprecipitation from patients with coeliac disease (a) and multiple sclerosis (b). OPG immunoprecipitated by serum from the index case (highlighted by arrow) was used as a positive control in each set of samples assessed. Protein loading was assessed by reprobing with labelled antibody against human immunoglobulin (lower part of image).

Using this technique, evidence of OPG precipitation was seen in serum from 15/46 (33%) patients with coeliac disease, 2/10 (20%) patients with rheumatoid arthritis,

1/10 (10%) patients with hypothyroidism and 8/10 (80%) patients with severe osteoporosis (defined as having bone mineral density T score less than -3.5).

Whilst the technique has an attractive simplicity in concept there are substantial difficulties in interpreting these results. A weak positive band of OPG was often observed in the negative control in the absence of serum and despite pre-incubation of the agarose beads with albumin (Figure 4.1 a, first column) indicative of non-specific binding of OPG by the agarose beads. This effect appears attenuated by use of a serum sample from a patient known to be negative for OPG antibodies (Figure 4.1 b, first column) but still raises the possibility of false positive tests using this technique. Despite standardisation of the protocols for protein loading and transfer, as well as duration of chemiluminescence exposure, the observed intensity of bands seen is highly variable undermining attempts at quantification of the signal seen (as seen in the arrowed bands in 4.1a and 4.1b). Expressing band intensity as a percentage of the signal seen in the positive control and with correction for protein loading was attempted but marked variability in the band intensity measured was seen. The inter-assay coefficient of variation in 10 coeliac samples was measured at 48%, with no improvement in the coefficient of variation (CV) observed by increasing the number of replicates to five. Hence although these results give an indication of OPG recognition, it is difficult to provide any confident estimate of prevalence of OPG antibodies.

4.3.1 Co-efficient of variation of ELISA protocol I

Serum from the index patient was included on every ELISA plate to act as a positive control, alongside serum from a patient known to be negative for OPG antibodies. The results of these quality control standards, as well as illustrative results for a sample of intermediate positivity are given in Table 4.1. Samples were analysed in duplicate wells, and on duplicate plates. In preliminary experiments very reasonable intra-assay variability of between 1 and 4% was noted for all quality controls, but a substantially higher inter-assay variability across all the samples of between 11 and 21%.

Stratification	OPG Ab ng/µl (Rep 1)	OPG Ab ng/µl (Rep 2)	Intra-assay CV %	Inter-assay CV %
Low	28.9 (±1.1)	34.1 (±1.1)	3.9, 3.3	11.6
Medium	227.6 (±0.7)	317 (±12.3)	0.31, 3.87	23.3
High	364 (±5.7)	490 (±1.7)	1.57, 0.36	20.9

Table 4.1 The effect of OPG antibody titre on coefficient of variation in ELISA protocol I. Assays were performed in duplicate on consecutive days.

4.3.2 Effect of freeze thaw cycles on ELISA I performance

The effects of repeated freeze thaw cycles on the results of OPG ELISA I were analysed in samples from the IBD cohort. Table 4.2 shows the baseline concentration of OPG antibody in a negative control, a weakly positive sample and serum from the index case. There is evidence of some degradation of the signal with repeated freeze thaw cycles which appears more marked in the sample with the lowest concentration of OPG antibody.

Stratification	OPG Ab (ng/µl)	% change d1 to d2	% change d2 to d3
Low	37.5 (±13.4)	-9.040	-60.173
Medium	227.5(±0.7)	+39.560	-19.0551
High	376.9(±32.4)	+31.464	-19.8789

Table 4.2 The effect of repeated freeze thaw cycles on the measured OPG antibody concentration using ELISA I. Assays were performed in duplicate on consecutive days with overnight freezing at -80ºC.

A further illustration of the adverse effects of multiple freeze thaw cycles was obtained by comparison of results in 38 samples that were sent to another lab for analysis of bone turnover markers. In this process samples underwent three freeze thaw cycles as well as being kept at 4˚C whilst being analysed. Comparison was made between samples analysed directly on defrosting of an original aliquot with these degraded samples. No correlation between the measured concentrations of

antibody were seen (Figure 4.3, R^2 =1%, p=0.552). A significant increase in the mean OPG antibody concentration was observed in the degraded samples (mean OPG antibody concentration 56.28 ± 33.122ng/µl compared to 29.94 ± 25.45ng/µl, p<0.001) which may represent contamination of the samples.

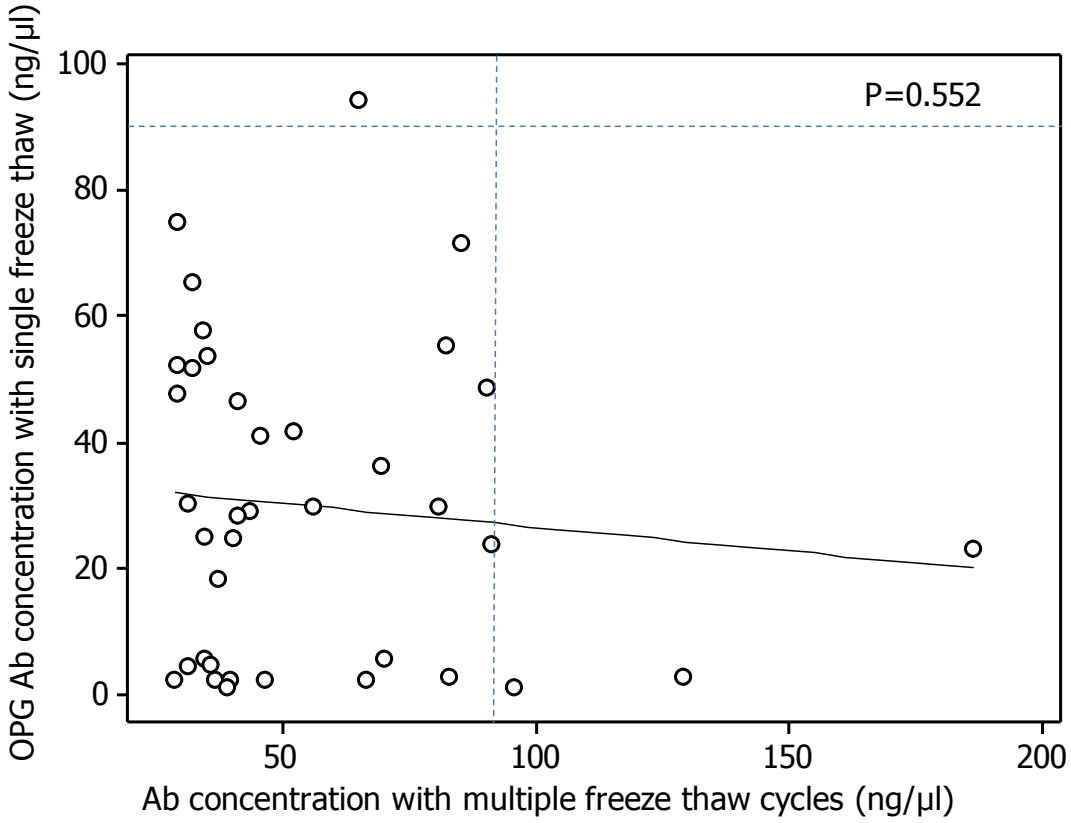

Figure 4.3 Effects of multiple freeze thaw cycles. No correlation observed between concentration of OPG antibody detected by ELISA I after repeated freeze thaw cycles. Most samples are below the threshold for a positive OPG antibody (marked by dotted line).

4.3.3 Effect of circulating RANKL/OPG on OPG antibody ELISA I

It is clearly possible that circulating OPG in the serum samples could compete with the capture OPG used in the assay, or that circulating sRANKL might recognise bound OPG and also interfere in the assay. To investigate this possibility we used a commercial ELISA for serum OPG and sRANKL to test a selection of serum samples for OPG and RANKL concentrations (Methods Section 2.4.1 to 2.4.3) Neither increasing OPG nor RANKL concentrations were associated with a reduction in the measured levels of OPG antibody by ELISA I. On the contrary a

non-significant trend to increasing levels of OPG antibody in those samples with increased serum OPG concentrations was observed (Figure 4.4a, p=0.068) and with increased levels of total RANKL (Figure 4.4b, p=0.033).

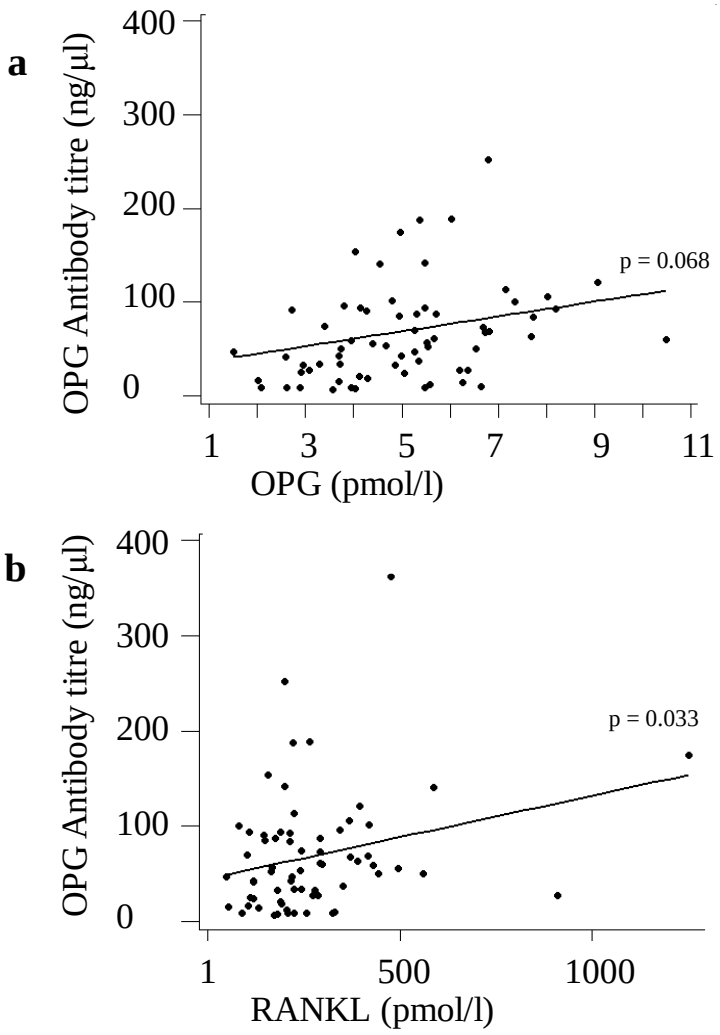

Figure 4.4 Correlation of OPG antibody concentration (ELISA I) with serum levels of circulating OPG (a) or total RANKL (b)

One commercial ELISA for free sRANKL uses OPG as a capture antigen (Biomedica BI-20452). A number of samples in this assay had very low, or even undetectable levels including serum taken from the index case which suggests that there might be interference by OPG antibodies on the performance of this ELISA. We also measured the performance of this assay in the same set of serum samples (Figure 4.5).

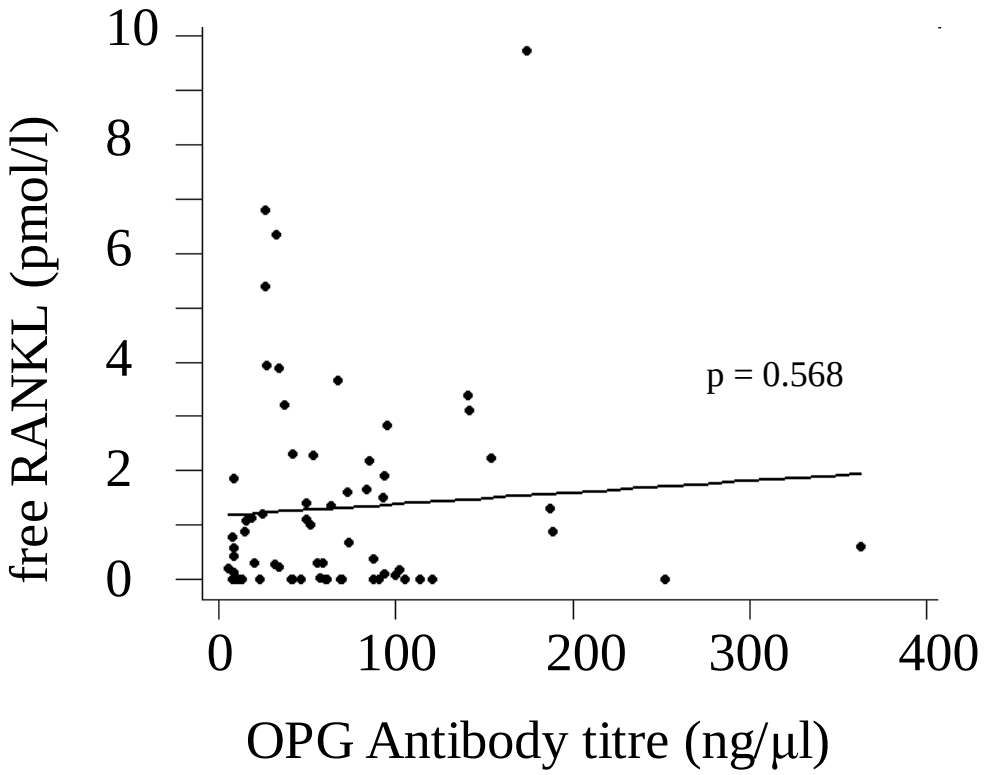

Figure 4.5 Correlation of OPG antibodies measured by ELISA I with serum levels of free RANKL.

No trend of any significance is observed in these samples (p=0.568). This is perhaps unsurprising given that most of the samples have low levels of OPG antibodies, but from this data it can be concluded that OPG antibodies are not a common cause of low or undetectable free RANKL in this assay.

4.3.4 Comparison of serum and plasma with ELISA I

Samples of plasma and serum samples taken at the same visit from 20 patients attending the rheumatology department were compared. The mean OPG Ab concentration measured did not differ significantly between the two samples (mean concentration in serum samples 60.2 ± 71.7ng/µl compared to plasma samples 51.8 ± 70.3ng/µl, p=0.265). A highly significant correlation between the values obtained in plasma and serum was seen (r^2=80.9%, p<0.001, Figure 4.6) suggesting that both sample types can be used.

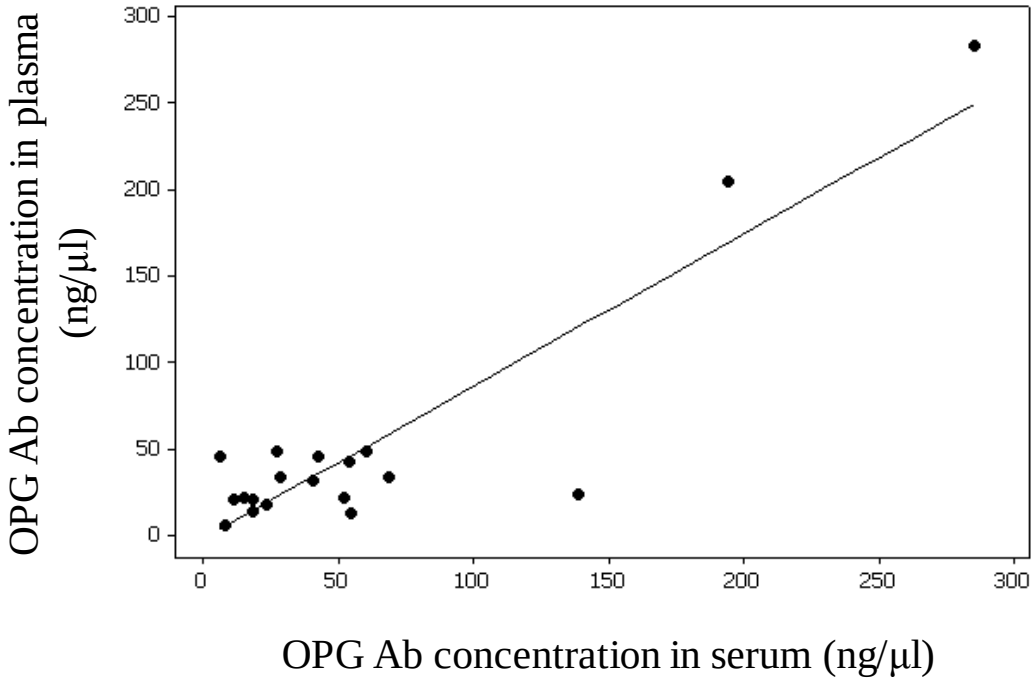

Figure 4.6 Correlation of OPG antibody concentration measured by ELISA I in plasma and serum.

4.4 Coefficient of variation of ELISA protocol II

In the revised version of the ELISA serum from the index patient was again included on every ELISA plate to act as a positive control, alongside serum from a patient known to be negative for OPG antibodies. The results of these quality control standards, as well as an illustrative result for a sample of intermediate positivity are given in Table 4.3. Samples were analysed in duplicate wells, and on duplicate plates. For positive samples a reasonable intra-assay CV of 1.1 to 8.2% is noted, and improved inter-assay CV of 11.5 to 12.7%. Higher variation is noted in the negative control sample presumably reflecting a greater influence of non-specific signal, and the inherent increase of CV with reduced mean sample values.

Stratification	OPG Ab ng/µl (Rep 1)	OPG Ab ng/µl (Rep 2)	Intra-assay CV %	Inter-assay CV %
Low	8.3 (±0.6)	6.7 (±1.1)	7.2, 16.4	15.1
Medium	30.3(±1.5)	25.3(±2.1)	5.0, 8.2	12.7
High	90.7(±1.2)	106.7(±1.2)	1.3, 1.1	11.5

Table 4.3 The effect of OPG antibody titre on coefficient of variation in ELISA protocol II. Assays were performed in duplicate on consecutive days.

4.5 Summary of ELISA characteristics

For reference a summary of the characteristics of the two iterations of the ELISA assay are presented in Table 4.3.

Characteristic	ELISA I	ELISA II
Standard curve	Polyclonal rabbit anti OPG	Dilution of serum from index case
Units	ng/µl	RU (relative units)
Threshold for positive sample	91ng/ul	14.3 RU
Value of positive control	364 to 490 ng/ul	90.7 to 106.7 RU (Standard 100RU)
Intra-assay CV	Low 3.3 to3.9% High 0.36 to 1.6%	Low 7.2 to 16.4% High 1.1 to 1.2%
Inter-assay CV	Low 11.6% High 20.9%	Low 15.1% High 11.5%

Table 4.3 Summary of characteristics of ELISA protocols I and II.

4.6 Discussion

Whilst the immunoprecipitation has an attractive simplicity in concept in practice there was high variability in the intensity of bands despite attempts to standardise the

assay, as well as concerns about false positive signals. Increased signals were seen in a small number of patients with severe osteoporosis as well as in the coeliac patients tested but it is difficult to quantify the levels of OPG antibody in these populations given the limitations of the assay. In practical terms since it takes 48 hours to perform the assay in just 10 samples it would never be a suitable assay to use in screening of large populations and in view of all these limitations attention turned to developing a high throughput and quantifiable assay.

Initially an indirect ELISA approach was adopted using commercial labelled anti-OPG antibodies to provide a signal that test serum samples would compete out. Proof of principle was established with clear suppression of signal seen with serum from the index case (Section 2.3.1). A standard curve was constructed using unlabelled commercial anti OPG but even with very high levels of this antibody complete suppression of the background signal could not be achieved. Unfortunately even after optimisation of the concentrations of OPG, and the quantity and type of primary antibody used, it became clear that this assay would lack the dynamic range needed to identify any but the most strongly positive of test samples.

Subsequently a direct ELISA was developed. Using the lessons learned from the indirect assay, an assay was developed that was able to show greater than 10 fold increase in signalling with the positive control over negative serum samples, and appeared much more promising to use as a screening tool. No direct effect of serum OPG or sRANKL levels on the performance of the ELISA was observed. The performance of the assay did appear to be affected by repeated freeze thaw cycles with substantial variability observed already after one, and particularly after two, freeze thaw cycles. An apparent increase in the concentration of antibody seen after freeze thaw may simply reflect day to day variability in the assay performance seen particularly with predominantly negative samples, but does raise concerns about interpretation of results in such samples. As a result samples were only analysed after a single freeze thaw cycle.

A major challenge has been ensuring reproducibility of results using the direct ELISA. Refinements were made to the number of washes, the temperature and timing of labelling steps, the coating protocol as well as the plate reader algorithm itself. After optimisation ELISA I showed good *intra-assay* variability of approximately 0.4 to 3.9% but higher *inter-assay* variability of 11.6 to 20.9%. With the additional serum from the index case it was possible to create a standard curve using human immunoglobulin which avoids any criticism that having separate species of immunoglobulin in the test wells and the standard curve might have generated, as well as potentially removing a further cause in variation in day to day performance. In terms of reproducibility this assay performed similarly with average *intra-assay* CV of 1.1 to 16.4% and *inter-assay* CV of 11.5 to 16.1% overall.

There is an inherent difficulty in assaying predominantly negative samples. Results are more likely to be influenced by non-specific effects and there is an inherent inflation of CV as absolute values near zero. Consequently whilst it remains an aspiration to develop an assay capable of demonstrating excellent reproducibility in all samples, it is more realistic to aim to achieve reproducibility in the positive samples. Here results are more encouraging with the most recent results showing *intra-assay* variability of 1.1 to 1.2 % only and *inter-asssay* variability of 11.5%. In view of this observed variability all samples were measured on two separate days and assayed in duplicate.

High background levels of signalling were seen in both the direct and indirect assays for OPG. Whilst purification of immunoglobulins from the samples attenuated this effect so too did sample dilution, and for simplicity the latter approach was adopted. With either approach, there is some possible loss of sensitivity. The possible effects of circulating RANKL and OPG were assessed. There was no evidence of reduced OPG antibody detection in association with increased levels of these cytokines, with if anything, a trend to increased OPG antibody concentrations seen with increased levels of OPG and RANKL. This observation makes it most unlikely that circulating cytokines are having a significant effect on the performance of the assay (an

inherently plausible conclusion given the very low concentrations of circulating OPG and RANKL in human serum).

Importantly a positive ELISA result does not reveal the affinity or epitope specificity of the antibody identified. An attempt was made to develop a screening assay that would simultaneously allow identification and functional assessment but this proved unsuccessful (proximity bead based assay discussed in Appendix A4.1). Consequently whilst the direct ELISA results are useful for hypothesis generation in the populations screened, this information should ideally also be combined with a separate assessment of the functional activity of such antibodies.

Chapter 5: Prevalence and correlation with bone traits of OPG antibodies in a general population cohort

5.1 Abstract

5.1.1 Introduction

Cardiovascular diseases (CVD) and osteoporosis frequently co-exist, and epidemiological studies suggest both may share a common pathophysiological basis. OPG has been suggested as a link between these conditions (Section 1.3.4). Neutralising antibodies to OPG might play a pathogenic role in both osteoporosis and cardiovascular disease.

5.1.2 Materials and methods

Plasma was obtained from participants of the ORCADES study who have already been assessed extensively for CVD and osteoporosis (Section 2.6.1). OPG antibodies were identified using ELISA I (Section 2.3.4). Samples of serum from 20 volunteers with normal bone density were used to define a normal range (Section 2.3.3). Vascular calcification on the lateral DEXA image was scored according to validated methodology (Section 2.5).

5.1.3 Results

Raised levels of OPG antibody were found in 14/864 (1.6%) of the ORCADES population, similar to levels seen in healthy controls. No significant association between presence of OPG antibody and bone density or turnover was observed, but significantly higher vascular calcification scores were observed even after adjustment for age and sex.

5.1.4 Conclusions

OPG antibodies did not contribute significantly to osteoporosis in this population cohort. The association of OPG antibodies with vascular calcification is intriguing but requires replication in an independent cohort.

5.2 Prevalence of OPG antibodies in ORCADES population

An analysis was performed on 864 plasma samples taken from the ORCADES cohort using ELISA I. Analysis of the OPG antibodies was performed either taking the absolute level of OPG antibody as a continuous variable, or alternatively treating the presence of antibodies to OPG as a categorical variable. In the latter analysis presence of OPG antibody was defined as a titre of OPG antibody by ELISA greater than the mean OPG antibody level in healthy controls plus three standard deviations (91ng/µl). Within this cohort the prevalence of OPG antibodies was low at 1.6% (n=14) with the small sample size limiting the study's power to detect any effect. No significant difference in the titre of OPG antibody was observed between cases and controls (controls median OPG antibody level 23.7 (IQR 23.5), ORCADES cohort median OPG Ab level 27.3 (IQR 20.7), p=0.11). Characteristics of participants in the ORCADES study are presented in Table 5.1.

Characteristic	**High antibody level (n=14)**	**Normal antibody level (n=850)**	**p value**
Age	59(±11.6)	56(±14.0)	0.35
Sex	7 male(50%)	357 male(42%)	0.24
BMI	27.42 (±4.8)	28.15(±14.0)	0.98
Spine BMD Z score	0.33(±1.7)	0.44(±1.5)	0.72
Hip BMD Z score	0.40(±1.1)	0.56(±1.1)	0.77
Spine BMD T score	-0.68 (±1.8)	-0.47(±1.5)	0.66
Hip BMD T score	-0.34(±1.2)	-0.12 (±1.1)	0.71
Bone turnover (CTX) (n=350)	0.56 (±0.32)	0.56(±0.32)	0.99

Table 5.1 Characteristics of ORCADES participants by OPG antibody status

No significant differences were observed between participants with or without OPG antibodies (p values represent 2 sided student T test for continuous, or Chi square test for categorical variables). Similarly no association between OPG antibody titre and BMD was observed.

5.3 Regression modelling within ORCADES population

Linear regression modelling was performed with the response taken as Z scores of the spine and hip. Age, weight, height and OPG antibody concentration were included as continuous variables with sex included as a categorical variable (female sex assigned value of 0, male sex 1). Possible correlations between these factors and the concentration of OPG antibody were explored with no significant correlations observed (Table 5.2). Since OPG antibody concentration is not normally distributed a Spearman's rank correlation coefficient was calculated for the continuous variables. Very similar OPG antibody concentration levels were observed in both women (median concentration 27.8, interquartile range 20.3) and men (median concentration 25.6, interquartile range 21.1) with a MWU test suggesting there was no significant difference (p=0.19).

FACTOR	Spearman's rho	P value
Age (yrs)	0.052	0.13
Weight (kg)	-0.04	0.3
Height (cm)	-0.04	0.3

Table 5.2 No correlation observed between key variables and OPG antibody concentration

Linear regression modelling was then performed using Z scores of the spine and hip as the response variable, with the full results of univariate and multivariate modelling given in table 5.3. Univariate regression analysis within the ORCADES population found no association with either spine bone density Z-score (p=0.86) or hip bone density Z-score (p=0.86) with the presence of OPG antibodies (Figure 5.1). Multivariate regression analyses against BMD scores revealed expected significant associations for sex, age, height and weight, however there was still no association with OPG antibody titre in this analysis either at the spine (p=0.86) or the hip (p=0.66).

Although plasma was available in further participants of the ORCADES cohort, given the low prevalence of antibody in the population there was estimated not to be sufficient power to detect an effect. Even had we extended the analysis to all 1,584

available participants this is estimated to give only 41% power to detect a difference of 0.5 SD in bone density or turnover and this was not pursued.

FACTOR	Analysis	Outcome	β co-efficient	SE	P value
Age	Univariate	Spine Z score	0.0305	0.0036	<0.001
Gender	Univariate	Spine Z score	0.184	0.0522	<0.001
Weight	Univariate	Spine Z score	0.020	0.0027	<0.001
Height	Univariate	Spine Z score	-0.006	0.0039	0.12
OPG Ab	Univariate	Spine Z score	-0.0003	0.0020	0.86
Age	Multivariate	Spine Z score	0.0318	0.0034	<0.001
Gender	Multivariate	Spine Z score	0.5647	0.0614	<0.001
Weight	Multivariate	Spine Z score	0.0312	0.0029	<0.001
Height	Multivariate	Spine Z score	0.0230	0.0043	<0.001
OPG Ab	Multivariate	Spine Z score	-0.00045	0.0027	0.865

FACTOR	Analysis	Outcome	β co-efficient	SE	P value
Age	Univariate	Hip Z score	0.0126	0.0027	<0.001
Gender	Univariate	Hip Z score	0.08718	0.0376	0.021
Weight	Univariate	Hip Z score	0.02146	0.00189	<0.001
Height	Univariate	Hip Z score	0.0004	0.0028	0.88
OPG Ab	Univariate	Hip Z score	-0.0003	0.0020	0.86
Age	Multivariate	Hip Z score	0.0138	0.0024	<0.001
Gender	Multivariate	Hip Z score	0.4617	0.0425	<0.001
Weight	Multivariate	Hip Z score	0.0316	0.0020	<0.001
Height	Multivariate	Hip Z score	0.0226	0.0030	<0.001
OPG Ab	Multivariate	Hip Z score	-0.00076	0.0017	0.66

Table 5.3 Regression modelling of predictors of Spine and Hip Z scores in the ORCADES population

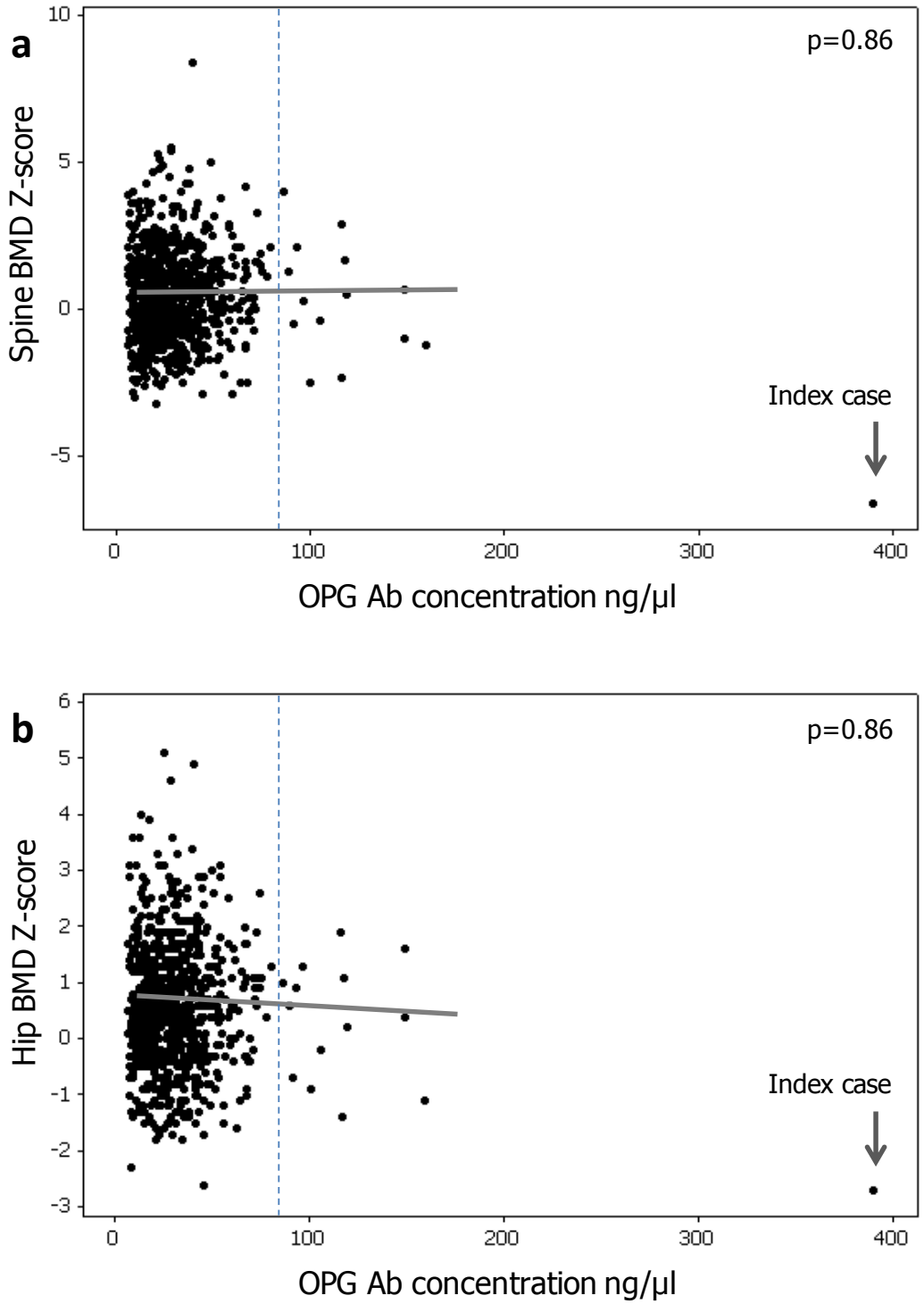

Figure 5.1 Univariate regression analysis reveals no association between OPG antibody concentration measured using ELISA I and spine BMD Z-score (a) or hip BMD Z-score (b). Threshold for positive OPG antibody status illustrated by dotted vertical line, and value seen in index case indicated by arrow.

In this and subsequent figures, results from the index case are illustrated (but not included in analysis) to allow approximate comparison between the two iterations of the ELISA). In a separate analysis no association was observed between OPG antibody titre and bone turnover markers (p=0.95) on either univariate or multivariate analyses.

5.4 Association of OPG antibodies with vascular calcification in ORCADES cohort

Vascular calcification was scored on the lateral image DEXA scan in all ORCADES participants that had undergone scanning and found to be present in 144/1578 (9.1%). The average calcification score of these participants was 2.6 (±1.6) based on an 8-point score, or 5.4 (± 4.07) based on a 24-point score. A regression analysis of the 24 point score against the 8 point score confirmed a highly significant correlation between the two ($p<0.001$) with an R^2 of 96.1% confirming that these two scores correspond closely.

OPG antibodies were measured by ELISA in plasma from a subgroup of 859 patients from the ORCADES cohort in whom lateral DEXA images were available. Within this group 91 cases (10.6%) had vascular calcification present with mean calcification scores of 2.7 (± 1.6) using the 8-point score and 5.6 (±4.0) using the 24-point score.

The titre of OPG antibody correlated significantly with presence of aortic calcification (p=0.015), although this effect was attenuated in a regression analysis including age and sex as covariates (p=0.08). Unsurprisingly age was a strong predictor of vascular calcification ($p<0.001$) though sex is not significant (p=0.368). Use of either the 8 or 24-point calcification scores substantially strengthened the observed association between OPG antibodies and vascular calcification. In this analysis significance is maintained even after adjustment for age and sex with p value of 0.04 (8-point calcification score) or p value of 0.02 (24-point calcification score).

Analysis based on a categorical definition of antibody positivity (defined as levels of OPG antibody greater than the mean of healthy controls plus 3 standard deviations) similarly revealed highly significant differences in both the 8-point calcification score (mean score in antibody positive 1.3±2.6 vs 0.27±0.94, p<0.001) and the 24-point scores (mean score in antibody positive 2.64±5.5 vs 0.56±2.0, p<0.001) (Figure 5.2). Significance was maintained on a multivariate regression analysis including age and sex as covariates for both the 8-point score (p<0.001) and 24-point score (p=0.001) with presence of OPG antibodies.

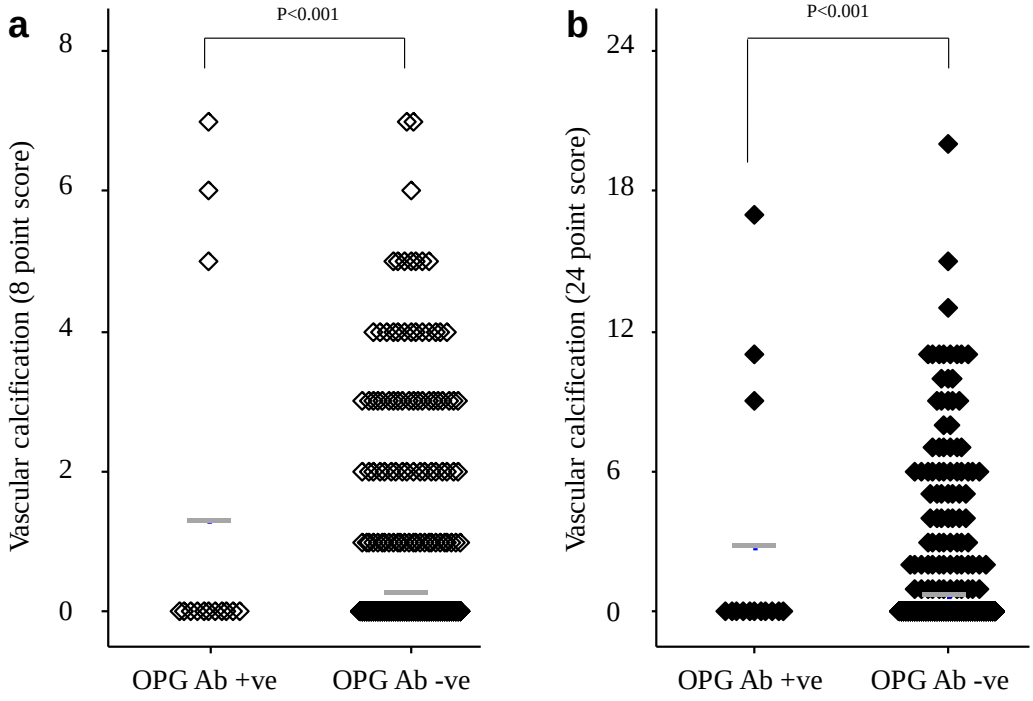

Figure 5.2 Vascular calcification grouped by presence or absence of OPG antibodies. Significantly higher calcification scores are seen in OPG antibody positive individuals. Scores based on an 8 point scoring system are shown in empty diamonds (panel a), and scores based on a 24 point scores are shown in filled diamonds (panel b). Means displayed as horizontal grey bar.

5.5 Discussion

Results of screening the ORCADES population cohort for the presence of OPG antibodies identified raised levels of autoantibodies to OPG in approximately 1.6% of the general population. The level that was set within the healthy control cohort as a threshold to define the presence of antibody was essentially arbitrary, and the absolute level measured in the ORCADES samples was correspondingly arbitrary. However the detection of any level of antibody to a circulating endogenous cytokine such as OPG in a healthy population is in itself surprising, and does raise an important issue about the frequency with which self-tolerance is breached in healthy populations. There is a single prior reference to OPG antibodies in the very specific context of a trial involving recombinant Fc-OPG fusion molecule[191]where it was quite reasonably assumed that the presence of the carrier protein, or some alteration in the conformation/post translational modification of expressed OPG itself allowed the development of an autoimmune response. It is intriguing that further examples have been recently reported of diverse clinical syndromes associated with the development of autoantibodies against self-antigens with the suggestion that this is such a widespread phenomenon that it makes more sense to consider diseases associated with autoantibodies to be a greatly exaggerated but fundamentally normal physiological occurence[193] . In keeping with this concept, a number of beneficial roles of naturally occurring antibodies with the capacity to recognise self-antigens have been recently described[194].

Within the ORCADES population, no association was seen between levels of OPG autoantibody and either lowered bone density or with markers of bone turnover, which would suggest that these antibodies do not have any adverse clinical effect, or if present any such effect is too small to be detected. Contradicting the notion that these antibodies are benign however was the observed significant association between vascular calcification and the presence of OPG autoantibodies. This could simply be a chance observation and it will require replication, however there is biological plausibility for a pathological role since OPG has been suggested as a possible common factor in the development of vascular calcification and osteoporosis (discussed in detail in Section 1.3.5). A simple explanation for this

association would be that calcium liberated by excess bone turnover had been deposited in the vasculature. This is difficult to reconcile with the normal bone turnover observed in these patients, though possibly the vascular calcification could represent evidence of a preceding and transient episode of increased bone turnover for which a compensating physiological response had been generated. Such responses could be immunological suppression of pathological neutralising antibody or an increase in levels of OPG itself. Alternatively there could be a direct role of OPG antibodies on the vasculature independently of an effect on bone density. This data is equally consistent with OPG antibodies being an epiphenomenon of vascular calcification or high bone turnover rather than pathological.

Chapter 6: Prevalence and correlation with bone traits of OPG antibodies in patients with osteoporosis

6.1 Abstract

6.1.1 Introduction

Neutralising antibodies to OPG have previously been described in a patient with severe osteoporosis who responded dramatically to treatment with bisphosphonate therapy. It is not known if OPG antibodies influence the risk of 'idiopathic' osteoporosis or its response to treatment.

6.1.2 Materials and methods

Serum was obtained from patients attending the osteoporosis service in Lothian, who completed lifestyle questionnaires at time of bone density scanning (Section 2.6.2). Prevalence of OPG antibodies was assessed in 315 patients by ELISA (Section 2.3.5 ELISA protocol II). Serum from healthy volunteers with normal bone density was used to define a normal range. Follow up bone density scans were available in 78 patients allowing treatment response to be evaluated.

6.1.3 Results

Raised levels of OPG antibodies were found in 37/315 (11.7%) of osteoporosis patients and titres of OPG antibodies were significantly higher than in age-matched non-osteoporotic controls. Within this cohort the presence of OPG antibodies was not associated with lower bone density. Serum calcium and ALP were raised but not serum CTX in patients with OPG antibodies. No difference in treatment response was observed between patients with and without OPG antibodies.

6.1.4 Conclusions

OPG antibody levels were higher in patients with osteoporosis consistent with a pathological role in a subset of these patients; however the presence of OPG antibodies did not predict more severe osteoporosis or a better response to treatment.

6.2 Prevalence of OPG antibodies in osteoporotic cohort

Serum samples were analysed from 315 patients attending the osteoporosis clinic by ELISA II (Section 2.3.6). In this cohort, 37/315 patients (11.7%) were found to have raised titres of OPG antibody as defined by levels greater than the mean plus 3 standard deviations of 101 healthy controls (14.3 RU). The titre of OPG antibodies was significantly raised when compared to healthy controls even after adjusting for age (median OPG antibody level 3.3 RU (IQR 4.0) in cases compared to 2.0 RU (IQR 4.5) in controls, p=0.01) (Figure 6.1)

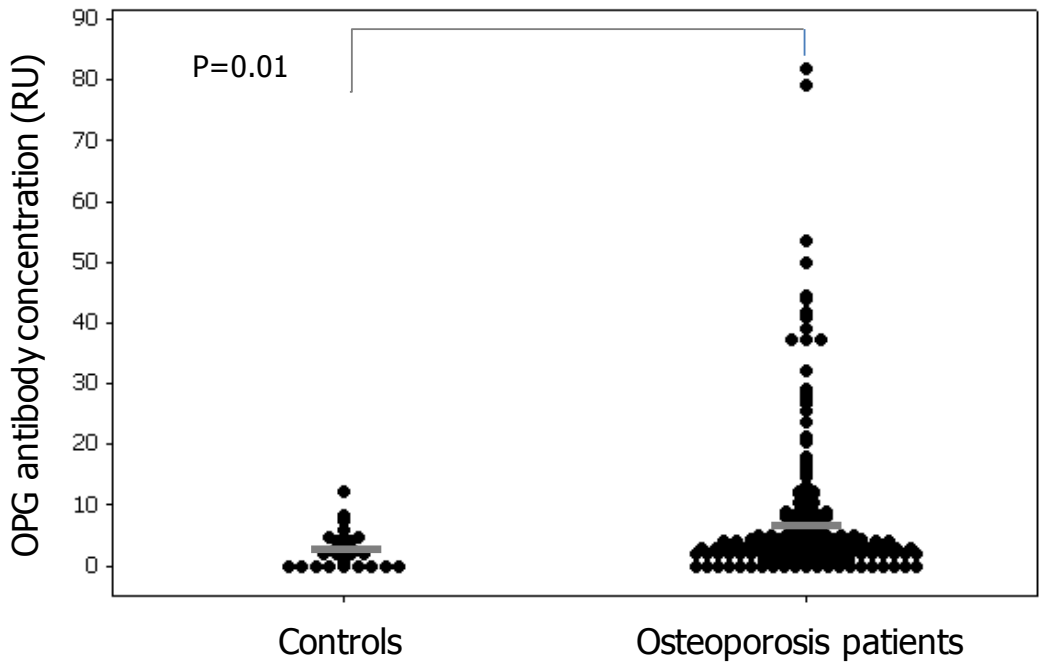

Figure 6.1 OPG antibody concentration in osteoporosis patients and age-matched controls. Significantly raised concentration of OPG antibody measured by ELISA II are seen in patients with osteoporosis.

The characteristics of these patients are given in Table 6.1. No significant differences were present between the groups as defined by OPG antibody status. No difference in BMD scores was observed between the groups.

Characteristic	High antibody level (n=37)	Normal antibody level (n=278)	p value
Age	69.5 (±12.8)	68.7 (±12.5)	0.70
Sex	5 male (13.5%)	58 male (20.1%)	0.38
BMI	24.1 (±6.2)	24.5 (±5.0)	0.61
Current smoker	6/37 (16%)	51/278(18%)	1.00
Calcium intake	926mg (±384)	845mg (±502)	0.34
Autoimmune disease	8/37 (21%)	50/278 (18%)	0.65
Spinal fracture	6/37 (16%)	65/278 (23%)	0.41
Spine BMD T score	-2.97 (±1.16)	-2.99 (±1.28)	0.94
Spine BMD Z score	-1.03 (±1.29)	-1.27 (±1.40)	0.33
Hip BMD T score	-2.76 (±0.87)	-2.43 (±0.95)	0.08
Hip BMD Z score	-1.03 (±0.87)	-0.82 (±1.01)	0.24

Table 6.1 Characteristics of osteoporosis patients by defined by OPG antibody status

6.3 Regression analyses in the osteoporotic cohort

No significant correlations between age, weight, height and OPG antibody concentration within the osteoporosis cohort were identified using Spearman's rank correlation coefficient (Table 6.2). Similarly no significant difference in the OPG antibody concentration between women (median concentration 3.4, interquartile range 4.6) and men was observed (median concentration 3.3, interquartile range 2.4) with a MWU test non-significant (p=0.57).

FACTOR	Spearman's rho	P value
Age (yrs)	0.096	0.09
Weight (kg)	0.006	0.92
Height (cm)	-0.004	0.95

Table 6.2 No correlation observed between key variables and OPG antibody concentration by ELISA II

Linear regression modelling was performed with the response taken as Z scores of the spine and hip. Age, weight, height and OPG antibody concentration were included as continuous variables with sex included as a categorical variable (female

sex assigned value of 0, male sex 1. Results of univariate and multivariate analyses against BMD Z scores are shown in table 6.3 with expected associations of age, gender and weight, though no association was seen between OPG antibody concentration or height, and BMD Z scores at either spine or hip.

FACTOR	Analysis	Outcome	β co-efficient	SE	P value
Age	Univariate	Spine Z score	0.0496	0.0060	<0.001
Gender	Univariate	Spine Z score	0.3608	0.1009	<0.001
Weight	Univariate	Spine Z score	0.0240	0.0060	<0.001
Height	Univariate	Spine Z score	-0.0130	0.0085	0.13
OPG Ab	Univariate	Spine Z score	0.0060	0.0075	0.42
Age	Multivariate	Spine Z score	0.0540	0.0055	<0.001
Gender	Multivariate	Spine Z score	0.5262	0.1090	<0.001
Weight	Multivariate	Spine Z score	0.0410	0.0056	<0.001
Height	Multivariate	Spine Z score	0.0038	0.0096	0.70
OPG Ab	Multivariate	Spine Z score	0.0043	0.0060	0.48

FACTOR	Analysis	Outcome	β co-efficient	SE	P value
Age	Univariate	Hip Z score	0.0272	0.0043	<0.001
Gender	Univariate	Hip Z score	0.2983	0.0705	<0.001
Weight	Univariate	Hip Z score	0.0149	0.0042	<0.001
Height	Univariate	Hip Z score	-0.0085	0.0058	0.15
OPG Ab	Univariate	Hip Z score	-0.0008	0.0053	0.88
Age	Multivariate	Hip Z score	0.0315	0.0042	<0.001
Gender	Multivariate	Hip Z score	0.4659	0.0806	<0.001
Weight	Multivariate	Hip Z score	0.0270	0.0042	<0.001
Height	Multivariate	Hip Z score	0.0078	0.0070	0.27
OPG Ab	Multivariate	Hip Z score	-0.0015	0.0045	0.74

Table 6.3 Regression modelling of predictors of BMD Z scores of the spine and hip in the osteoporosis cohort. Age, sex and weight are significantly associated with BMD but in this analysis neither height nor OPG antibody concentration are significantly associated.

Similarly univariate analysis of OPG antibody showed no association with spine T score (p=0.80) or hip T score (p=0.63), as well as multivariate analysis including age, sex and BMI also not showing any association with spine T score (p=0.46) or hip T score (p=0.65) (Figure 6.2).

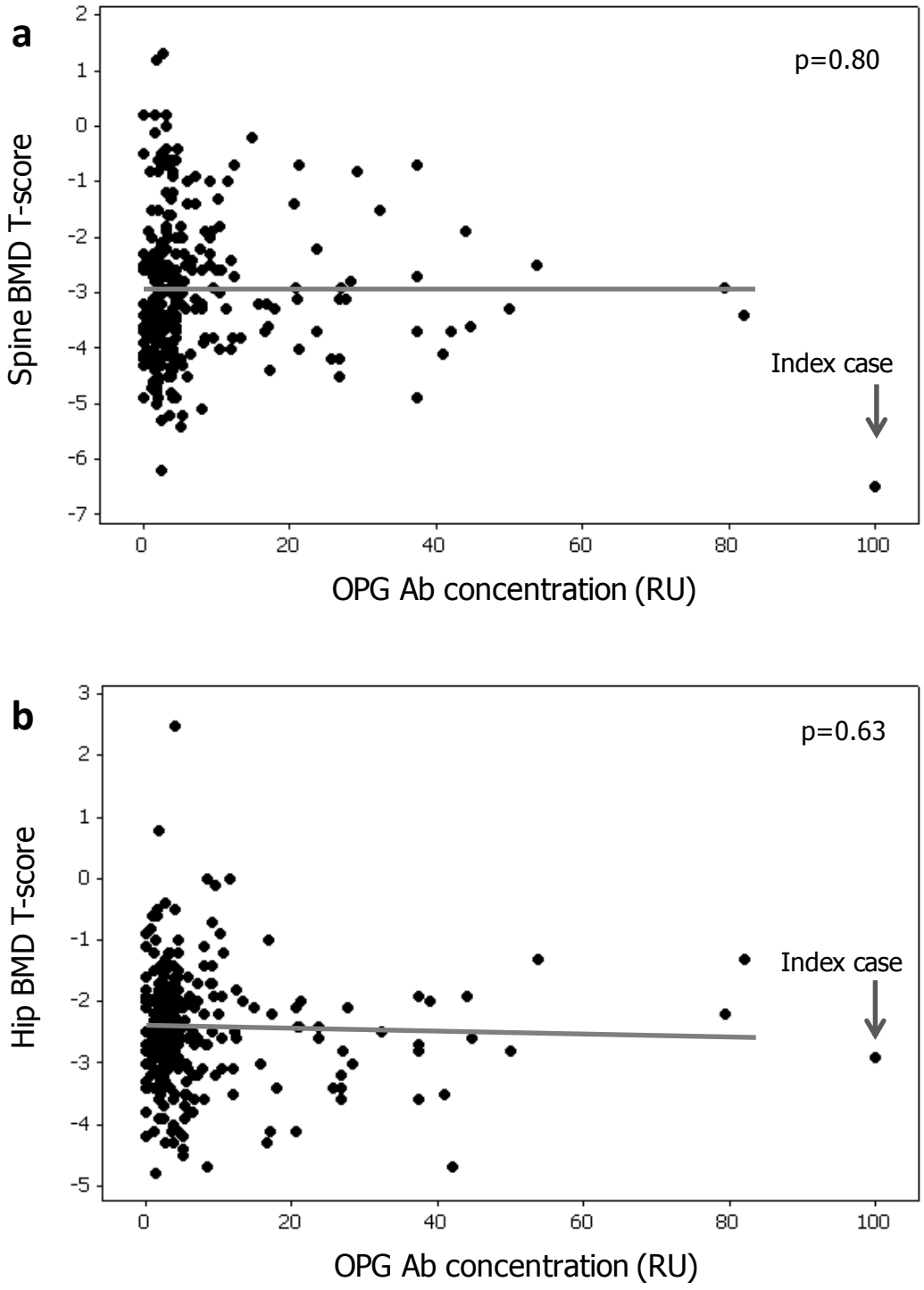

Figure 6.2 Association of BMD and OPG antibody in osteoporosis cohort. Univariate regression analysis revealed no significant association between OPG antibody concentration by ELISA II and spine BMD T-score (a) or total hip BMD T-score (b). Values for index case are shown to illustrate that in this cohort some samples approached levels of OPG antibody seen in index case.

6.4 Analysis of disease response in OPG antibody positive patients

The phenotype information that is held on the patients recruited to this study is currently being extended to include drug prescribing data, fracture data and results of biochemistry investigations. At the time of preparation of this manuscript, this data was available in 225 patients that had given a serum sample for assessment of OPG antibody. OPG antibodies were present in 31/225 (13.8%) and the baseline characteristics of these patients are given in Table 6.4.

Characteristic	**OPG Ab positive (n=31)**	**OPG Ab negative (n=194)**	**p value**
Spine BMD	0.71 (±0.14)	0.71 (±0.14)	0.97
Total Hip BMD	0.67 (±0.14)	0.68 (±0.13)	0.56
Fem Neck BMD	0.56 (±0.10)	0.58 (±0.10)	0.36
FRAX major fracture	23.55 (±17.6)	20.27 (±11.3)	0.19
FRAX hip fracture	12.31 (±15.3)	9.10 (±9.14)	0.11
Number of vertebral fractures	1.61 (±2.32)	1.13 (±1.51)	0.13
Serum Calcium	2.44 (±0.20)	2.37 (±0.12)	*0.02*
Serum ALP	99.71 (±29.67)	87.12 (±31.07)	*0.04*
Serum 25(OH)Vitamin D	51.19 (±39.23)	54.06 (±42.94)	0.78
CTX (n=104)	0.22 (±0.25)	0.22 (±0.25)	0.96

Table 6.4 Baseline characteristics of OPG antibody positive patient in osteoporosis cohort.

Once again no difference was observed in the BMD at any site between cases and controls. No difference in any individual component of the FRAX score, nor in the

consequent calculated fracture risk was seen, nor in the number of vertebral fractures seen. OPG antibody patients were found to have significantly higher serum calcium and ALP compatible with increased bone turnover; though in the subset of these patients for whom serum CTX data is available this marker was not different between cases and controls.

A subset of 78 patients has undergone repeat bone density scanning since recruitment allowing a preliminary assessment of treatment response to be made. Characteristics of these patients are shown in Table 6.3. Of these patients 27 were treated with a bisphosphonate (13 alendronate, 4 risedronate and 10 zoledronate) and 22 treated with PTH therapy (20 teriparatide and 2 preotact).
Patients treated with strontium ranelate, hormone replacement therapy, calcium and vitamin D alone or in whom prescribing information was incomplete were not included. The average duration of follow up was 3.15 (±2.28) years.

As might be expected, the greatest improvements in BMD were observed in the lumbar spine, and with teriparatide therapy. Significantly greater BMD improvements were seen with teriparatide treatment compared to bisphosphonate therapy. No significant change in either measure of hip BMD was observed within either treatment arm. Adjustment for the duration of treatment appeared to substantially improve the sensitivity of this analysis, with significantly greater effects of teriparatide shown in the lumbar spine over bisphosphonate in all comparisons performed (effects assessed in all treated patients, and subgroup analyses of patients with high or low OPG antibody status). No significant difference in response to either PTH or bisphosphonate treatment was seen between low or high OPG antibody status patients suggesting that presence of OPG antibody does not predict treatment response (Table 6.5).

Patient cohort	Lumbar spine		Total Hip		Fem Neck	
	ΔBMD	ΔBMD/ time	ΔBMD	ΔBMD/ time	ΔBMD	ΔBMD/ time
BP (all) n=27	0.044 (±0.045)	0.0139 (±0.013)	0.010 (±0.040)	0.006 (±0.027)	0.009 (±0.029)	0.005 (±0.015)
BP (low OPG) n=21	0.053 (±0.044)	0.0163 (±0.012)	0.003 (±0.027)	0.001 (±0.009)	0.007 (±0.028)	0.003 (±0.010)
BP (high OPG) n=6	0.014 (±0.042)	0.0056 (±0.014)	0.027 (±0.065)	0.0200 (±0.051)	0.014 (±0.035)	0.0108 (±0.026)
PTH (all) n=22	0.069 (±0.056)	0.0343 (±0.024)	-0.009 (±0.035)	-0.0042 (±0.014)	-0.002 (±0.039)	0.0006 (±0.019)
PTH (low OPG) n=17	0.061 (±0.060)	0.0315 (±0.026)	-0.014 (±0.038)	-0.0063 (±0.015)	-0.003 (±0.044)	0.0009 (±0.021)
PTH (high OPG) n=5	0.092 (±0.040)	0.0417 (±0.017)	0.007 (±0.019)	0.0030 (±0.009)	0.0002 (±0.022)	-0.0004 (±0.010)

p value for comparisons shown	Lumbar spine		Total Hip		Fem Neck	
	ΔBMD	ΔBMD/ time	ΔBMD	ΔBMD/ time	ΔBMD	ΔBMD/ time
BP (all) vs PTH (all)	0.119	***0.001***	0.128	0.116	0.313	0.386
BP (low OPG) vs BP (high OPG)	0.095	0.098	0.286	0.198	0.67	0.366
PTH (low OPG) vs PTH (high OPG)	0.293	0.442	0.255	0.194	0.877	0.904
BP (low OPG) vs PTH (low OPG)	0.679	***0.042***	0.185	0.111	0.458	0.681
BP (high OPG) vs PTH (high OPG)	***0.017***	***0.007***	0.543	0.481	0.480	0.398

Table 6.5 Change in BMD over time. ΔBMD calculated by subtracting the baseline BMD value from the BMD reading on the return visit (ie a positive value represents a gain in BMD). ΔBMD/time is calculated by dividing the ΔBMD by the time (in years) between baseline and follow-up scan.

6.5 Discussion

The prevalence of OPG antibodies in the osteoporosis cohort was estimated at 11.7% (ELISA protocol II) with the titre of OPG higher than in age-matched controls. These patients were no more likely to have autoimmune disease and overall had very similar demographic characteristics to patients without OPG autoantibodies. The higher level of OPG autoantibodies is consistent with a pathogenic role for OPG antibodies in a proportion of patients with osteoporosis, though also with antibodies being an epiphenomenon of osteoporosis.

It remains a striking observation that over 11% of patients attending the clinic were found to have autoantibodies to OPG and a number of preliminary analyses of the characteristics of disease in these patients have been carried out. Serum calcium and ALP were noted to be significantly raised in these patients which echoes the markedly elevated bone turnover observed in the index case. There is an inconsistency in that the results of serum CTX were not found to be raised and these results must be interpreted with some caution. Even if it is established that patients with OPG autoantibodies have higher bone turnover this does not necessarily infer that they will respond to antiresorptive therapy in the dramatic fashion seen in the index case. The number of patients in whom treatment response data are available at present is very small but no trend is seen to a better response in OPG antibody positive patients compared to OPG negative to bisphosphonate, or indeed a differential response to PTH treatment. This analysis will need to be repeated with larger numbers of patients, and it would be of particular interest to observe the effects of more potent bisphosphonates such as zoledronate and denosumab.

Chapter 7: Prevalence and correlation with bone traits of OPG antibodies in coeliac and inflammatory bowel disease

7.1 Abstract

7.1.1 Introduction

Osteoporosis is a recognised complication of coeliac disease and inflammatory bowel disease (IBD). It is not known if autoantibodies to OPG contribute to the pathogenesis of osteoporosis in coeliac disease or IBD.

7.1.2 Materials and Methods

Serum samples were obtained from patients attending gastroenterology disease clinics in Lothian with bone density scanning performed in line with routine clinical practice (Section 2.6.3). OPG antibodies were identified by ELISA, with the IBD cohort assessed using ELISA protocol I (Section 2.3.3) and the coeliac patients using ELISA protocol II (Section 2.3.5). Serum from volunteers with normal bone density was used to define a normal range.

7.1.3 Results

Raised levels of OPG antibody were seen in 14/282 (5.0%) patients with coeliac disease and this was associated with reduced spine BMD. Functional inhibition of OPG was shown by 3/14 (21.4%) of the OPG antibody positive samples. No improvement in case finding was shown by inclusion of OPG antibodies into a risk prediction score for osteoporosis. Raised levels of OPG antibodies were found in 5/141 (3.5%) of IBD patients with the presence of antibodies associated with reduced bone density Z-scores of the hip. This result was confounded by features of increased disease severity in OPG antibody positive patients.

7.1.4 Conclusion

Results are consistent with a pathological role of OPG antibodies in a proportion of patients with coeliac disease. Whilst similar trends were observed in the IBD cohort the association with BMD is confounded by features of increased disease severity.

7.2 Prevalence of OPG antibodies in patients with IBD

Levels of OPG autoantibody were measured using ELISA I in a cohort of 141 patients with IBD in whom stored serum samples was available. The titre of OPG antibody was not significantly higher in the cases (median concentration 23.1 ng/µl, IQR 25.1) than in controls (median concentration 23.0 ng/µl, IQR 37.0); p=0.08 MWU) (Fig 7.1).

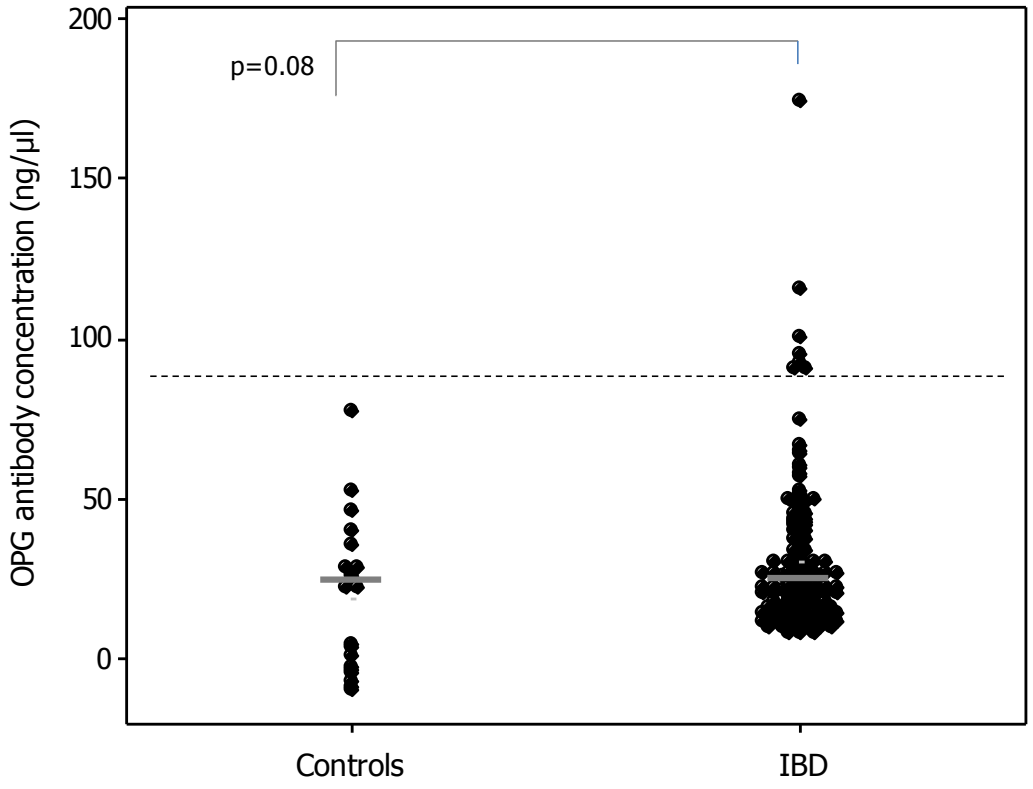

Figure 7.1 OPG antibody levels in IBD patients and controls. The concentration of OPG antibody is not significantly raised in IBD patients (n=141) when compared to healthy controls (n=20). OPG antibodies measured using ELISA protocol 1, with a threshold of mean plus three standard deviations indicated by the grey dotted line, and the median value in each cohort by a horizontal grey bar.

A total of 5/141 (3.5%) of the IBD patients had elevated levels of OPG autoantibodies as defined by values >3 SD above the mean in 20 healthy controls (91 ng/µl). The characteristics of these patients are shown in Table 7.1 with p values

based on 2 sided student T test for continuous variables, and Chi square or Fishers Exact test for categorical variables. Lower hip BMD Z-scores were associated with presence of OPG antibodies, though the difference in spine BMD Z-scores was not statistically significant. This association was potentially confounded by features of more severe disease with a younger age of onset, and non-significantly lower BMI in cases with OPG antibodies.

Characteristic	**High antibody level (n=5)**	**Normal antibody level (n=136)**	**p value**
Age	44(±17.2)	46(±14.6)	0.36
Sex	2(40%)	61(43%)	1.00
BMI	22.2(±2.37)	25.1(±4.3)	0.07
Age of onset	18(±7.2)	32.6(±14.5)	**0.01**
Crohns disease	5/5(100%)	88(65%)	0.17
Spine T score	-1.4(±0.97)	-0.93(±1.3)	0.39
Spine Z score	-1.05(±0.97)	-0.48(±1.3)	0.17
Hip T score	-1.8(±0.14)	-0.63(±1.1)	0.07
Hip Z score	-1.6(±1.06)	-0.39(±0.94)	**0.01**

Table 7.1 Characteristics of OPG antibody positive patients in IBD cohort

7.3 Regression analyses in patients with IBD

Linear regression modelling was performed with the response taken as Z scores of the spine and hip. Age, weight, height and OPG antibody concentration were included as continuous variables with sex included as a categorical variable (female sex assigned value of 0, male sex 1).

Possible confounding was investigated by looking at Spearman's correlation coefficient between age, weight, height and age of onset of inflammatory bowel disease with OPG antibody concentration (Table 7.2). Within this cohort age of onset of inflammatory bowel disease was significantly associated with the concentration of OPG antibody as measured by ELISA I. No significant correlations between age,

weight, height and OPG antibody concentration within the IBD cohort were identified however. Similar concentrations of OPG antibody were observed in women (median concentration 22.7, interquartile range 24.7) and men (median concentration 26.7, interquartile range 25.4) with a MWU test non-significant (p=0.58).

FACTOR	Spearman's rho	P value
Age (yrs)	-0.10	0.24
Weight (kg)	-0.06	0.51
Height (cm)	0.02	0.77
Age of onset IBD	-0.25	<0.05

Table 7.2 No correlation observed between key variables and OPG antibody concentration by ELISA I

Further modelling was then performed using Z score of the spine as the response variable, with the full results of univariate and multivariate modelling given in table 7.3. Univariate regression analyses revealed significant associations for sex, age, weight and age of onset of IBD. Significance for all these factors was maintained on multivariate analysis with the exception of age of onset. No association was seen between OPG antibody concentration and spine Z score.

FACTOR	Analysis	Outcome	β co-efficient	SE	P value
Age	Univariate	Spine Z score	0.0190	0.007	0.01
Gender	Univariate	Spine Z score	0.2838	0.109	0.01
Weight	Univariate	Spine Z score	0.0192	0.008	0.02
Height	Univariate	Spine Z score	-0.0045	0.012	0.71
OPG Ab	Univariate	Spine Z score	-0.006	0.004	0.16
Age of onset	Univariate	Spine Z score	0.0160	0.007	0.03
Age	Multivariate	Spine Z score	0.0185	0.008	0.02
Gender	Multivariate	Spine Z score	0.6087	0.146	<0.001
Weight	Multivariate	Spine Z score	0.0243	0.009	0.01
Height	Multivariate	Spine Z score	0.0317	0.017	0.07
OPG Ab	Multivariate	Spine Z score	-0.0046	0.004	0.29
Age	Multivariate	Spine Z score	0.0223	0.011	<0.05
Gender	Multivariate	Spine Z score	0.6029	0.147	<0.001
Weight	Multivariate	Spine Z score	0.0251	0.009	0.01
Height	Multivariate	Spine Z score	0.0304	0.018	0.09
OPG Ab	Multivariate	Spine Z score	-0.0054	0.005	0.25
Age of onset	Multivariate	Spine Z score	-0.0055	0.011	0.63

Table 7.3 Regression modelling of spine BMD Z score in IBD patients

The same analysis was performed using hip BMD Z score as the response variable (Table 7.4). In these analyses weight is consistently and highly significantly associated with hip Z score. The presence of OPG antibodies was significantly associated with hip BMD Z scores on univariate analysis (p=0.01) (Figure 7.2). On multivariate analysis including age, sex, height and weight, significance remained (p=0.025), and was demonstrated also for hip T score (p=0.046). However, this result was confounded by features of more severe disease in these patients including a significantly lower age of disease onset such that if age of onset was included in a multivariate analysis then significance was lost for the association of hip Z score and OPG antibody (p=0.08).

FACTOR	Analysis	Outcome	β co-efficient	SE	P value
Age	Univariate	Hip Z score	0.0041	0.006	0.49
Gender	Univariate	Hip Z score	0.1347	0.0865	0.12
Weight	Univariate	Hip Z score	0.0233	0.006	<0.001
Height	Univariate	Hip Z score	0.0018	0.010	0.85
OPG Ab	Univariate	Hip Z score	-0.0092	0.003	0.01
Age of onset	Univariate	Hip Z score	0.0119	0.006	0.04
Age	Multivariate	Hip Z score	0.0009	0.006	0.9
Gender	Multivariate	Hip Z score	0.2984	0.112	0.01
Weight	Multivariate	Hip Z score	0.0290	0.007	<0.001
Height	Multivariate	Hip Z score	0.0054	0.013	0.69
OPG Ab	Multivariate	Hip Z score	-0.0076	0.003	0.02
Age	Multivariate	Hip Z score	-0.0083	0.008	0.32
Gender	Multivariate	Hip Z score	0.3090	0.112	0.01
Weight	Multivariate	Hip Z score	0.0274	0.007	<0.001
Height	Multivariate	Hip Z score	0.0077	0.014	0.57
OPG Ab	Multivariate	Hip Z score	-0.0062	0.003	0.08
Age of onset	Multivariate	Hip Z score	0.0107	0.009	0.22

Table 7.4 Regression modelling of hip BMD Z score in IBD patients

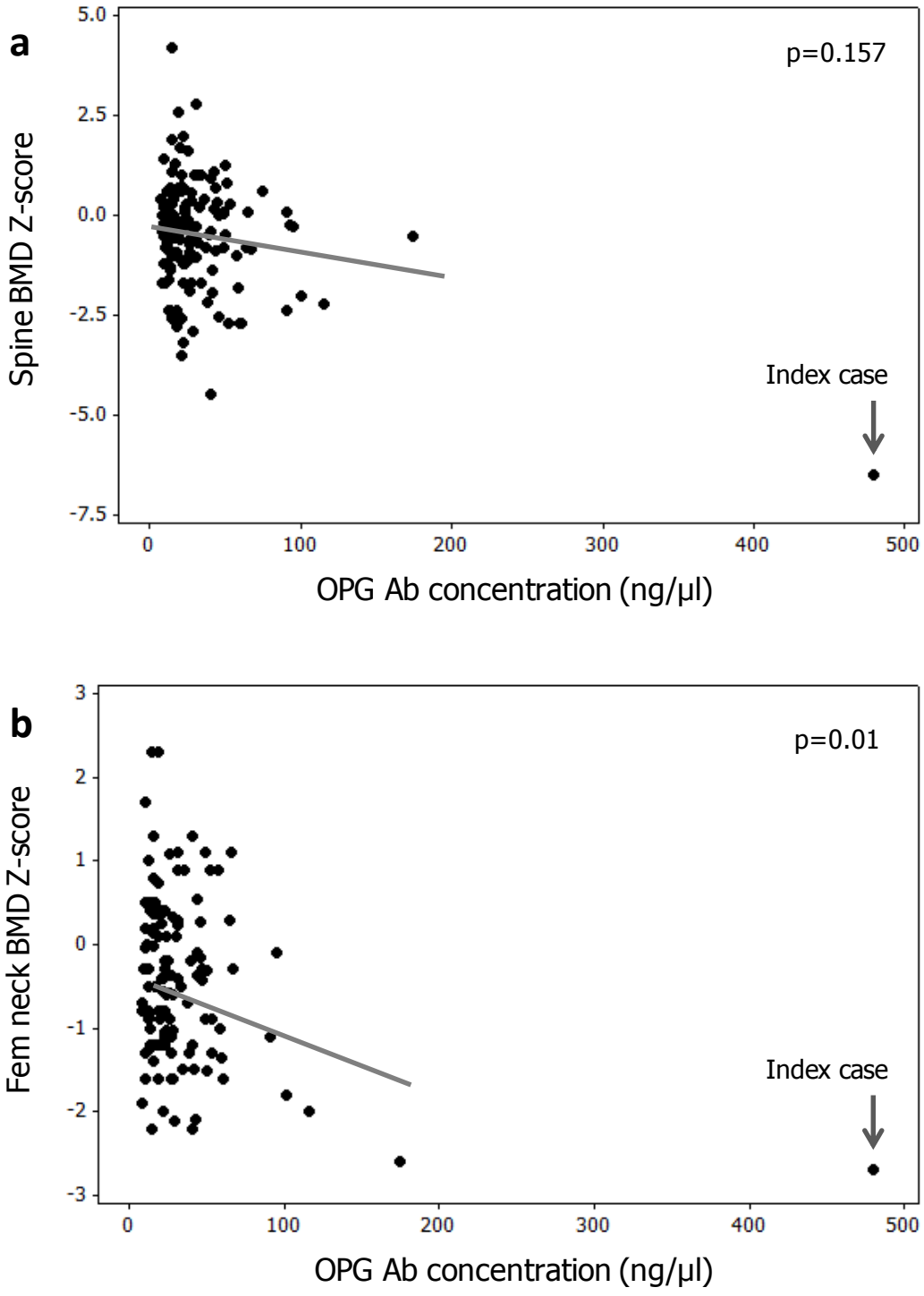

Figure 7.2 Association of BMD and OPG antibody in IBD cohort. Univariate regression analyses revealed no association between OPG antibody concentration by ELISA I and spine BMD Z-score (a) but a significant association between femoral neck BMD Z-score (b). Values for index case shown for illustrative purposes only.

7.4 Prevalence of OPG antibodies in patients with coeliac disease

Serum samples were analysed from 282 patients with coeliac disease recruited through gastroenterology clinics in Lothian using ELISA II (Section 2.3.6). The concentration of OPG antibodies was significantly raised when compared to levels seen in healthy age matched controls (Figure 7.4). The median OPG antibody level in coeliac cases was 4.0 RU (IQR 4.6) compared to a median of 2.6 RU (IQR 3.1) in the controls.

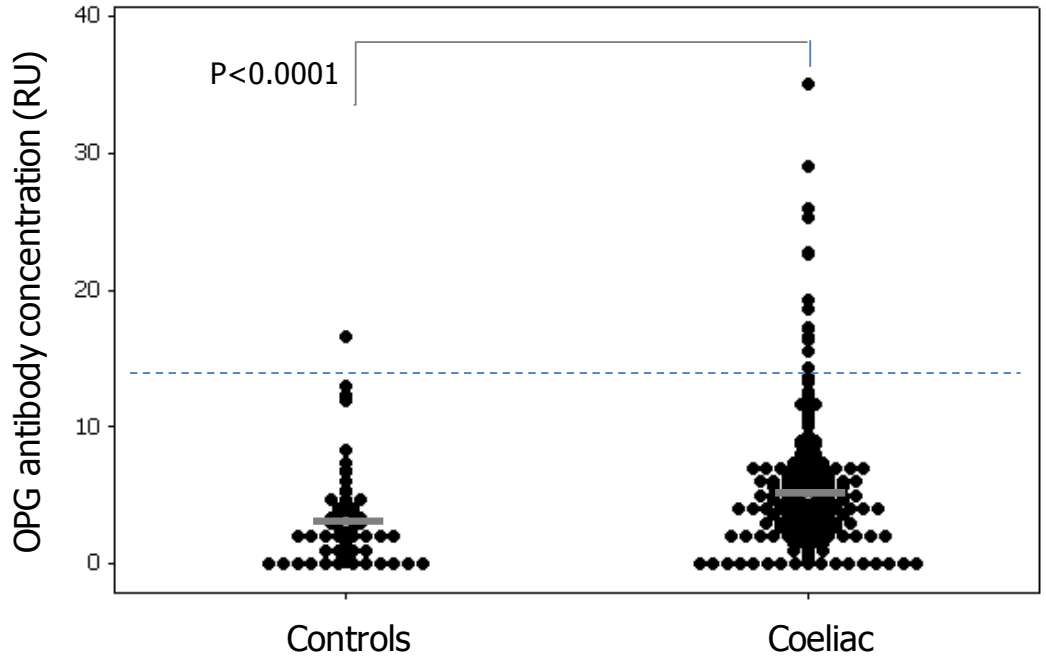

Figure 7.3 Raised concentrations of OPG antibody by ELISA II are seen in a coeliac cohort compared to age matched controls. Threshold for positive antibody status indicated by horizontal dotted line.

A reference range was derived from the mean plus three standard deviations of concentrations seen in 101 volunteers with normal BMD (14.3RU). Within the coeliac cohort, 14/282 patients (5.0%) were found to have raised levels of antibody (defined as greater than the mean plus 3SD of levels seen in 101 volunteers of normal BMD). BMD data was available in 254 of these patients of whom 11/254 had

elevated titres of OPG antibody. The characteristics of patients with raised or normal levels of antibody within this cohort are given in Table 7.5.

Characteristic	**High antibody level (n=14)**	**Normal antibody level (n=268)**	**p value**
Age	56.2 (±15.8)	55.5 (±15.0)	0.85
Female	8/14 (57%)	199/268 (74%)	0.16
Bisphosphonate (ever)	4/14 (29%)	39/268(14%)	0.25
Steroid use (ever)	1/12 (8%)	16/251 (6%)	0.56
Ca/D (ever)	10/13 (77%)	122/252 (48%)	0.05
BMI	25.7 (±4.0)	25.7 (±4.8)	0.87
Number of raised TTG results since diagnosis	1.6(±3.2)	0.7 (±1.1)	0.33
Months since diagnosis of CD	118 (±116)	103 (±114)	0.58
Current smoker	1/12(9%)	27/251 (12%)	1.00
Alcohol (units/week)	8.9 (±10.4)	5.3(±8.3)	0.27
Spine BMD T-score (n=254)	-2.00 (±1.2)	-1.05 (±1.3)	0.02
Spine BMD Z-score (n=254)	-1.12 (±1.39)	-0.10 (±1.2)	<0.01
Hip BMD T-score (n=254)	-1.36 (±0.99)	-1.01 (±1.10)	0.29
Hip BMD Z-score (n=254)	-0.38 (±0.84)	-0.03 (±0.97)	0.24

Table 7.5 Characteristics of OPG antibody positive patients in coeliac cohort. Bone density data was only available in 254 patients. p values represent results of 2-tailed student T test for normally distributed continuous data, or Mann-Whitney U test where data was not normally distributed, Fishers exact test for categorical variables.

No significant differences between patients with raised OPG antibody levels and those with normal levels were observed in terms of conventional risk factors for osteoporosis, namely age, sex, BMI, smoking, alcohol consumption or use of steroid medication. Significantly lower BMD at the spine was observed in patients with high OPG antibody levels (both T-score and Z-score). Whilst numerically lower bone density was seen at the hip, this was not statistically significant.

This difference was not contributed to by treatment effects since a greater proportion of patients in the high OPG antibody group were receiving bone active treatments both bisphosphonate therapy and combined vitamin D and calcium (the latter narrowly failing to reach statistical significance p=0.051).

7.5 Regression analyses in patients with coeliac disease

Prior to performing linear regression possible associations between the variables of interest and OPG antibody by ELISA II in the coeliac cohort were explored. Spearman's rho was calculated for the continuous variables age, weight and height. No significant correlation was seen between any of the factors analysed and OPG antibody concentration by ELISA II (Table 7.6). Very similar concentrations of OPG antibody were seen in women with median concentrations 4RU (IQR 4.5), and in men median concentrations 4RU (IQR 5.1) with no significant difference on Mann Whitney U test (p= 0.78)

FACTOR	Spearman's rho	P value
Age (yrs)	0.01	0.86
Weight (kg)	-0.04	0.54
Height (cm)	0.07	0.28

Table 7.6 Correlation analysis of OPG antibody concentration in coeliac patients

Linear regression modelling was then performed with the response taken as Z scores of the spine and total hip. Age, weight and height were included as continuous variables with sex included as a categorical variable (female sex assigned value of 0, male sex 1). On univariate regression analysis the titre of OPG antibody was significantly associated with spine BMD T-score (p=0.005) and Z-score (p=0.006), though not total hip T-score (p=0.10) or Z-score (p=0.17) (Table 7.7 and Figure 7.4).

The result was consistent when analysed by OPG antibody status with significant association maintained with spine T-score (p=0.021) and Z-score (p=0.006), but not total hip T-score (p=0.34) or Z-score (p=0.24). A multivariate analysis of OPG antibody concentration which included age, sex, height and weight as covariates, found significant associations with spine T score (p=0.004) and spine Z-score (p=0.015), though again no association was seen with total hip T score (p=0.13) or total hip Z-score (p=0.31). Expression as a categorical variable did not change this analysis; association with T-score of the spine (p=0.03) and Z-score of the spine (p=0.03) was maintained, though again no association was found with either hip T-score (p=0.34) or hip Z-score (p=0.45). In a further sensitivity analysis the OPG antibody concentration was log transformed but statistical significance for the association of OPG antibody and spine BMD Z score was maintained on both univariate and multivariate analysis (p<0.05).

FACTOR	Analysis	Outcome	β co-efficient	SE	P value
Age	Univariate	Spine Z score	0.0122	0.005	0.02
Gender	Univariate	Spine Z score	0.2848	0.08	0.001
Weight	Univariate	Spine Z score	0.0227	0.005	<0.001
Height	Univariate	Spine Z score	0.0009	0.009	0.92
OPG Ab	Univariate	Spine Z score	-0.0461	0.016	0.005
Age	Multivariate	Spine Z score	0.0154	0.005	<0.005
Gender	Multivariate	Spine Z score	0.5150	0.099	0.58
Weight	Multivariate	Spine Z score	0.0271	0.006	<0.001
Height	Multivariate	Spine Z score	0.0173	0.011	0.131
OPG Ab	Multivariate	Spine Z score	-0.0436	0.016	0.015

FACTOR	Analysis	Outcome	β co-efficient	SE	P value
Age	Univariate	Hip Z score	0.0001	0.004	0.98
Gender	Univariate	Hip Z score	-0.1197	0.073	0.10
Weight	Univariate	Hip Z score	0.0289	0.004	<0.001
Height	Univariate	Hip Z score	0.0107	0.008	0.17
OPG Ab	Univariate	Hip Z score	-0.0185	0.013	0.17
Age	Multivariate	Hip Z score	-0.0044	0.004	0.30
Gender	Multivariate	Hip Z score	-0.0113	0.067	0.09
Weight	Multivariate	Hip Z score	0.0326	0.005	<0.001
Height	Multivariate	Hip Z score	-0.0144	0.008	0.08
OPG Ab	Multivariate	Hip Z score	-0.0134	0.012	0.27

Table 7.7 Regression analysis of spine and hip Z -scores in coeliac patients

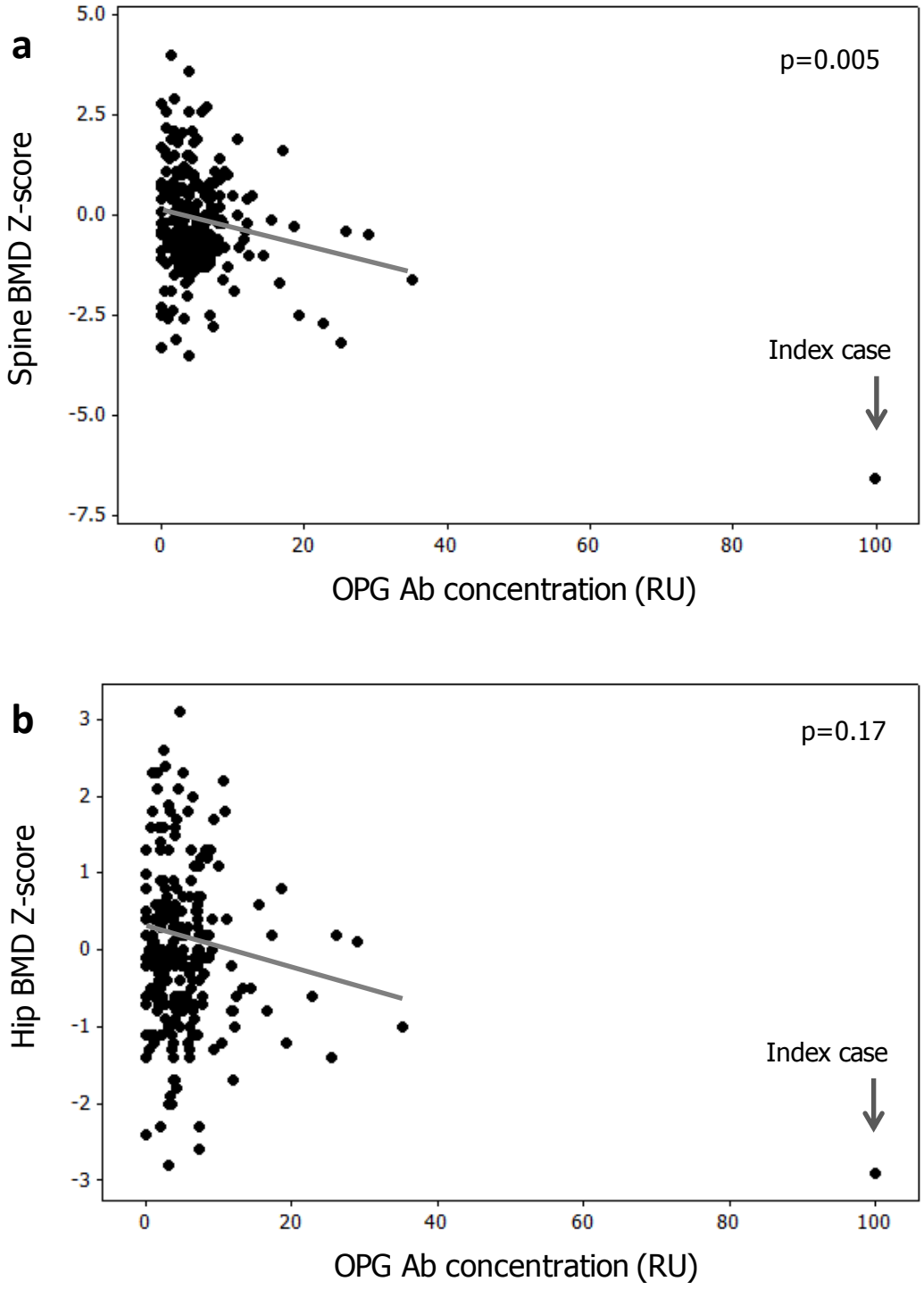

Figure 7.4 Association of BMD and OPG antibody in coeliac cohort. Univariate regression analyses revealed significant association between OPG antibody concentration by ELISA II and spine BMD Z-score (a) but no significant association with total hip BMD Z-score (b). Values for index case shown for illustrative purposes only.

A number of coeliac disease specific factors were also analysed. A numerically greater number of raised TTG antibody tests and longer disease duration were seen in patients with raised OPG antibody concentrations, but neither difference was statistically significant. There was a suggestion that higher titres of OPG antibody were observed in patients in the early part of their disease, rather than in established disease, though it is not possible to draw firm conclusions from this small sample. Specifically of the 14 samples that are positive for OPG antibody the mean disease duration of the highest 7 samples, was significantly shorter than that in the lowest 7 samples (mean duration of disease 46.1 months (± 70.6 months) in highest OPG antibody patients, compared to mean duration of disease 189.9 months (± 112 months) in the lowest OPG antibody patients (Figure 7.5a, $p<0.01$ MWU test). Within this small cohort the duration of disease however was not a significant predictor of OPG antibody concentration either on univariate regression (Figure 7.5b, $p=0.09$, data log transformed to ensure a normal distribution of disease duration) or multivariate regression including age and gender ($p=0.16$).

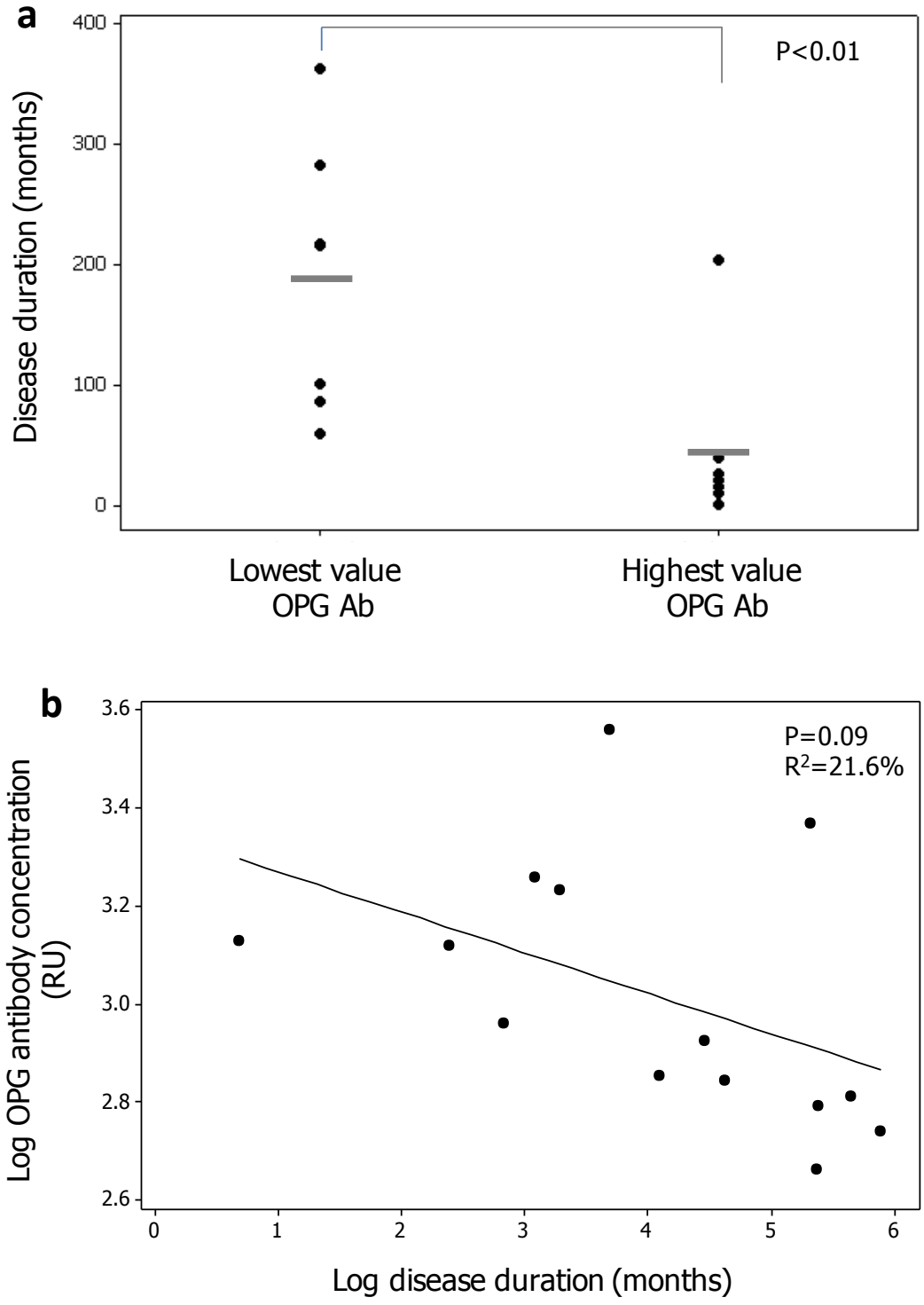

Figure 7.5 Mean disease duration is shorter in those OPG antibody positive patients with the highest titre, compared to those with the lowest titre (a) however disease duration is not a significant predictor of OPG antibody titre (b).

7.6 Assessment of functional activity of OPG antibodies

All samples identified as having raised levels of OPG antibody in the coeliac cohort have also been assessed for their ability to inhibit OPG function using the methodology described in Section 2.2.3.

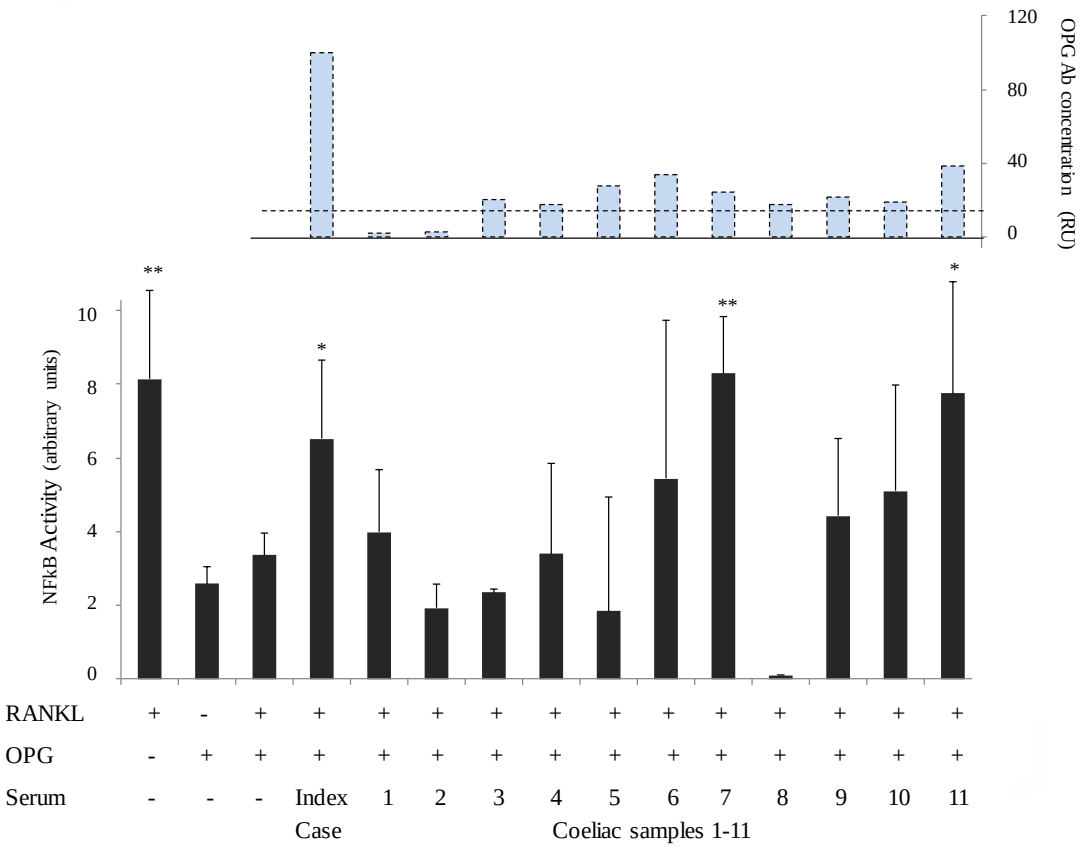

Figure 7.6 Assessment of OPG inhibition by serum samples negative for OPG antibodies (coeliac samples 1-2) and samples known to be positive for OPG antibodies (coeliac samples 3 to 11). Levels of NFκB *activation were compared to that observed in cells treated with both RANKL and OPG alone (RANKL/OPG + +, third column). Significantly increased signalling compared to this background level, is seen in serum from the index case which was used as a positive control, as well as samples 7 and 11. *represents $p<0.05$, ** represents $p<0.01$. Results are means plus SD of triplicate samples. The ELISA OPG Ab value for each serum sample analysed is displayed above each sample (inset columns in light blue, dotted line representing threshold for positive OPG antibody) suggesting there is no simple correlation between titre of OPG antibody and functional inhibition.*

Three of the 14 positive samples screened showed significant inhibition of OPG similar if not greater than that shown by serum from the index case. Overall there was substantial variation in the extent of inhibition of OPG function demonstrated in the samples from coeliac patients. No significant correlation between the level of OPG antibody and the extent of inhibition was observed (Pearson correlation coefficient 0.33, p=0.23). In turn this implies that the affinity or specificity of the antibody may play a more important role in antibody function than absolute titre.

7.7 Clinical utility of testing for OPG antibodies in coeliac disease

The results presented so far demonstrate that OPG antibodies are found more commonly in coeliac disease and correlate with reduced BMD. In order to translate this knowledge into improvements in the management of coeliac disease it will be necessary to show that the identification of OPG antibodies can help in either the identification or in the treatment of osteoporosis. Despite the frequency with which osteoporosis complicates coeliac disease, there are no reliable models that can predict the development of osteoporosis[195] and an exploratory study was performed to see if OPG antibodies might be of value in osteoporosis risk prediction.

7.7.1 Utility of the FRAX tool in predicting osteoporosis in coeliac disease

A number of fracture risk assessment tools have been developed that can aid in the management of patients at risk of osteoporosis, and which have recently been advised for use in selecting patients for bone density scanning (see Section 1.1) . The FRAX algorithm, developed by the World Health Organization, is the most widely available, and incorporates clinical risk factors that include causes of secondary osteoporosis such as coeliac disease (Figure 7.6) [196]. Based on these variables a 10-year probability of hip fracture and major osteoporotic fracture is generated as well as management advice on whether patients should be given empirical treatment, be selected for BMD scanning, or offered lifestyle advice only.

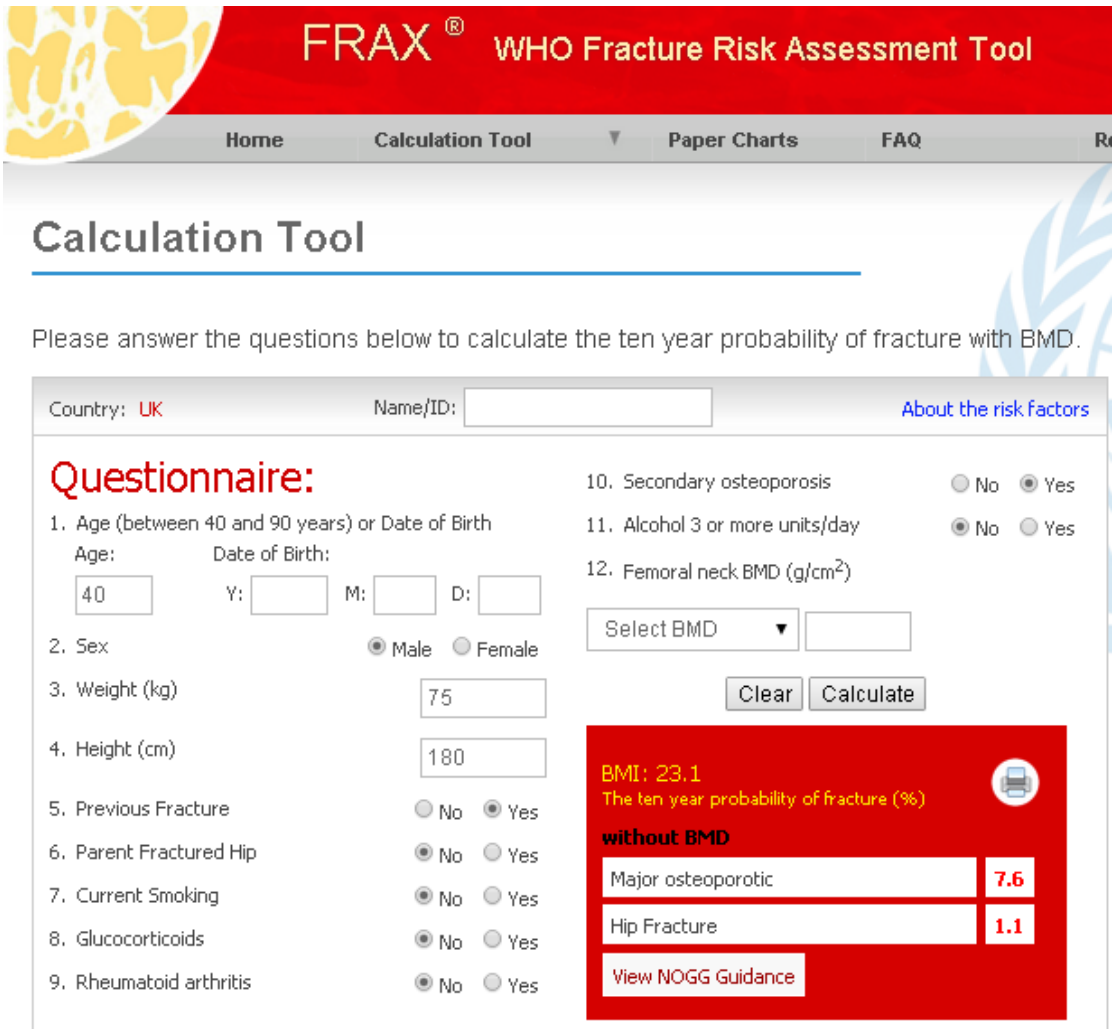

Figure 7.7 Screenshot of the FRAX risk assessment tool displaying the 10 year major osteoporotic and hip fracture probabilities for a patient with characteristics of the index case. The National osteoporosis guidelines group (NOGG) guidance in this example was to measure BMD.

Within the cohort of 282 patients with coeliac disease, there were 254 in whom BMD scans had been performed. Patients that had not received a bone density scan were necessarily excluded from further analysis. Of note the excluded patients had a significantly shorter duration of disease prior to recruitment (median 5 months compared to 254 months, MWU test $p<0.01$) as well as having been recruited more recently (median recruitment date 481 days into the study, rather than 276 days, MWU test $p=0.05$) suggesting that one reason for their not having a scan was simply that they had not yet been appointed. The excluded patients were significantly younger however (average age 39.7±16.1 years compared to 57.2±14.7 years,

p<0.01) suggesting that they are also less likely to have osteoporosis and this limits the generalisability of the models.

Characteristic	**Osteoporosis (n=45)**	**Controls (n=209)**	**p value**
Age at DEXA (yrs)	65.3 (±12.1)	52.1 (±14.6)	<0.001
Sex (Female)	36/45 (80.0%)	153/209 (73.2%)	0.45
Weight, kg	62.7 (±8.8)	71.9 (±14.7)	<0.001
Height, cm	1.61 (±0.08)	1.66 (±0.08)	<0.001
History of low trauma fracture	13/45 (28.9%)	52/209 (24.9%)	0.58
Parental hip fracture	1/45 (2.2%)	18/209 (8.6%)	0.21
Current smoker	7/45 (15.6%)	21/209 (10.0%)	0.30
History of glucocorticoid use	6/45 (13.3%)	11/209 (5.2%)	0.09
Alcohol, >3units/week	0/45 (0%)	14/195 (6.7%)	0.14
FRAX major fracture	18.4 (±11.3)	10.1%(±8.1)	<0.001
FRAX hip fracture	7.80 (±7.61)	2.69 (±4.27)	<0.001
NOGG guidance	Lifestyle 5(11.1%) Measure 24(53.3%) Treat 16(35.6%)	Lifestyle 43 (20.6%) Measure 129 (61.7%) Treat 37 (17.7%)	0.02

Table 7.8 Distribution of FRAX risk prediction variables in coeliac patients depending on osteoporosis status

Of the patients that had received a scan 45/254 (17.7%) had osteoporosis based on the WHO classification of BMD T score ≤ -2.5. The distribution of risk factors used in the FRAX algorithm between patients with or without osteoporosis is displayed in

Table 7.8 (p values based on 2-sided student T test for continuous variables or Fishers exact test for categorical variables).

Age, height and weight are statistically different between cases and controls. The patient details were entered into the online FRAX tool (data entry performed September 2014) to generate 10-year estimates of major fracture and hip fracture risk, as well as the NOGG management advice (treat, measure BMD or offer lifestyle advice only). BMD data were not included since utility in predicting osteoporosis was to be assessed. Patients with osteoporosis were identified as being at highly significantly greater risk of fracture and were more likely to be recommended for active management (Table 7.3).

The utility of the NOGG guidance and FRAX fracture prediction scores in predicting osteoporosis within the coeliac cohort were analysed using Receiver Operating Characteristic (ROC) analysis. Of these, the FRAX fracture prediction scores both yielded a fair result, though the NOGG guidance was a poor test (Table 7.9).

Prediction variable	**Area under curve**	**Std Error**	**95% CI**
NOGG guidance	0.61	0.047	0.52-0.70
FRAX Major Fracture	0.741	0.043	0.66-0.82
FRAX Hip Fracture	0.767	0.041	0.68-0.85

Table 7.9 ROC curve analysis of the FRAX tool output variables in predicting the presence of osteoporosis

To illustrate this, if the NOGG guidance to measure or treat are both taken as an indication for bone density scan referral, this yielded a test with a sensitivity for osteoporosis of 89% but a specificity of only 20.6%. Alternatively use of a FRAX major fracture risk score of ≥10% (which is the proposed threshold for bone density scan referral under the forthcoming SIGN guidelines) yielded a sensitivity of only 73.3% and a specificity of 64.1%. These results suggest that there are significant

shortcomings in the currently available risk assessment tools, and justify a re-evaluation of the predictors of osteoporosis in coeliac disease.

7.7.2 Utility of the QFracture tool in predicting osteoporosis

The QFracture algorithm is an alternative to FRAX which has been derived and validated in large UK primary care patient cohorts utilising the records of over 4.5 million patients[197]. The current revision of QFracture incorporates 26 risk factors, has been validated in patients aged between 30 and 100, and can generate a risk of hip or any osteoporotic fracture over 1 to 10 years. Malabsorption is included in the risk equation for all fractures, but is not included in the hip fracture equation. All the inputs used in FRAX are also included in QFracture, with QFracture utilising a graded score for smoking and alcohol to reflect levels of consumption. Unlike FRAX there is no option within QFracture to input BMD. The distribution of additional risk factors found within the coeliac patient cohort is shown in Table 7.10 (p values represent Fishers exact test).

Characteristic	**Osteoporosis (n=45)**	**Controls (n=209)**	**p value**
Depression	0/45 (0%)	3/209 (1.4%)	1.0
Cancer	3/45 (6.6%)	13/209 (6.2%)	1.0
Asthma	1/45 (2.2%)	2/209 (0.96%)	0.47
Cardiovascular disease	5/45 (11.1%)	9/209 (4.3%)	0.08
Endocrine disorder	3/45 (6.6%)	6/209 (2.9%)	0.20
Falls	5/45 (11.1%)	23/209 (11%)	1.0
Hormone replacement	2/45 (4.4%)	10/209 (4.8%)	1.0
Rheumatoid arthritis	3/45 (6.6%)	4/209 (1.9%)	0.12
Type 1 diabetes	1/45 (2.2%)	0/209 (0%)	0.17
Caucasian ethnicity	44/45 (97.8)	207/209 (99%)	0.44

Table 7.10 Additional risk factors utilised in the QFracture algorithm

Whilst none of these factors reached statistical significance this is not surprising given the small numbers of patients with each individual condition. Across all medical conditions, with the exception of depression, an absolute higher prevalence was seen in the osteoporotic patients, consistent with the results reported in the derivation of QFracture. Whilst dementia, residence in institutional care, epilepsy, chronic liver disease, type II diabetes, Parkinson's disease and renal failure are components of this score there were no patients with these conditions identified by the patient completed questionnaire.

Open source software generating the QFracture scores is freely available online and this was used to generate both 5 and 10 year risk scores, for both all fractures and hip fractures (download performed November 2014). The algorithms were verified by comparison with the output from the online tool. The only discrepancies noted were instances in which the all fracture model generated a lower score than the hip fracture model. In these cases in order to avoid logical absurdity the online tool appears to raise the all fracture score so that it is brought in line with the hip fracture score. The utility of the QFracture scores in predicting osteoporosis within the coeliac cohort were analysed using ROC analysis (Table 7.11). Five and 10 year risk scores for each algorithm performed in a very similar fashion, and once again the hip fracture risk performs somewhat better than the all fracture risk in predicting osteoporosis. With an AUC of 0.799, the QFracture neck of femur algorithm appeared to perform somewhat better than the FRAX neck of femur score (AUC 0.767) though the confidence intervals overlapped widely.

Prediction variable	**Area under curve**	**Std Error**	**95% CI**
QFracture NOF 5 yr	0.799	0.036	0.728-0.871
QFracture NOF 10yr	0.799	0.036	0.727-0.870
QFracture Any 5 yr	0.779	0.038	0.705-0.854
QFracture Any 10yr	0.779	0.038	0.705-0.854

Table 7.11 ROC curve analysis of the QFracture tool output variables in predicting the presence of osteoporosis

If a threshold of 10% is taken with the QFracture 10 year all fracture risk in line with recent SIGN guidelines then this yields a test with a poor sensitivity of 33.3%, though excellent specificity of 92.8%. This finding highlighted important differences between FRAX and QFracture in terms of the absolute risk predicted and the dangers of assuming equivalence when setting threshold of risk for example in referral for bone density scanning. Setting a lower QFracture 10-year all fracture risk of 5% would give a sensitivity of 68.9% and specificity 76.1% which shows poorer sensitivity to FRAX whilst improving specificity. Overall this would suggest there remains a need for improved risk stratification within the context of the coeliac population.

7.7.3 Identification of disease specific risk factors

Identification of further disease specific factors with a possible contribution to the development of osteoporosis were identified by case note review. The distribution of these factors between cases and controls is illustrated in Table 7.12 (2 sided student T test for continuous variables, and Fishers exact test for categorical variables).

Characteristic	Osteoporosis (n=45)	Controls (n=209)	p value
Baseline TTG off scale	12/45 (26.7%)	33/209 (15.8%)	0.09
Duration of disease	92.91 (±94.37)	115.41 (±120.00)	0.23
<2 yrs disease duration	13/45 (28.9%)	46/209 (22.0%)	0.33
Number TTG positive	0.84 (±1.29)	0.74 (±1.43)	0.68
% TTG test positive	25.0% (±34.9)	22.6% (±36.9)	0.72
Biopsy grading (n=129)	Marsh 1: 0/21 Marsh 2: 0/21 Marsh 3a: 14/21 Marsh 3b: 4/21 Marsh 3c: 3/21	Marsh 1: 10/108 Marsh 2: 0 Marsh 3a: 65/108 Marsh 3b: 9/108 Marsh 3c: 21/108	0.27
Number of co-morbidities	0.60 (±0.81)	0.39 (±0.69)	0.08
OPG Ab concentration	6.67 RU (±6.52)	4.71 RU (±4.24)	**0.01**
OPG antibody status	5/45 (11.1%)	6/209 (2.9%)	**0.03**
Ca intake (daily)	875mg (± 297)	896mg (± 355)	0.72
Age of menopause (n=112)	47.12 (± 5.57)	48.88 (± 4.56)	0.08
Premature menopause (<45 yrs)	9/45 (20%)	12/209 (5.7%)	**<0.01**

Table 7.12 Disease specific risk factors for osteoporosis in coeliac disease cohort. OPG antibody determined by ELISA II. Antibody status defined as level greater than the mean plus three standard deviations in healthy controls (14.3RU)

Only OPG antibody (whether as a continuous variable or categorical variable) and premature menopause were significantly associated with osteoporosis in this case control analysis. Premature menopause remained significantly associated with development of osteoporosis even on multivariate analysis including gender and age ($p=0.015$) suggesting that this could be a useful risk modifier. A markedly elevated TTG levels at baseline and the number of comorbidities missed statistical significance relatively narrowly and may be worth pursuing in a larger cohort. Overall duration of disease was not correlated with development of osteoporosis though it is plausible that both short duration (due to the immediate effects of coeliac disease) and long disease duration (simply due to an association with ageing) would be associated with increased risk of osteoporosis. As evidence of the latter phenomenon a strong correlation was observed between disease duration and age at recruitment (Pearson correlation coefficient 0.19, $p=0.002$). Interestingly a disease duration <2 years is associated with osteoporosis on a multivariate analysis that included age as a covariate ($p<0.05$) suggesting that this could be a useful addition to a multivariate risk prediction model. Although biopsy grading has been reported to be a predictor of osteoporosis[159] in coeliac disease this was not replicated in this dataset. Unfortunately in this cohort the pathological report was available in just over half of cases only, and the Marsh grading had to be inferred from the report, rather than being consistently reported which are significant limitations in this analysis. A number of measures aimed at assessing dietary compliance indirectly using TTG levels showed no evidence of difference between the groups.

7.7.4 Utility of novel factors in a risk prediction model

Whilst the number of cases within this cohort remains small, a preliminary assessment of the utility of the identified variables in a risk prediction model was performed. Variables with significant association with osteoporosis status were selected, namely OPG antibody titre, premature menopause and disease duration less than 2 years and modelled in female patients. The QFracture and FRAX hip scores were taken forward as performing slightly better on the ROC analysis than their respective all fracture prediction counterparts. In combination with either of these hip scores OPG antibody titre, premature menopause and disease duration less than 2 years were analysed by best subset analysis on Minitab. The output generated with

inclusion of the FRAX hip score (Table 7.13) and QFracture hip score (Table 7.14) are shown.

Variable	R-Sq	FRAX hip score	Premature menopause	OPG Antibody titre	Disease duration <2yrs
1	17.1%	**X**			
1	6%		**X**		
1	4.4%			**X**	
1	0.4%				**X**
2	21%	**X**	**X**		
2	21.3%	**X**		**X**	
2	18.1%	**X**			**X**
2	10.6%		**X**	**X**	
2	6.6%		**X**		**X**
3	25.4%	**X**	**X**	**X**	
3	22.1%	**X**	**X**		**X**
3	22.8%	**X**		**X**	**X**
3	11.6%		**X**	**X**	**X**
4	27.1%	**X**	**X**	**X**	**X**

Table 7.13 Best subset analysis incorporating FRAX hip score

The greatest contributors in each case are the individual fracture risk scores explaining 15.7 to 17.1% of the variability and both significantly associated with osteoporosis status ($p<0.001$). Premature menopause contributed 6% of the R^2 individually, and approximately 5% increase in R^2 in combination whilst remaining significantly associated with outcome ($p=0.001$). Inclusion of OPG antibodies increased the R^2 value by 4% either alone or in combination and was also significantly associated with outcome in this model ($p=0.001$). Disease duration less than 2 years contributed a modest 0.4% increase in the R^2 value only and in this analysis was not significantly associated with outcome ($p=0.11$) suggesting that it should be removed from future models.

Variable	R-Sq	QFracture hip score	Premature menopause	OPG Antibody titre	Disease duration <2yrs
1	15.7%	**X**			
1	6.0%		**X**		
1	4.4%			**X**	
1	0.4%				**X**
2	19.6%	**X**	**X**		
2	19.9%	**X**		**X**	
2	16.4%	**X**			**X**
2	10.6%		**X**	**X**	
2	6.6%		**X**		**X**
3	24%	**X**	**X**	**X**	
3	20.4%	**X**	**X**		**X**
3	20.9%	**X**		**X**	**X**
3	11.6%		**X**	**X**	**X**
4	25.2%	**X**	**X**	**X**	**X**

Table 7.14 Best subset analysis incorporating QFracture hip score

A model incorporating FRAX hip score, premature menopause and OPG antibody improved all parameters over the FRAX score alone with an R^2 of 27.1. Similar results were seen with the use of the QFracture hip score with a modestly lower R^2 of 25.2%.

7.8 Discussion

OPG autoantibodies were significantly raised in patients with coeliac disease compared to healthy controls with a prevalence of 5% (ELISA protocol II). Within this cohort the presence and titre of OPG autoantibody was associated with significantly lower spine BMD, and a non-significant trend to lower BMD at the hip. The association is driven by a relatively small number of positive cases and needs to be treated with some caution. The association is robust and unaffected by log transformation of the data, which will reduce the influence of more extreme results. Similarly the association withstood multivariate analyses of potential confounders such as age, sex, weight and height and is consistent with a pathogenic role for these antibodies in a subset of patients with coeliac disease.

Within the IBD cohort whilst numerically lower bone density scores were seen in patients with OPG antibodies, the statistical association was weaker than in the coeliac cohort. Significant association between OPG antibodies and reduced BMD was seen only with hip Z scores on univariate analysis, though adjustment for age revealed significant association with hip T scores also. These associations were confounded by features of worsened disease severity since the patients with OPG antibodies suffered a significantly longer disease duration as well as all having Crohn's disease. Perhaps unsurprisingly for a condition not associated with autoantibody production, the absolute titres of OPG antibody were not significantly raised in this cohort when compared to healthy controls. From this small cohort it was not possible to conclude that OPG antibodies are associated with the development of osteoporosis in IBD therefore.

The clinical utility of measuring OPG antibodies has not been established. Whilst OPG antibodies appeared to be an independent predictor of osteoporosis in coeliac disease further work will be required to demonstrate that there is a clinical utility in identifying OPG antibodies. A number of observations can still be made from this modelling work. In general the available fracture risk scores do not provide a clinically useful guide to the development of osteoporosis in coeliac disease. In women premature menopause appears to be a useful additional factor in a risk

prediction model with increased explanatory power apparently added in models incorporating both premature menopause and OPG antibodies, and it will be interesting to explore the utility of these factors in a larger cohort of coeliac patients.

The finding that only a proportion of the serum samples with OPG antibodies were able to demonstrate functional inhibition of OPG may go some way to explain the difficulties in establishing a link between the presence of OPG antibodies and clinical outcomes. It is well established that naturally occurring antibodies recognising self-antigens occur, though these are typically thought to be of low affinity and rarely pathogenic. Such natural antibodies are usually IgM antibodies which would not be expected to be purified in the Protein G agarose beads that were used here, however IgG natural autoantibodies are also recognised[198]. It is of course important to consider not just the affinity but also the epitope specificity of the antibody with recognition of a non-functional domain of the OPG presumably less likely to cause functional inhibition.

Chapter 8: Discussion

8.1 Introduction

Many different factors are involved in the determination of peak bone mass and subsequent bone loss. In all patients identified as having osteoporosis a search should be undertaken for underlying conditions that may predispose toward osteoporosis. The very severe phenotype of the patient presented in Chapter 3 prompted extensive further investigation into an underlying cause. Such investigations are justified on two counts. Firstly the identification of a treatable underlying condition will directly affect the management of the individual patient. Secondly the investigation of patients with extreme phenotypes can yield important insights into the pathogenesis and treatment of disease in patients with more typical presentations[199].

This patient was identified as having coeliac and thyroid disease yet his bone density deteriorated despite appropriate management of these conditions. Whilst osteoporosis is a common complication of many autoimmune diseases it is typically attributed to disease specific factors or steroid treatment rather than a direct autoimmune process[147, 200]. It is well recognised however that patients with an autoimmune condition are more likely to develop other autoimmune diseases[193] and autoantibodies to endogenous cytokines are increasingly recognised as a cause of disease pathogenesis[174]. This prompted a search for an autoimmune aetiology of the patient's high bone turnover osteoporosis, and ultimately led to the identification of autoantibodies to OPG.

This is the first report of a bone disease occurring in association with the spontaneous development of autoantibodies to OPG. OPG antibodies have previously been reported, but occurred in the context of treatment with a recombinant immunoglobulin Fc region-OPG construct resulting in the discontinuation of treatment but no apparent disease [191]. The bone disease in this index patient was extreme, with bone density T score falling to a nadir of -7.1 in the spine, multiple vertebral fractures resulting in height loss of 6cm and very high bone turnover. Unlike many patients with coeliac disease there was no improvement in his bone

density with a gluten-free diet and calcium and vitamin D replacement, yet his response to treatment with the anti-resorptive zoledronate (Aclasta) was astonishing. Treatment with the anti-RANKL monoclonal denosumab (Prolia) did not prove as effective in this patient despite this intuitively being a more attractive approach. It is possible that the usual treatment regime for osteoporosis was inadequate in this patient, and even conceivable that the loss of efficacy was the result of a further autoantibody response to the denosumab treatment, though this is speculation. The high and persisting levels of OPG antibody seen in the index patient even raise the possibility of treatment with B cell depleting therapies such as rituximab (Mabthera), though given the potentially serious adverse effects reported with the therapy this approach has not been adopted to date[201].

8.2 Challenges

8.2.1 Identification of OPG autoantibodies

The first aim of this thesis was to establish if immunoglobulins isolated from the index patient were capable of recognising OPG in-vitro. An assay for OPG autoantibodies was developed initially by modifying a commonly used immunoprecipitation technique for the identification of cellular proteins. Instead of probing for the presence of a protein with specific antibody however, OPG was introduced and the assay used to test for the presence of recognising antibody. This technique did indeed result in robust precipitation of OPG using serum from the index case providing an initial proof of concept that OPG autoantibodies were present. As has been discussed in Section 4.8 even with serum from the index case there was substantial variability in the intensity of bands seen despite attempts to standardise the assay and whilst an OPG signal was seen in a small number of patients with severe osteoporosis and coeliac disease this proved both laborious and difficult to quantify. Given these practical limitations attention turned to developing an alternative assay.

There were considerable challenges in developing a quantifiable, and high throughput, assay for OPG autoantibodies. The initial indirect ELISA approach (Section 2.3.1) again demonstrated proof of principle that serum from the index case

would compete out the signal from commercial anti-OPG autoantibodies, but the dynamic range of the assay was very limited and unlikely to yield a test capable of recognising anything but a very strong signal equivalent to that seen in the index case. Subsequently a direct ELISA was developed which did show a greater than 10 fold increase in signalling with the positive control over negative serum samples, and appeared much more promising to use as a screening tool. A major challenge with this assay has been ensuring reproducibility of results using the direct ELISA. (a detailed discussion of the refinements to the assay are given in Section 4.8). The variability in results seen, as well as the essentially arbitrary nature of any threshold chosen to define the presence of an antibody mean that the estimates of prevalence of antibodies in different populations must be treated with caution. At a fundamental level these results support the thesis that the occurrence of OPG autoantibodies was not a unique event, but is also occurring in a small proportion of patients with established osteoporosis or immune mediated disease.

8.2.2 Demonstration of inhibition of OPG function

The pathological significance of any autoantibody is likely to be influenced by a combination of titre, affinity and epitope specificity, with the most compelling evidence of pathogenicity provided by transmission of disease in vivo with transfer of autoantibody. The ELISA assay is able to demonstrate the presence of autoantibody recognising part(s) of the whole OPG protein, but in order to provide additional evidence of possible pathological effect an in-vitro assay was developed to identify if the autoantibody was also capable of blocking the effects of OPG in vitro.

A number of cell signalling systems were explored in this respect (Section 2.2) with more physiological systems based on the generation of alkaline phosphatase in macrophage based RAW cell lines unfortunately not proving suitable as the cells were not responsive to RANKL. Fortuitously a HEK 293 cell line that was stably transfected with an Nf-κB luciferase reporter was found to respond to RANKL and with this it proved possible to demonstrate that serum from the index patient and serum from a proportion of the positive samples found from populations screened were capable of inhibiting the function of OPG in vitro. This result corroborated the result of the IP assay and ELISA, and also lends credence to the concept that the

autoantibodies identified were capable of inhibiting the function of OPG in-vivo and so causing disease. The finding that only a proportion of the serum samples with OPG antibodies were able to demonstrate functional inhibition of OPG may go some way to explain the difficulties in establishing a link between the presence of OPG antibodies and clinical outcomes, with these positive samples by ELISA potentially representing false positives, antibodies directed against non-functional epitopes or low affinity antibodies incapable of interfering in OPG function.

8.2.3 Clinical significance of OPG autoantibodies

Within a general population autoantibodies to OPG were identified in 1.6% based on an arbitrary cut-off of the mean plus 3 standard deviations of healthy controls. No correlation with bone density or bone turnover was observed in these patients suggesting that these antibodies are not pathological and represent false positives or non-functional antibodies. This also implies that OPG antibodies are not a common cause of osteoporosis in the general population. An association with vascular calcification was observed which conflicts with the conclusion that these OPG antibodies are benign but requires replication in view of the small number of samples with positive OPG antibodies in this cohort. If confirmed, this could be explained by the identified OPG antibodies being a marker for a previous episode of high bone turnover resolved by some compensatory biological response, or by OPG antibodies being directly implicated in vascular calcification independently of effects on bone. Equally this result could be explained by OPG antibodies representing an epiphenomenon of increased bone turnover or vascular calcification.

Within a cohort of patients with osteoporosis, an increased prevalence of OPG antibodies was observed, though this does not act as a marker of lower bone density and was associated with inconsistent changes in markers of bone turnover. Within this cohort, most patients have already been treated with antiresorptive therapies which would be expected to influence these results. An increased prevalence of OPG antibodies was also seen in patients with coeliac disease, which is unsurprising given the manifest tendency to autoimmunity in these patients. In this cohort, the presence of OPG antibodies is associated with lower bone density again consistent with a

pathological role of the antibodies, though compatible also with OPG antibodies being an epiphenomenon of bone disease ie association does not prove causality. The *in-vitro* studies showing that a proportion of these antibodies are functional support the conclusion that for some patients at least OPG antibodies contribute to the pathogenesis of osteoporosis.

The clinical utility of measuring OPG antibodies has not been established however. In an exploratory analysis it would appear that identification of OPG antibodies might help in identifying osteoporosis in coeliac patients, though it is unlikely that this small additive benefit would mean a move away from current practice of screening all newly diagnosed patients by DEXA scanning. Similarly in the osteoporosis cohort the subgroup of patients identified as having OPG autoantibodies did not respond differently to treatment than the patients without antibodies. At present these results provide evidence for an additional autoimmune mechanism of disease in osteoporosis, but have not demonstrated that identification of OPG autoantibodies would materially influence the management of any individual patient.

In a study of this nature there is an inherent danger of over interpreting chance observations in the context of relatively small disease cohorts. The significant associations observed between OPG antibody presence and reduced bone mineral density in the IBD and coeliac cohorts are driven by relatively small numbers of patients with the highest antibody concentrations. Given the extreme phenotype seen in the index case excluding the most extreme results runs the risk of excluding the most relevant patients from the study, but at the same time such outliers will heavily influence the results. The association of OPG antibody with reduced hip bone density observed in the IBD cohort may indeed be a chance effect influenced by confounding features of increased disease severity. The association of OPG antibody with reduced spine bone density in the coeliac cohort appears more robust. Standard regression diagnostics confirmed that the model satisfied assumptions of linear regression, and. repeating the analysis with log transformed data did not materially alter the conclusions. Equally the finding was not affected by inclusion of common confounders in a multivariate analysis, and a search for potential disease associated

confounders did not reveal any significant correlations with OPG antibody. Clearly in a complex disease such as osteoporosis it is difficult to control for all the many potential confounding disease and treatment associated factors and given these difficulties it will be critical to see these results replicated in larger and independent cohorts.

8.3 Context of the current study

The current case report remains the only description of disease associated with the development of autoantibodies to OPG[202]. In the original published report an immunoprecipitation assay was used to identify autoantibodies and, as has been discussed already (Section 4.2), this assay was found to be unsuitable for population screening. Developing a more sensitive and reproducible assay has been difficult even with a positive control sample with which to guide optimisation of assay conditions. It is disappointing, though perhaps not surprising, that to date no further case of disease associated with OPG autoantibodies has been reported. The only work published to date that has attempted to replicate this work screened a small cohort of 30 coeliac patients using the immunoprecipitation assay without finding any positive samples[203].

Naturally occurring self-reactive autoantibodies have long been recognized, though their role in normal physiology, as well as in disease pathogenesis, is the subject of ongoing research [174, 194, 204]. This appears to be a promising field of research offering insights into diverse conditions previously considered unexplained or idiopathic. This is an expanding field with the power of protein arrays and mass spectrometry technologies facilitating the identification of novel autoantigens. What this thesis highlights is the many practical difficulties that translating a proof of concept that a novel autoantibody does occur naturally, into knowledge that can be used in some clinically useful manner. This includes the difficulty of developing robust assays to both identify and characterise novel autoantibodies, but equally given the many contributors to complex diseases such as osteoporosis it highlights the importance of building biobanks of samples from well phenotyped patients to allow the clinical significance of such antibodies over a patient's disease course to be evaluated.

OPG was identified as a key inhibitor of osteoclast development and this thesis has naturally focussed primarily on the possible skeletal manifestations of autoantibodies to OPG, but there are other potential applications of the study. As has been mentioned in the introduction (Section 1.3.5) there is already substantial evidence for a role of OPG in the development of vascular calcification with this concept supported by human studies, animal models and in-vitro work[104,105,106 107]. This may be explained by effects on RANKL with elevated levels of RANK and RANKL having been identified in atherosclerotic lesions where they are associated with increased expression of BMP-2 as well as decreased expression of matrix Gla protein (MGP) a key inhibitor of mineralisation[108], however an alternative mechanism independent of RANKL has also been suggested. OPG acts as a decoy receptor for TNF related apoptosis inducing ligand (TRAIL) and both TRAIL and OPG have been identified in atherosclerotic plaques, with TRAIL also shown to enhance the mineralisation of VSMCs *in-vitro*[114].

TRAIL is primarily known as a lymphokine that induces apoptosis in tumour cells, implicating OPG in cancer biology[205]. This is in addition to the direct recognition of OPG via a heparin binding domain that has been implicated in myeloma bone disease[206]. Further complexity is added by studies showing the proteoglycans in the tumour milieu are capable of binding OPG and interfering with OPG activity in a mouse model of osteosarcoma[207]. An array of reported roles for OPG has recently been reviewed with the binding of glycosaminoglycans by OPG potentially contributing to chemotaxis of monocytes and even the migration of endothelial cells, and an interaction with von Willebrand factor and Factor VII/von Willebrand factor complex suggesting a role for OPG in vascular injury and thrombus formation[208]. To date the index case has not been identified as having any other serious manifestations of disease associated with OPG deficiency, though mild vascular calcification was detected on a screening CT scan.

8.4 Future aims

The immediate priority will be to expand the numbers of patients with coeliac disease and established osteoporosis that have been presented here, and reassess the associations with bone mineral density and fracture in larger numbers, as well as the clinical significance of identified OPG antibodies. It is anticipated that these results should be available for submission within the year. Current collaborations have already looked at the results of the OPG ELISA in cohorts of patients with rheumatic disease such as rheumatoid arthritis and ankylosing spondylitis[209]. There great potential to expand this work with interest expressed from a number of potential collaborators already in possession of serum samples from well phenotyped population and study cohorts. The rate limiting factor in this has been the performance of the ELISA which has hindered development of such collaborations. Some modifications have been made by Prof Bill Fraser in University of East Anglia and approaches have been made to biotechnology companies interested in this field which it is hoped will allow replication of these findings in other settings. This is progressing, albeit slowly.

The current ELISA uses whole recombinant OPG as a capture antigen in order to identify autoantibodies recognising all exposed epitopes of OPG. The results presented in this thesis have shown that functional inhibition of OPG is demonstrable only in a proportion of the positive samples identified by ELISA. It is possible that only antibodies against specific regions within OPG are capable of inhibiting function, and as such work has already been undertaken to generate recombinant fragments of OPG in order to fine map this immune response. OPG consists of four amino terminal cysteine rich domains required for the binding of RANKL[210, 211], as well as a heparin binding domain and two death domain homologous regions at the carboxy terminal end[210, 212]. Two large ~100 amino acid fragments of OPG from the functional domains of OPG have been expressed in bacterial plasmids and both have shown reactivity to serum from the index patient and selected positive samples[213]. The large fragments used in these experiments were unable to detect any differential epitope specificity in the serum samples analysed although this work has already established that the OPG autoantibody response is capable of recognising diverse

epitopes within OPG in keeping with a polyclonal antibody response. Further work with smaller fragments could be useful to fine map these responses.

8.5 Conclusions

The results presented here identify a novel mechanism of osteoporosis mediated by autoantibodies to OPG. Whilst the clinical presentation of the index case was exceptionally severe and appears rather unique, the results of screening populations of idiopathic osteoporosis patients and patients with coeliac disease are consistent with a pathogenic role for OPG antibodies in a number of these patients with more typical presentations of osteoporosis. Whilst this is an interesting observation, it should be tempered by the practical observation that no clinical utility in identifying the presence of OPG antibodies has been demonstrated in either cohort. Clearly it remains possible that an analysis of larger cohorts, or better characterisation of the antibody functionality may yet yield clinically useful insight. It will also be important to identify patients who have recently developed OPG antibodies in whom treatment effect, or potentially physiological compensation, will not have occurred. The coeliac cohort lends itself particularly well to this work, since they are clearly a population at heightened risk of developing autoantibodies in whom intervention with antiresorptive therapies is not usually given in the initial period after diagnosis, hence removing this important confounding effect on bone density and bone turnover. Work is ongoing to build a large cohort of coeliac patients in whom these questions can be further addressed.

Reference List

1. Assessment of fracture risk and its application to screening for postmenopausal osteoporosis. Report of a WHO Study Group. World Health Organization technical report series 1994;843:1-129.

2. Wright NC, Looker AC, Saag KG et al. The recent prevalence of osteoporosis and low bone mass in the United States based on bone mineral density at the femoral neck or lumbar spine. J Bone Miner Res 2014;29(11):2520-2526.

3. Looker AC, Melton LJ, III, Harris TB, Borrud LG, Shepherd JA. Prevalence and trends in low femur bone density among older US adults: NHANES 2005-2006 compared with NHANES III. J Bone Miner Res 2010;25(1):64-71.

4. Cummings SR, Black DM, Nevitt MC et al. Bone density at various sites for prediction of hip fractures. The Study of Osteoporotic Fractures Research Group. Lancet 1993;341(8837):72-75.

5. Holroyd C, Cooper C, Dennison E. Epidemiology of osteoporosis. Best Practice & Research Clinical Endocrinology & Metabolism 2008;22(5):671-685.

6. Svedbom A, Hernlund E, Ivergard M et al. Osteoporosis in the European Union: a compendium of country-specific reports. Arch Osteoporos 2013;8(1-2):137.

7. Brauer CA, Coca-Perraillon M, Cutler DM, Rosen AB. Incidence and mortality of hip fractures in the United States. JAMA 2009;302(14):1573-1579.

8. Alendronate, etidronate risedronate, raloxifene, strontium ranelate and teriparatide for the secondary prevention of osteoporotic fragility fractures in postmenopausal women (amended). NICE Clinical Guideline 161 2008.

9. Management of osteoporosis and the prevention of fragility fracture. SIGN Guideline No 142 2015;(ISBN 978 1 909103 35 1).

10. National Institute for Health and Clinical Excellence. Osteoporosis: assessing the risk of fragility fracture: Clinical Guideline CG146: Aug. 2012

11. National Osteoporosis Foundation. Clinician's Guide to Prevention and Treatment of Osteoporosis. Washington, DC: National Osteoporosis Foundation. 2013

12. Mattinson A, Hauser B, Gillett H et al. The Frax Algorithm is of Limited Utility in Predicting Osteoporosis in Coeliac Disease. Gut 2013;62 (Supplement 1):A263.

13. Clarke B. Normal Bone Anatomy and Physiology. Clinical Journal of the American Society of Nephrology 2008;3(Supplement 3):S131-S139.

14. Baron R, Kneissel M. WNT signaling in bone homeostasis and disease: from human mutations to treatments. Nat Med 2013;19(2):179-192.

15. Huddleston AL, Rockwell D, Kulund DN, Harrison RB. Bone mass in lifetime tennis athletes. JAMA 1980;244(10):1107-1109.

16. Suda T, Takahashi N, Udagawa N, Jimi E, Gillespie MT, Martin TJ. Modulation of osteoclast differentiation and function by the new members of the tumor necrosis factor receptor and ligand families. Endocr Rev 1999;20:345-357.

17. Garabedian M, Holick MF, DeLuca HF, Boyle IT. Control of 25-hydroxycholecalciferol metabolism by parathyroid glands. Proc Natl Acad Sci U S A 1972;69(7):1673-1676.

18. Bouillon R, Van CS, Carmeliet G. Intestinal calcium absorption: Molecular vitamin D mediated mechanisms. J Cell Biochem 2003;88(2):332-339.

19. Zaidi M, Inzerillo AM, Moonga BS, Bevis PJ, Huang CL. Forty years of calcitonin--where are we now? A tribute to the work of Iain Macintyre, FRS. Bone 2002;30(5):655-663.

20. Krum SA, Miranda-Carboni GA, Hauschka PV et al. Estrogen protects bone by inducing Fas ligand in osteoblasts to regulate osteoclast survival. EMBO J 2008;27(3):535-545.

21. Nakamura T, Imai Y, Matsumoto T et al. Estrogen prevents bone loss via estrogen receptor alpha and induction of Fas ligand in osteoclasts. Cell 2007;130(5):811-823.

22. Zallone A. Direct and indirect estrogen actions on osteoblasts and osteoclasts. Ann N Y Acad Sci 2006;1068:173-179.

23. Riggs BL, Wahner HW, Melton LJ, Richelson LS, Judd HL, Offord KP. Rates of bone loss in the appendicular and axial skeletons of women. J Clin Invest 1986;77:1487-1491.

24. Brown LB, Streeten EA, Shapiro JR et al. Genetic and environmental influences on bone mineral density in pre- and post-menopausal women. Osteoporos Int 2005;16(12):1849-1856.

25. McGuigan FE, Murray L, Gallagher A et al. Genetic and environmental determinants of peak bone mass in young men and women. J Bone Miner Res 2002;17(7):1273-1279.

26. Rubin LA, Hawker GA, Peltekova VD, Fielding LJ, Ridout R, Cole DE. Determinants of peak bone mass: clinical and genetic analyses in a young female Canadian cohort. Journal of Bone & Mineral Research 1999;14(4):633-643.

27. Koller DL, Zheng HF, Karasik D et al. Meta-analysis of genome-wide studies identifies WNT16 and ESR1 SNPs associated with bone mineral density in premenopausal women. J Bone Miner Res 2013;28(3):547-558.

28. Armstrong VJ, Muzylak M, Sunters A et al. Wnt/beta-catenin signaling is a component of osteoblastic bone cell early responses to load-bearing and requires estrogen receptor alpha. J Biol Chem 2007;282(28):20715-20727.

29. Gunter K, Baxter-Jones AD, Mirwald RL et al. Impact exercise increases BMC during growth: an 8-year longitudinal study. J Bone Miner Res 2008;23(7):986-993.

30. Estrada K, Styrkarsdottir U, Evangelou E et al. Genome-wide meta-analysis identifies 56 bone mineral density loci and reveals 14 loci associated with risk of fracture. Nat Genet 2012;44(5):491-501.

31. Riggs BL, Khosla S, Melton LJ, III. A unitary model for involutional osteoporosis: estrogen deficiency causes both type I and type II osteoporosis in postmenopausal women and contributes to bone loss in aging men. J Bone Miner Res 1998;13(5):763-773.

32. Felson DT, Zhang Y, Hannan MT, Kiel DP, Wilson PW, Anderson JJ. The effect of postmenopausal estrogen therapy on bone density in elderly women. N Engl J Med 1993;329(16):1141-1146.

33. Laurent M, Gielen E, Claessens F, Boonen S, Vanderschueren D. Osteoporosis in older men: recent advances in pathophysiology and

treatment. Best Pract Res Clin Endocrinol Metab 2013;27(4):527-539.

34. Khosla S, Melton LJ, III, Riggs BL. The unitary model for estrogen deficiency and the pathogenesis of osteoporosis: is a revision needed? J Bone Miner Res 2011;26(3):441-451.

35. Manolagas SC. From estrogen-centric to aging and oxidative stress: a revised perspective of the pathogenesis of osteoporosis. Endocr Rev 2010;31(3):266-300.

36. Pye SR, Devakumar V, Boonen S et al. Influence of lifestyle factors on quantitative heel ultrasound measurements in middle-aged and elderly men. Calcif Tissue Int 2010;86(3):211-219.

37. Gomez-Cabello A, Ara I, Gonzalez-Aguero A, Casajus JA, Vicente-Rodriguez G. Effects of training on bone mass in older adults: a systematic review. Sports Med 2012;42(4):301-325.

38. Painter SE, Kleerekoper M, Camacho PM. Secondary osteoporosis: a review of the recent evidence. Endocr Pract 2006;12(4):436-445.

39. Hofbauer LC, Hamann C, Ebeling PR. Approach to the patient with secondary osteoporosis. Eur J Endocrinol 2010;162(6):1009-1020.

40. van Staa T. The Pathogenesis, Epidemiology and Management of Glucocorticoid-Induced Osteoporosis. Calcif Tiss Int 2006;79(3):129-137.

41. Hofbauer LC, Gori F, Riggs BL et al. Stimulation of Osteoprotegerin Ligand and Inhibition of Osteoprotegerin Production by Glucocorticoids in Human Osteoblastic Lineage Cells: Potential Paracrine Mechanisms of Glucocorticoid-Induced Osteoporosis. Endocrinology 1999;140(10):4382-4389.

42. Schakman O, Kalista S, Barbe C, Loumaye A, Thissen JP. Glucocorticoid-induced skeletal muscle atrophy. Int J Biochem Cell Biol 2013;45(10):2163-2172.

43. Mackie EJ, Tatarczuch L, Mirams M. The skeleton: a multi-functional complex organ. The growth plate chondrocyte and endochondral ossification. J Endocrinol 2011;211(2):109-121.

44. Sroga GE, Vashishth D. Effects of bone matrix proteins on fracture and fragility in osteoporosis. Curr Osteoporos Rep 2012;10(2):141-150.

45. Long F. Building strong bones: molecular regulation of the osteoblast lineage. Nat Rev Mol Cell Biol 2012;13(1):27-38.

46. Komori T. Regulation of osteoblast differentiation by transcription factors. J Cell Biochem 2006;99(5):1233-1239.

47. St-Jacques B, Hammerschmidt M, McMahon AP. Indian hedgehog signaling regulates proliferation and differentiation of chondrocytes and is essential for bone formation. Genes Dev 1999;13(16):2072-2086.

48. Karp SJ, Schipani E, St-Jacques B, Hunzelman J, Kronenberg H, McMahon AP. Indian hedgehog coordinates endochondral bone growth and morphogenesis via parathyroid hormone related-protein-dependent and -independent pathways. Development 2000;127(3):543-548.

49. Liu ZJ, Zhuge Y, Velazquez OC. Trafficking and differentiation of mesenchymal stem cells. J Cell Biochem 2009;106(6):984-991.

50. Krause C, Korchynskyi O, de RK et al. Distinct modes of inhibition by sclerostin on bone morphogenetic protein and Wnt signaling pathways. J Biol Chem 2010;285(53):41614-41626.

51. Balemans W, Patel N, Ebeling M et al. Identification of a 52 kb deletion downstream of the SOST gene in patients with van Buchem disease. J Med Genet 2002;39(2):91-97.

52. Balemans W, Van Den EJ, Freire Paes-Alves A et al. Localization of the gene for sclerosteosis to the van Buchem disease- gene region on chromosome 17q12-q21. Am J Hum Genet 1999;64(6):1661-1669.

53. Semenov MV, He X. LRP5 mutations linked to high bone mass diseases cause reduced LRP5 binding and inhibition by SOST. J Biol Chem 2006;281(50):38276-38284.

54. Gong Y, Slee RB, Fukai N et al. LDL Receptor-Related Protein 5 (LRP5) Affects Bone Accrual and Eye Development. Cell 2001;107(4):513-523.

55. Yadav VK, Ryu JH, Suda N et al. Lrp5 controls bone formation by inhibiting serotonin synthesis in the duodenum. Cell 2008;135(5):825-837.

56. Cui Y, Niziolek PJ, MacDonald BT et al. Reply to Lrp5 regulation of bone mass and gut serotonin synthesis. Nat Med 2014;20(11):1229-1230.

57. DeKoter RP, Walsh JC, Singh H. PU.1 regulates both cytokine-dependent proliferation and differentiation of granulocyte/macrophage progenitors. EMBO J 1998;17(15):4456-4468.

58. Kwon OH, Lee CK, Lee YI, Paik SG, Lee HJ. The hematopoietic transcription factor PU.1 regulates RANK gene expression in myeloid progenitors. Biochem Biophys Res Commun 2005;335(2):437-446.

59. Kodama H, Nose M, Niida S, Yamasaki A. Essential role of macrophage colony-stimulating factor in the osteoclast differentiation supported by stromal cells. J Exp Med 1991;173(5):1291-1294.

60. Kong YY, Yoshida H, Sarosi I et al. OPGL is a key regulator of osteoclastogenesis, lymphocyte development and lymph-node organogenesis. Nature 1999;397(6717):315-323.

61. Mellis DJ, Itzstein C, Helfrich MH, Crockett JC. The skeleton: a multi-functional complex organ. The role of key signalling pathways in osteoclast differentiation and in bone resorption. J Endocrinol 2011;211(2):131-143.

62. Iotsova V, Caamano J, Loy J, Yang Y, Lewin A, Bravo R. Osteopetrosis in mice lacking NF-kappaB1 and NF-kappaB2 [see comments]. Nat Med 1997;3:1285-1289.

63. Ikeda F, Nishimura R, Matsubara T et al. Critical roles of c-Jun signaling in regulation of NFAT family and RANKL-regulated osteoclast differentiation. J Clin Invest 2004;114(4):475-484.

64. Franzoso G, Carlson L, Xing L et al. Requirement for NF-kappaB in osteoclast and B-cell development. Genes & Development 1997;11(24):3482-3496.

65. Grigoriadis AE, Wang ZQ, Cecchini MG et al. c-Fos: a key regulator of osteoclast-macrophage lineage determination and bone remodeling. Science 1994;266(5184):443-448.

66. Takayanagi H, Kim S, Koga T et al. Induction and activation of the transcription factor NFATc1 (NFAT2) integrate RANKL signaling in terminal differentiation of osteoclasts. Dev Cell 2002;3(6):889-901.

67. Mocsai A, Humphrey MB, Van Ziffle JA et al. The immunomodulatory adapter proteins DAP12 and Fc receptor gamma-chain (FcRgamma) regulate development of functional osteoclasts through the Syk tyrosine kinase. Proc Natl Acad Sci U S A 2004;101(16):6158-6163.

68. Hwang SY, Putney JW. Orai1-mediated calcium entry plays a critical role in osteoclast differentiation and function by regulating activation of the transcription factor NFATc1. FASEB J 2012;26(4):1484-1492.

69. Zou W, Reeve JL, Liu Y, Teitelbaum SL, Ross FP. DAP12 couples c-Fms activation to the osteoclast cytoskeleton by recruitment of Syk. Mol Cell 2008;31(3):422-431.

70. Barrow AD, Raynal N, Andersen TL et al. OSCAR is a collagen receptor that costimulates osteoclastogenesis in DAP12-deficient humans and mice. J Clin Invest 2011;121(9):3505-3516.

71. Nakashima T, Hayashi M, Takayanagi H. New insights into osteoclastogenic signaling mechanisms. Trends Endocrinol Metab 2012;23(11):582-590.

72. Blair HC, Teitelbaum SL, Ghiselli R, Gluck S. Osteoclastic bone resorption by a polarized vacuolar proton pump. Science 1989;245(4920):855-857.

73. Eastell R, Ebeling P. Bone turnover markers: a key tool for understanding osteoporosis. Osteoporosis Int 2009;20(0):237-238.

74. Balemans W, Van WL, Van HW. A clinical and molecular overview of the human osteopetroses. Calcif Tissue Int 2005;77(5):263-274.

75. Villa A, Guerrini M, Cassani B, Pangrazio A, Sobacchi C. Infantile Malignant, Autosomal Recessive Osteopetrosis: The Rich and The Poor. Calcif Tiss Int 2009;84(1):1-12.

76. Harre U, Georgess D, Bang H et al. Induction of osteoclastogenesis and bone loss by human autoantibodies against citrullinated vimentin. J Clin Invest 2012;122(5):1791-1802.

77. Bonewald LF. The amazing osteocyte. J Bone Miner Res 2011;26(2):229-238.

78. Xiao Z, Dallas M, Qiu N et al. Conditional deletion of Pkd1 in osteocytes disrupts skeletal mechanosensing in mice. FASEB J 2011;25(7):2418-2432.

79. Robling AG, Niziolek PJ, Baldridge LA et al. Mechanical Stimulation of Bone in Vivo Reduces Osteocyte Expression of Sost/Sclerostin. J Biol Chem 2008;283(9):5866-5875.

80. Nakashima T, Hayashi M, Fukunaga T et al. Evidence for osteocyte regulation of bone homeostasis through RANKL expression. Nat Med 2011;17(10):1231-1234.

81. Qing H, Ardeshirpour L, Pajevic PD et al. Demonstration of osteocytic perilacunar/canalicular remodeling in mice during lactation. J Bone Miner Res 2012;27(5):1018-1029.

82. Feng JQ, Ward LM, Liu S et al. Loss of DMP1 causes rickets and osteomalacia and identifies a role for osteocytes in mineral metabolism. Nat Genet 2006;38(11):1310-1315.

83. Liu S, Zhou J, Tang W, Jiang X, Rowe DW, Quarles LD. Pathogenic role of Fgf23 in Hyp mice. Am J Physiol Endocrinol Metab 2006;291(1):E38-E49.

84. Liu S, Zhou J, Tang W, Menard R, Feng JQ, Quarles LD. Pathogenic role of Fgf23 in Dmp1-null mice. Am J Physiol Endocrinol Metab 2008;295(2):E254-E261.

85. Zhang LN, Yang G, Cheng C et al. Plasma FGF23 levels and heart rate variability in patients with stage 5 CKD. Osteoporos Int 2014.

86. Boukhris R, Becker KL. Calcification of the Aorta and Osteoporosis: A Roentgenographic Study. JAMA: The Journal of the American Medical Association 1972;219(10):1307-1311.

87. Anderson JB, Barnett E, Nordin BEC. The Relation between Osteoporosis and Aortic Calcification. The British Journal of Radiology 1964;37(444):910-912.

88. Alexopoulos N, Raggi P. Calcification in atherosclerosis. Nat Rev Cardiol 2009;6(11):681-688.

89. Sage AP, Tintut Y, Demer LL. Regulatory mechanisms in vascular calcification. Nat Rev Cardiol 2010;7(9):528-536.

90. Schulz E, Arfai K, Liu X, Sayre J, Gilsanz V. Aortic Calcification and the Risk of Osteoporosis and Fractures. Journal of Clinical Endocrinology Metabolism 2004;89(9):4246-4253.

91. Hyder JA, Allison MA, Wong N et al. Association of Coronary Artery and Aortic Calcium With Lumbar Bone Density: The MESA Abdominal Aortic Calcium Study. Am J Epidemiol 2009;169(2):186-194.

92. Sennerby U, Melhus H, Gedeborg R et al. Cardiovascular Diseases and Risk of Hip Fractures. JAMA: The Journal of the American Medical Association 2009;302(15):1666-1673.

93. Murshed M, Harmey D, Millan JL, McKee MD, Karsenty G. Unique coexpression in osteoblasts of broadly expressed genes accounts for the spatial restriction of ECM mineralization to bone. Genes Dev 2005;19(9):1093-1104.

94. Shanahan CM, Cary NR, Salisbury JR, Proudfoot D, Weissberg PL, Edmonds ME. Medial localization of mineralization-regulating proteins in association with Monckeberg's sclerosis: evidence for smooth muscle cell-mediated vascular calcification. Circulation 1999;100(21):2168-2176.

95. Kirton JP, Wilkinson FL, Canfield AE, Alexander MY. Dexamethasone downregulates calcification-inhibitor molecules and accelerates osteogenic differentiation of vascular pericytes: implications for vascular calcification. Circ Res 2006;98(10):1264-1272.

96. Reynolds JL, Joannides AJ, Skepper JN et al. Human vascular smooth muscle cells undergo vesicle-mediated calcification in response to changes in extracellular calcium and phosphate concentrations: a potential mechanism for accelerated vascular calcification in ESRD. J Am Soc Nephrol 2004;15(11):2857-2867.

97. Owens GK, Kumar MS, Wamhoff BR. Molecular regulation of vascular smooth muscle cell differentiation in development and disease. Physiol Rev 2004;84(3):767-801.

98. Alexander MR, Owens GK. Epigenetic control of smooth muscle cell differentiation and phenotypic switching in vascular development and disease. Annu Rev Physiol 2012;74:13-40.

99. Sage AP, Tintut Y, Demer LL. Regulatory mechanisms in vascular calcification. Nat Rev Cardiol 2010;7(9):528-536.

100. Matsumoto T, Yamada A, Aizawa R et al. BMP-2 Induced Expression of Alx3 That Is a Positive Regulator of Osteoblast Differentiation. PLoS One 2013;8(6):e68774.

101. Chen G, Deng C, Li YP. TGF-beta and BMP signaling in osteoblast differentiation and bone formation. Int J Biol Sci 2012;8(2):272-288.

102. Csiszar A, Ahmad M, Smith KE et al. Bone morphogenetic protein-2 induces proinflammatory endothelial phenotype. Am J Pathol 2006;168(2):629-638.

103. Persy V, Haese P. Vascular calcification and bone disease: the calcification paradox. Trends in molecular medicine 15[9], 405-416. 1-9-2009.
Ref Type: Abstract

104. Min H, Morony S, Sarosi I et al. Osteoprotegerin Reverses Osteoporosis by Inhibiting Endosteal Osteoclasts and Prevents Vascular Calcification by Blocking a Process Resembling Osteoclastogenesis. J Exp Med 2000;192(4):463-474.

105. Rezg R, Barreto FC, Barreto DV, Liabeuf S, Drueke TB, Massy ZA. Inhibitors of vascular calcification as potential therapeutic targets. J Nephrol 2011;24(4):416-427.

106. Bucay N, Sarosi I, Dunstan CR et al. Osteoprotegerin-deficient mice develop early onset osteoporosis and arterial calcification. Genes & Development 1998;12(9):1260-1268.

107. Whyte MP, Singhellakis PN, Petersen MB, Davies M, Totty WG, Mumm S. Juvenile Paget's disease: the second reported, oldest patient is homozygous for the TNFRSF11B "Balkan" mutation (966_969delTGACinsCTT), which elevates circulating immunoreactive osteoprotegerin levels. J Bone Miner Res 2007;22(6):938-946.

108. Osako MK, Nakagami H, Koibuchi N et al. Estrogen inhibits vascular calcification via vascular RANKL system: common mechanism of

osteoporosis and vascular calcification. Circ Res 2010;107(4):466-475.

109. Wei T, Wang M, Wang M, Gan L-Y, Li X. Relationship of sRANKL Level and Vascular Calcification Score to Cardiovascular Events in Maintenance Hemodialysis Patients. Blood Purification 2009;28(4):342-345.

110. Bezerra MC, Calomeni GD, Caparbo VF, Gebrim ES, Rocha MS, Pereira RMR. Low bone density and low serum levels of soluble RANK ligand are associated with severe arterial calcification in patients with Takayasu arteritis. Rheumatology 2005;44(12):1503-1506.

111. Nitta K, Akiba T, Uchida K et al. Serum osteoprotegerin levels and the extent of vascular calcification in haemodialysis patients. Nephrol Dial Trans 2004;19(7):1886-1889.

112. Jono S, Ikari Y, Shioi A et al. Serum Osteoprotegerin Levels Are Associated With the Presence and Severity of Coronary Artery Disease. Circulation 2002;106(10):1192-1194.

113. Rogers A, Eastell R. Circulating osteoprotegerin and receptor activator for nuclear factor kappaB ligand: clinical utility in metabolic bone disease assessment. J Clin Endocrinol Metab 2005;90(11):6323-6331.

114. Chasseraud M, Liabeuf S, Mozar A et al. Tumor necrosis factor-related apoptosis-inducing ligand and vascular calcification. Ther Apher Dial 2011;15(2):140-146.

115. Cranenburg EC, Vermeer C, Koos R et al. The circulating inactive form of matrix Gla Protein (ucMGP) as a biomarker for cardiovascular calcification. J Vasc Res 2008;45(5):427-436.

116. Hodges SJ, Akesson K, Vergnaud P, Obrant K, Delmas PD. Circulating levels of vitamins K1 and K2 decreased in elderly women with hip fracture. J Bone Miner Res 1993;8(10):1241-1245.

117. Somjen D, Weisman Y, Kohen F et al. 25-hydroxyvitamin D3-1alpha-hydroxylase is expressed in human vascular smooth muscle cells and is upregulated by parathyroid hormone and estrogenic compounds. Circulation 2005;111(13):1666-1671.

118. Khosla S. Minireview: The OPG/RANKL/RANK System. Endocrinology 2001;142(12):5050-5055.

119. Lacey DL, Timms E, Tan HL et al. Osteoprotegerin ligand is a cytokine that regulates osteoclast differentiation and activation. Cell 1998;93(2):165-176.

120. Blair JM, Zheng Y, Dunstan CR. RANK ligand. The International Journal of Biochemistry & Cell Biology 2007;39(6):1077-1081.

121. Simonet WS, Lacey DL, Dunstan CR et al. Osteoprotegerin: a novel secreted protein involved in the regulation of bone density. Cell 1997;89(2):309-319.

122. Gori F, Hofbauer LC, Dunstan CR, Spelsberg TC, Khosla S, Riggs BL. The expression of osteoprotegerin and RANK ligand and the support of osteoclast formation by stromal-osteoblast lineage cells is developmentally regulated. Endocrinology 2000;141(12):4768-4776.

123. Brandstrom H, Bjorkman T, Ljunggren OO. Regulation of Osteoprotegerin Secretion from Primary Cultures of Human Bone Marrow Stromal Cells. Biochem Biophys Res Commun 2001;280(3):831-835.

124. Udagawa N, Takahashi N, Yasuda H et al. Osteoprotegerin produced by osteoblasts is an important regulator in osteoclast development and function. Endocrinology 2000;141(9):3478-3484.

125. Rivadeneira F, Styrkársdottir U, Estrada K et al. Twenty bone-mineral-density loci identified by large-scale meta-analysis of genome-wide association studies. Nat Genet 2009;41(11):1199-1206.

126. Chong B, Hegde M, Fawkner M et al. Idiopathic hyperphosphatasia and TNFRSF11B mutations: relationships between phenotype and genotype. J Bone Miner Res 2003;18(12):2095-2104.

127. Hughes AE, Ralston SH, Marken J et al. Mutations in TNFRSF11A, affecting the signal peptide of RANK, cause familial expansile osteolysis. Nat Genet 2000;24(1):45-48.

128. Whyte MP, Hughes AE. Expansile skeletal hyperphosphatasia is caused by a 15-base pair tandem duplication in TNFRSF11A encoding RANK and is allelic to familial expansile osteolysis. J Bone Miner Res 2002;17(1):26-29.

129. Akiyama T, Shimo Y, Yanai H et al. The tumor necrosis factor family receptors RANK and CD40 cooperatively establish the thymic

medullary microenvironment and self-tolerance. Immunity 2008;29(3):423-437.

130. Loser K, Mehling A, Loeser S et al. Epidermal RANKL controls regulatory T-cell numbers via activation of dendritic cells. Nat Med 2006;12(12):1372-1379.

131. Danks L, Takayanagi H. Immunology and bone. J Biochem 2013;154(1):29-39.

132. Hsu H, Lacey DL, Dunstan CR et al. Tumor necrosis factor receptor family member RANK mediates osteoclast differentiation and activation induced by osteoprotegerin ligand. Proc Natl Acad Sci U S A 1999;96(7):3540-3545.

133. Theill LE, Boyle WJ, Penninger JM. RANK-L AND RANK: T Cells, Bone Loss, and Mammalian Evolution. Annual Review of Immunology 2002;20(1):795-823.

134. Kong YY, Feige U, Sarosi I et al. Activated T cells regulate bone loss and joint destruction in adjuvant arthritis through osteoprotegerin ligand. Nature 1999;402(6759):304-309.

135. Cohen SB, Dore RK, Lane NE et al. Denosumab treatment effects on structural damage, bone mineral density, and bone turnover in rheumatoid arthritis: A twelve-month, multicenter, randomized, double-blind, placebo-controlled, phase II clinical trial. Arth Rheum 2008;58(5):1299-1309.

136. Zhao W, Liu Y, Cahill CM, Yang W, Rogers JT, Huang X. The role of T cells in osteoporosis, an update. Int J Clin Exp Pathol 2009;2(6):544-552.

137. Yun TJ, Chaudhary PM, Shu GL et al. OPG/FDCR-1, a TNF receptor family member, is expressed in lymphoid cells and is up-regulated by ligating CD40. J Immunol 1998;161(11):6113-6121.

138. Weitzmann MN. The Role of Inflammatory Cytokines, the RANKL/OPG Axis, and the Immunoskeletal Interface in Physiological Bone Turnover and Osteoporosis. Scientifica (Cairo) 2013;2013:125705.

139. Li Y, Li A, Yang X, Weitzmann MN. Ovariectomy-induced bone loss occurs independently of B cells. J Cell Biochem 2007;100(6):1370-1375.

140. Leibbrandt A, Penninger JM. RANK/RANKL: Regulators of Immune Responses and Bone Physiology. Annals of the New York Academy of Sciences 2008;1143:123-150.

141. Bord S, Ireland DC, Beavan SR, Compston JE. The effects of estrogen on osteoprotegerin, RANKL, and estrogen receptor expression in human osteoblasts. Bone 2003;32(2):136-141.

142. Yano K, Tsuda E, Washida N et al. Immunological Characterization of Circulating Osteoprotegerin/Osteoclastogenesis Inhibitory Factor: Increased Serum Concentrations in Postmenopausal Women with Osteoporosis. J Bone Miner Res 1999;14(4):518-527.

143. Moschen AR, Kaser A, Enrich B et al. The RANKL/OPG system is activated in inflammatory bowel disease and relates to the state of bone loss. Gut 2005;54(4):479-487.

144. Rogers A, Eastell R. Circulating Osteoprotegerin and Receptor Activator for Nuclear Factor {kappa}B Ligand: Clinical Utility in Metabolic Bone Disease Assessment. Journal of Clinical Endocrinology Metabolism 2005;90(11):6323-6331.

145. Findlay D, Chehade M, Tsangari H et al. Circulating RANKL is inversely related to RANKL mRNA levels in bone in osteoarthritic males. Arthritis Research & Therapy 2008;10(1):R2.

146. Lacey DL, Boyle WJ, Simonet WS et al. Bench to bedside: elucidation of the OPG-RANK-RANKL pathway and the development of denosumab. Nat Rev Drug Discov 2012;11(5):401-419.

147. Bianchi ML, Bardella MT. Bone and Celiac Disease. Calcif Tiss Int 2002;71(6):465-471.

148. Noble C, Mc Cullough J, Ho W et al. Low body mass not vitamin D receptor polymorphisms predict osteoporosis in patients with inflammatory bowel disease. Alimentary Pharmacology & Therapeutics 2008;27(7):588-596.

149. van Staa TP, Geusens P, Bijlsma JW, Leufkens HG, Cooper C. Clinical assessment of the long-term risk of fracture in patients with rheumatoid arthritis. Arthritis Rheum 2006;54(10):3104-3112.

150. Romas E, Gillespie MT, Martin TJ. Involvement of receptor activator of NF[kappa]B ligand and tumor necrosis factor-[alpha] in bone destruction in rheumatoid arthritis. Bone 2002;30(2):340-346.

151. Taranta A, Fortunati D, Longo M et al. Imbalance of osteoclastogenesis-regulating factors in patients with celiac disease. J Bone Miner Res 2004;19(7):1112-1121.

152. Goldring SR, Gravallese EM. Mechanisms of bone loss in inflammatory arthritis: diagnosis and therapeutic implications. Arthritis Res 2000;2(1):33-37.

153. Klareskog L, R+Ânnelid J, Lundberg K, Padyukov L, Alfredsson L. Immunity to Citrullinated Proteins in Rheumatoid Arthritis. Annual Review of Immunology 2008;26(1):651-675.

154. Hoff M, Boyesen P, Haugeberg G et al. High disease activity is a predictor of cortical hand bone loss in post-menopausal patients with established rheumatoid arthritis: a 5-year multicentre longitudinal study. Rheumatology (Oxford) 2010;49(9):1676-1682.

155. Hauser B, Riches PL, Wilson JF, Horne AE, Ralston SH. Prevalence and clinical prediction of osteoporosis in a contemporary cohort of patients with rheumatoid arthritis. Rheumatology (Oxford) 2014.

156. Vis M, Havaardsholm EA, Haugeberg G et al. Evaluation of bone mineral density, bone metabolism, osteoprotegerin and receptor activator of the NFkappaB ligand serum levels during treatment with infliximab in patients with rheumatoid arthritis. Ann Rheum Dis 2006;65(11):1495-1499.

157. West J, Logan RFA, Hill PG et al. Seroprevalence, correlates, and characteristics of undetected coeliac disease in England. Gut 2003;52(7):960-965.

158. Olmos M, Antelo M, Vazquez H, Smecuol E, Maurino E, Bai JC. Systematic review and meta-analysis of observational studies on the prevalence of fractures in coeliac disease. Dig Liver Dis 2008;40(1):46-53.

159. Garcia-Manzanares A, Tenias JM, Lucendo AJ. Bone mineral density directly correlates with duodenal Marsh stage in newly diagnosed adult celiac patients. Scand J Gastroenterol 2012;47(8-9):927-936.

160. Janssen HC, Samson MM, Verhaar HJ. Vitamin D deficiency, muscle function, and falls in elderly people. Am J Clin Nutr 2002;75(4):611-615.

161. Meyer D, Stavropolous S, Diamond B, Shane E, Green PHR. Osteoporosis in a North American adult population with celiac

disease. American Journal of Gastroenterology 2001;96(1):112-119.

162. Wexler JA, Sharretts J. Thyroid and bone. Endocrinol Metab Clin North Am 2007;36(3):673-705, vi.

163. Murphy E, Williams GR. The thyroid and the skeleton. Clin Endocrinol (Oxf) 2004;61(3):285-298.

164. Abe E, Marians RC, Yu W et al. TSH is a negative regulator of skeletal remodeling. Cell 2003;115(2):151-162.

165. Vestergaard P, Mosekilde L. Hyperthyroidism, bone mineral, and fracture risk--a meta-analysis. Thyroid 2003;13(6):585-593.

166. Murphy E, Gluer CC, Reid DM et al. Thyroid function within the upper normal range is associated with reduced bone mineral density and an increased risk of nonvertebral fractures in healthy euthyroid postmenopausal women. J Clin Endocrinol Metab 2010;95(7):3173-3181.

167. Coindre J, David J, Riviere L et al. Bone loss in hypothyroidism with hormone replacement. A histomorphometric. Arch Intern Med 1986;146:48-53.

168. Ali T, Lam D, Bronze MS, Humphrey MB. Osteoporosis in inflammatory bowel disease. Am J Med 2009;122(7):599-604.

169. van Staa TP, Cooper C, Brusse LS, Leufkens H, Javaid MK, Arden NK. Inflammatory bowel disease and the risk of fracture. Gastroenterology 2003;125(6):1591-1597.

170. Silvennoinen JA, Karttunen TJ, Niemela SE, Manelius JJ, Lehtola JK. A controlled study of bone mineral density in patients with inflammatory bowel disease. Gut 1995;37(1):71-76.

171. Silvennoinen JA, Lehtola JK, Niemela SE. Smoking is a risk factor for osteoporosis in women with inflammatory bowel disease. Scand J Gastroenterol 1996;31(4):367-371.

172. Targownik LE, Bernstein CN, Leslie WD. Risk factors and management of osteoporosis in inflammatory bowel disease. Curr Opin Gastroenterol 2014;30(2):168-174.

173. Lleo A, Invernizzi P, Gao B, Podda M, Gershwin ME. Definition of human autoimmunity: autoantibodies versus autoimmune disease. Autoimmunity Reviews 2010;9(5):A259-A266.

174. Browne SK, Holland SM. Immunodeficiency secondary to anticytokine autoantibodies. Curr Opin Allergy Clin Immunol 2010;10(6):534-541.

175. Ferry H, Jones M, Vaux DJ, Roberts ISD, Cornall RJ. The Cellular Location of Self-antigen Determines the Positive and Negative Selection of Autoreactive B Cells. J Exp Med 2003;198(9):1415-1425.

176. Quirke AM, Fisher BAC, Kinloch AJ, Venables PJ. Citrullination of autoantigens: Upstream of TNF+¦ in the pathogenesis of rheumatoid arthritis. FEBS Lett 2011;585(23):3681-3688.

177. de Vries RRP, van der Woude D, Houwing JJ, Toes REM. Genetics of ACPA-positive rheumatoid arthritis: the beginning of the end? Annals of the Rheumatic Diseases 2011;70(Suppl 1):i51-i54.

178. Saderbergh A, Myhre AG, Ekwall O et al. Prevalence and Clinical Associations of 10 Defined Autoantibodies in Autoimmune Polyendocrine Syndrome Type I. Journal of Clinical Endocrinology & Metabolism 2004;89(2):557-562.

179. Wildin RS, Smyk-Pearson S, Filipovich AH. Clinical and molecular features of the immunodysregulation, polyendocrinopathy, enteropathy, X linked (IPEX) syndrome. Journal of Medical Genetics 2002;39(8):537-545.

180. Littleton E, Dreger M, Palace J, Vincent A. Immunocapture and Identification of Cell Membrane Protein Antigenic Targets of Serum Autoantibodies. Molecular & Cellular Proteomics 2009;8(7):1688-1696.

181. Auger I, Balandraud N, Rak J, Lambert N, Martin M, Roudier J. New autoantigens in rheumatoid arthritis (RA): screening 8268 protein arrays with sera from patients with RA. Annals of the Rheumatic Diseases 2009;68(4):591-594.

182. Whyte MP, Obrecht SE, Finnegan PM et al. Osteoprotegerin deficiency and juvenile Paget's disease. N Engl J Med 2002;347(3):175-184.

183. Helfrich MH, Ralston S.H. Bone Research Protocols (ISBN 1-58829-044-1). Humana Press; 2003.

184. Cecelja M, Frost M, Spector T, Chowienczyk P. Abdominal Aortic Calcification Detection Using Dual-Energy X-Ray Absorptiometry: Validation Study in Healthy Women Compared to Computed Tomography. Calcif Tissue Int 2013;1-6.

185. Genant HK, Wu CY, van Kuijk C, Nevitt MC. Vertebral fracture assessment using a semiquantitative technique. J Bone Miner Res 1993;8(9):1137-1148.

186. Minich WB, Lenzner C, Morgenthaler NG. Antibodies to TSH-receptor in thyroid autoimmune disease interact with monoclonal antibodies whose epitopes are broadly distributed on the receptor. Clin Exp Immunol 2004;136(1):129-136.

187. Peacock M, Robertson WG, Nordin BEC. Relation between serum and urinary calcium with particular reference to parathyroid activity. Lancet 1969;i:384-386.

188. Bianchi ML, Bardella M. Bone in celiac disease. Osteoporosis Int 2008;19(12):1705-1716.

189. Pazianas M, Butcher GP, Subhani JM et al. Calcium absorption and bone mineral density in celiacs after long term treatment with gluten-free diet and adequate calcium intake. Osteoporos Int 2005;16(1):56-63.

190. Carr AJ, Smith R, Athanasou N, Woods CG. Fibrogenesis imperfecta ossium. J Bone Joint Surg Br 1995;77(5):820-829.

191. Bekker PJ, Holloway DL, Rasmussen AS et al. A single-dose placebo-controlled study of AMG 162, a fully human monoclonal antibody to RANKL, in postmenopausal women. J Bone Miner Res 2004;19(7):1059-1066.

192. O'Neill SG, Isenberg DA, Rahman A. Could antibodies to C-reactive protein link inflammation and cardiovascular disease in patients with systemic lupus erythematosus? Ann Rheum Dis 2007;66(8):989-991.

193. Denham JM, Hill ID. Celiac disease and autoimmunity: review and controversies. Curr Allergy Asthma Rep 2013;13(4):347-353.

194. Panda S, Ding JL. Natural Antibodies Bridge Innate and Adaptive Immunity. J Immunol 2015;194(1):13-20.

195. Lewis NR, Scott BB. Guidelines for osteoporosis in inflammatory bowel disease and coeliac disease. http://www bsg org uk 2009.

196. Kanis JA, Johnell O, Oden A, JOhansson H, McCloskey E. FRAX and the assessment of fracture probability in men and women from the UK. Osteoporos Int 2008;19(4):385-397.

197. Hippisley-Cox J, Coupland C. Derivation and validation of updated QFracture algorithm to predict risk of osteoporotic fracture in primary care in the United Kingdom: prospective open cohort study. Br Med J 2012;344:e3427.

198. Gronwall C, Silverman GJ. Natural IgM: beneficial autoantibodies for the control of inflammatory and autoimmune disease. J Clin Immunol 2014;34 Suppl 1:S12-S21.

199. Little RD, Carulli JP, Del Mastro RG et al. A mutation in the LDL receptor-related protein 5 gene results in the autosomal dominant high-bone-mass trait. Am J Hum Genet 2002;70(1):11-19.

200. Goldring SR, Gravallese EM. Mechanisms of bone loss in inflammatory arthritis: diagnosis and therapeutic implications. Arthritis Res 2000;2(1):33-37.

201. Clifford DB, Ances B, Costello C et al. Rituximab-associated progressive multifocal leukoencephalopathy in rheumatoid arthritis. Arch Neurol 2011;68(9):1156-1164.

202. Riches PL, McRorie E, Fraser WD, Determann C, Hof Rv, Ralston SH. Osteoporosis Associated with Neutralizing Autoantibodies against Osteoprotegerin. The New England Journal of Medicine 2009;361(15):1459-1465.

203. Larussa T, Suraci E, Nazionale I et al. No evidence of circulating autoantibodies against osteoprotegerin in patients with celiac disease. World Journal of Gastroenterology 2012;14(18):1622-1627.

204. Nagele EP, Han M, Acharya NK, DeMarshall C, Kosciuk MC, Nagele RG. Natural IgG autoantibodies are abundant and ubiquitous in human sera, and their number is influenced by age, gender, and disease. PLoS One 2013;8(4):e60726.

205. Sheridan JP, Marsters SA, Pitti RM et al. Control of TRAIL-induced apoptosis by a family of signaling and decoy receptors [see comments]. Science 1997;277(5327):818-821.

206. Standal T, Seidel C, Hjertner O et al. Osteoprotegerin is bound, internalized, and degraded by multiple myeloma cells. Blood 2002;100(8):3002-3007.

207. Lamoureux F, Picarda G, Garrigue-Antar L et al. Glycosaminoglycans as potential regulators of osteoprotegerin therapeutic activity in osteosarcoma. Cancer Res 2009;69(2):526-536.

208. Baud'huin M, Duplomb L, Teletchea S et al. Osteoprotegerin: multiple partners for multiple functions. Cytokine Growth Factor Rev 2013;24(5):401-409.

209. Hauser B, Riches PL, Gilchrist T, Visconti MR, Wilson JF, Ralston SH. Autoantibodies to osteoprotegerin are associated with increased bone resorption in rheumatoid arthritis. Ann Rheum Dis 2015.

210. Luan X, Lu Q, Jiang Y et al. Crystal structure of human RANKL complexed with its decoy receptor osteoprotegerin. J Immunol 2012;189(1):245-252.

211. Schneeweis LA, Willard D, Milla ME. Functional dissection of osteoprotegerin and its interaction with receptor activator of NF-kappaB ligand. J Biol Chem 2005;280(50):41155-41164.

212. Yamaguchi K, Kinosaki M, Goto M et al. Characterization of structural domains of human osteoclastogenesis inhibitory factor. J Biol Chem 1998;273(9):5117-5123.

213. Real A, Gilbert N, Hauser B et al. Characterisation of Osteoprotegerin Autoantibodies in Coeliac Disease. Calcif Tissue Int 2015.

Appendices

A1 Materials and Reagents

All **materials** and **reagents** are listed in the table below in an alphabetical order.

Materials and reagents	**Supplier**
A Minimum Essential Medium (α MEM)	Sigma Aldrich, Dorset, UK
alamarBlue™ reagent	Invitrogen, Paisley, UK
Amersham Hybond™-P	GE Healthcare Life Sciences, Buckinghamshire, UK
Bicinchoninic acid (BCA) protein assay	Sigma Aldrich, Dorset, UK
Bovine serum albumin (A7906)	Sigma Aldrich, Dorset, UK
Bromophenol blue	BDH Laboratory Supplies, Poole, Dorset, UK
Centrifuge tubes (15 and 50ml)	Fisher Scientific, Leicestershire, UK
Coating buffer (C3041)	Sigma Aldrich, Dorset, Kent
Copper (II)-sulfate	Sigma Aldrich, Dorset, UK
Costar ELISA plate (3369 EIA/RIA)	Fisher Scientific, Leicestershire, UK
Criterion™ XT pre-cast gels (12% Bis-Tris)	Bio-Rad Laboratories, Hertfordshire, UK
D Minimum Essential Medium (dMEM)	Sigma Aldrich, Dorset, UK
DL-Dithiothreitol (DTT)	Sigma Aldrich, Dorset, UK
DMSO	Sigma Aldrich, Dorset, UK
EDTA	Sigma Aldrich, Dorset, UK
Electrophoresis power supply	Anachem, Bedfordshire, UK
Ethanol absolute	Fisher Scientific, Leicestershire, UK
Extra thick blot papers	Bio-Rad Laboratories, Hertfordshire, UK
Fetal calf serum (FCS)	Fisher Scientific, Leicestershire, UK
HEK 293 luciferase reporter cell line (RC0014)	eBioscience Ltd,Hatfield, UK

Human recombinant RANKL	Gift from Dr. Patrick Mollat (Proskelia SASU)
IgG elution buffer (Cat 21004)	Fisher Scientific, Leicestershire, UK
Jackson ImmunoResearch Anti-rabbit secondary antibody	Stratech Scientific Unit, Newmarket Suffolk, UK
Kaleidoscope markers	Bio-Rad Laboratories, Hertfordshire, UK
L-Glutamine	Invitrogen, Paisley, UK
LPS (IMG-2204)	Imgenex,2B scientific, Oxford, UK
Low molecular weight DNA ladder	New England Biolabs, Hertfordshire, UK
Magic Marker	Invitrogen, Paisley, UK
Melon™ Gel IgG Spin Purification Kit Thermo Scientific 45206	Fisher Scientific, Leicestershire, UK
Methanol	Fisher Scientific, Leicestershire, UK
Micro titre plate (Sterilin, 611F96)	Fisher Scientific, Leicestershire, UK
Neubauer haemocytometer	*Hawksley*, Lancing, UK
Osteoprotegerin (Human recombinant Cat 185-05)	R&D Systems, Abingdon, UK
Osteoprotegerin ELISA Biomedica, BI-20403	Oxford Biosystems, Oxford, UK
PBS tablets	Invitrogen, Paisley, UK
Penicillin/Streptomycin	Invitrogen, Paisley, UK
Pierce Protein G IgG Binding Buffer 21019	Fisher Scientific, Leicestershire, UK
Pierce SuperSignal® West Dura Extended Duration Substrate	Fisher Scientific, Leicestershire, UK
Pierce Protein G spin columns	Fisher Scientific, Leicestershire, UK
Primary mouse monoclonal antibody to OPG (Cat Ab1194 – clone number 98A1071)	AbCam, Cambridge, UK
Primary rabbit polyclonal antibody to OPG (Cat Ab 9986)	AbCam, Cambridge, UK
Primary rabbit polyclonal antibody to-OPG biotin conjugated (Cat Ab18068)	AbCam, Cambridge, UK
Protein G IgG Binding Buffer (Cat 21019)	Fisher Scientific, Leicestershire, UK

Quant-iT™ PicoGreen® assay	Invitrogen, Paisley, UK
RANKL ELISA Total (Biovendor RD193004200R)	Oxford Biosystems, Oxford, UK
RANKL ELISA Free (Biomedica BI-20452)	Oxford Biosystems, Oxford, UK
RAW 264.7 SEAP reporter cell line (IML-120)	Imgenex, 2B Scientific, Oxford, UK
RAW 264.7 cell line (91062702)	ECACC, Porton Down, UK
SEAP reporter Alkaline Phosphatase assay (Imgenex Cat 10055K)	Imgenex, 2B Scientific, Oxford, UK
Secondary anti-human peroxidase conjugated antibody (109-035-088)	Stratech Scientific Unit, Newmarket Suffolk, UK
Secondary anti- mouse secondary antibody (Cat 715-035-151)	Stratech Scientific Unit, Newmarket Suffolk, UK
Sodium dodecyl sulphate (SDS)	Bio-Rad Laboratories, Hertfordshire, UK
Steady-Glo reagent	Promega, Southampton, UK,
Stripettes (5, 10, 25 and 50ml)	Sarstedt Ltd, Leicester, UK
Syngene BIO imaging system	Fisher Scientific, Leicestershire, UK
Syringes (all sizes)	Becton Dickinson, Berkshire, UK
TBS 10x (T5912)	Sigma Aldrich, Dorset, UK
TBE buffer 10X	Invitrogen, Paisley, UK
2%TCH (serum replacement)	MP-Biomedicals, Cambridge, UK
Tissue culture 75cm^2 flasks	Fisher Scientific, Leicestershire, UK
Tissue culture microplates (6– 96well plates)	Fisher Scientific, Leicestershire, UK
TMB Stop solution (50-85-06)	KPL, Maryland, USA
Toluidine Blue	Sigma Aldrich, Dorset, UK
Tris	Bio-Rad Laboratories, Hertfordshire, UK
Tris-EDTA buffer	Sigma Aldrich, Dorset, UK
Triton X-100™	Sigma Aldrich, Dorset, UK
Trizol reagent	Invitrogen, Paisley, UK
Trizol® Reagent	Invitrogen, Paisley, UK

Trypsin/EDTA	Sigma Aldrich, Dorset, UK
Tween-20 (27,434-8)	Sigma Aldrich, Dorset, UK
UV 96 well plates for plate reader	Fisher Scientific, Leicestershire, UK
XT-MOPS	Bio-Rad Laboratories, Hertfordshire, UK
Xylene	Sigma Aldrich, Dorset, UK

A2 Apparatus

All **apparatus** are listed in the table below in alphabetical order.

Apparatus	**Supplier**
AA Hoefer® protein transfer apparatus	Fisher Scientific, Leicestershire, UK
Balancer Fisherbrand	Fisher Scientific, Leicestershire, UK
Bench-top centrifuge	SciQuip, Shropshire, UK
Benchtop Eppendorf centrifuge	Fisher Scientific, Leicestershire, UK
Bio-Tek Synergy HT plate reader	Fisher Scientific, Leicestershire, UK
Envair Bio2 safety cabinets	H&V Commissioning Services Ltd., Ayrshire, UK
Grant OLS 200 water bath	Thistle Scientific, Glasgow, UK
Nichiryo America Inc. Pipettes (2, 10, 100, 200 and 1000µl)	Thistle Scientific, Glasgow, UK
NoAir Class II Biological safety cabinet	TripleRed Ltd., Buckinghamshire, UK
Origo PSU-400/200 power supply for electrophoresis,	Anachem, Bedfordshire, UK
PowerPac basic™	Bio-Rad Laboratories, Hertfordshire, UK
Syngene GeneGenius Gel Bio-Imaging system	Fisher Scientific, Leicestershire, UK
SynSyngene GeneGnome Bio-Imaging system for chemiluminescence	Fisher Scientific, Leicestershire, UK
Vertical Criterion™ gel tanks	Bio-Rad Laboratories, Hertfordshire, UK

All **software** are listed in the table below in alphabetical order.

Software	**Supplier**
Bio-Tek Gen5^{TM} plate reader software	Fisher Scientific, Leicestershire, UK
Minitab Release 16.2.4	Minitab Inc., Pennsylvania, US
SPSS statistics 19	SPSS Inc
Syngene GeneSnap software	Fisher Scientific, Leicestershire, UK
Syngene GeneTool software	Fisher Scientific, Leicestershire, UK

A3 Solutions

APPENDIX 3.1 SOLUTIONS FOR PAGE AND WESTERN BLOT

i. Electrophoresis running buffer

50ml of XT-MOPS (20X) in 1000ml of dH2O

ii. Sample loading protein buffer (5X stock)

5.2ml of 1M Tris-HCl pH adjusted to 6.8, 1g of DL-Dithiothreitol (DTT), 3g SDS, 6.5ml glycerol and 130µl of 10% (w/v) bromophenol blue. Stored at -20˚C.

iii. Transfer buffer

3.63g of Tris, 14.4g of glycine, 200ml of methanol and 3.75ml of 10% (w/v) SDS made up to 1,000ml with dH_2O. Stored at room temperature.

iv. TBS

1M of Tris and 1M Tris-HCl, pH adjusted to 7.9 prior to addition of 3M sodium chloride. Stored at room temperature.

v. TBST

0.1% (v/v) Tween-20 in TBS. Stored at room temperature.

vi. Stripping buffer

1mM DTT, 2% (w/v) SDS and 62.5mM Tris-HCl (pH 6.7). Stored at room temperature.

APPENDIX 3.2 SOLUTION FOR CELL LYSIS

RIPA Lysis buffer

1% Triton 100X, 0.5% (w/v) sodium deoxycholate, 0.1% (w/v) sodium dodecyl sulphate (SDS), 50mM Tris-HCl (pH 7.4) and 150nM sodium chloride were dissolved in dH_2O.

APPENDIX 3.3 SOLUTION FOR ELISA

TBST wash buffer

0.05 % (v/v) Tween 20 in TBS (pH 7.4) made up in dH2O.

Coating buffer

Carbonate/bicarbonate buffer 0.2 M, pH 9.6, prepared commercially with deionised water from sigma and buffer capsules C3041-100cap.

A4 Protocols for assays of functional inhibition of OPG

A number of models were explored to find a system that would demonstrate the functional activity of OPG antibodies, but were found not to be suitable. I acknowledge the technical assistance of Tamara Gilchrist in the performance of these assays.

A4.1 Principles of the AlphaLISA assay

A potential functional assay of OPG antibodies was investigated using the AlphaLISA bead based protocol (Perkin Elmer). This is a proximity assay of protein interactions, in which a signal is emitted when coupled beads are brought together by linked protein pairs.

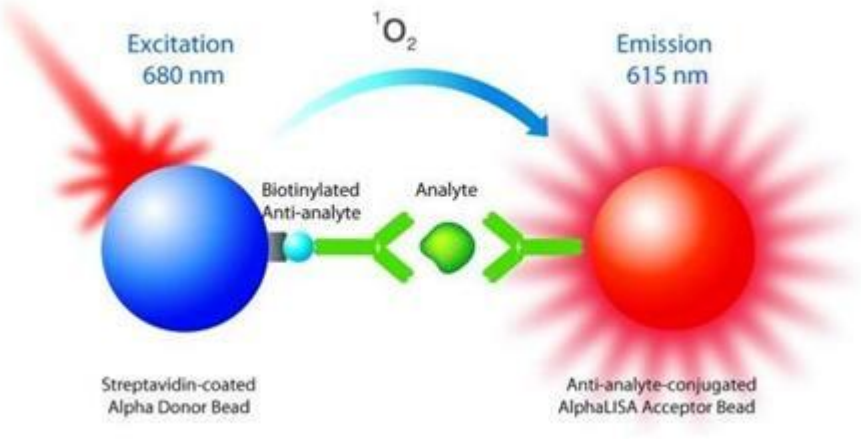

In this exploratory assay, OPG was bound to 'donor' beads and RANKL bound to separate 'acceptor' beads. If a robust dose response to increasing OPG beads could be established, then this in turn could potentially be inhibited by the presence of OPG antibodies. Diminution of signal in such an assay would allow both the quantification of antibodies to OPG (or indeed RANKL) and simultaneously demonstrate that these antibodies were functional inhibitors of the OPG-RANKL interaction.

The beads are supplied with a variety of ligands with glutathione acceptor beads linked to GST tagged RANKL, and Nickel chelate donor beads then linked with his-tagged OPG. Dose ranging experiments were performed using a variety of concentrations of OPG and RANKL. Inconsistent results were observed despite a variety of blocking buffers being assessed to see if these could improve the assay performance (Table A4.1).

A4.2 Protocol for the AlphaLISA assay

All beads prepared in subdued lighting (covered in foil for all incubations).

1) Add 10µl of the appropriate 1x buffer to the corresponding wells (see plate plan).

- Prepare 5ml of 1% BSA in TBST
- Prepare 5ml of 1x AlphaLISA Universal buffer (5 x stock) by adding:
  1ml stock to 4ml of 0.2µM filtered dH20
- Prepare 5ml of 1x AlphaLISA HiBlock buffer and AlphaLISA Immunoassay buffer (10x stock) by adding:
  500µl stock to 4.5ml 0.2µM filtered dH20

2) Prepare 4 x 180nM OPG and RANKL protein solutions (1 in each buffer) and use to prepare 5 x concentrated working stock solutions to create a concentration gradient for each buffer:

- Produce 4 x 55µl of a 180nM his-tagged OPG solution by adding:
  0.9µl of OPG stock (0.5 mg/ml) to 54.1µl of the appropriate buffer
- Prepare 4 x 55µl of a 180 nM GST-tagged RANKL solution by adding:
  46.5µl of RANKL stock (10 µg/ml) to 8.5µl of the appropriate buffer
- Use the 180nM protein solutions to prepare 4 lots of the following OPG and RANKL solutions (1 gradient for each buffer):

Final concentration in well	Working concentration prepared	Volume of protein required	Volume of buffer
36nM	180nM	55µl of 180nM solution	None
8.0nM	40nM	11µl of 180nM solution	38.5µl
2.4nM	12nM	15µl of 40nM solution	35µl

0.0nM	0.0nM	None	50µl

3) Add 10µl of OPG and 10µl of the RANKL solutions to the appropriate wells (see plate plan).

4) Seal plate firmly, wrap in foil and incubate at 37^{o}C (± 2^{o}C) for 1 hour.

5) Prepare 4 x working solutions of Glutathione Acceptor beads (1 in each buffer):

- Prepare 4 x 175µl of 100 µg/ml solutions (5 x) of glutathione acceptor beads by adding 3.5µl beads (at 5 mg/ml) to 171.5µl of the appropriate buffer

6) After initial incubation, allow plate to equilibrate to room temperature for 5 minutes. Subsequently, add 10µl of the 100µg/ml acceptor beads (final concentration 20µg/ml) to the appropriate wells of the plate (See plan).

7) Seal plate firmly, cover in foil and incubate at room temperature (24^{o}C ± 2^{o}C) for 1 hour.

8) Prepare 4 x working solutions of Nickel chelate donor beads:

- Prepare 4 x 175µl of 100µg/ml solutions (5x) of Nickel chelate donor beads by adding 3.5µl beads (at 5mg/ml) to 171.5µl of the appropriate buffer.

9) After second incubation, add 10µl of the 100µg/ml donor beads (final concentration 20µg/ml) to each well.

10) Seal plate, cover in foil and incubate at room temperature (24˚C ± 2˚C) for 1 hour.

11) Record results using the EnVision plate reader.

	1	2	3	4	5	6	7	8	9 - 24
A	36 nM OPG 36 nM RANKL 1 % BSA TBST	36 nM OPG 8 nM RANKL 1 % BSA TBST	36 nM OPG 2.4 nM RANKL 1 % BSA TBST	36 nM OPG 0 nM RANKL 1 % BSA TBST	36 nM OPG 36 nM RANKL Universal buffer	36 nM OPG 8 nM RANKL Universal buffer	36 nM OPG 2.4 nM RANKL Universal buffer	36 nM OPG 0 nM RANKL Universal buffer	Blank
B	8 nM OPG 36 nM RANKL 1 % BSA TBST	8 nM OPG 8 nM RANKL 1 % BSA TBST	8 nM OPG 2.4 nM RANKL 1 % BSA TBST	8 nM OPG 0 nM RANKL 1 % BSA TBST	8 nM OPG 36 nM RANKL Universal buffer	8 nM OPG 8 nM RANKL Universal buffer	8 nM OPG 2.4 nM RANKL Universal buffer	8 nM OPG 0 nM RANKL Universal buffer	Blank
C	2.4 nM OPG 36 nM RANKL 1 % BSA TBST	2.4 nM OPG 8 nM RANKL 1 % BSA TBST	2.4 nM OPG 2.4 nM RANKL 1 % BSA TBST	2.4 nM OPG 0 nM RANKL 1 % BSA TBST	2.4 nM OPG 36 nM RANKL Universal buffer	2.4 nM OPG 8 nM RANKL Universal buffer	2.4 nM OPG 2.4 nM RANKL Universal buffer	2.4 nM OPG 0 nM RANKL Universal buffer	Blank
D	0 nM OPG 36 nM RANKL 1 % BSA TBST	0 nM OPG 8 nM RANKL 1 % BSA TBST	0 nM OPG 2.4 nM RANKL 1 % BSA TBST	0 nM OPG 0 nM RANKL 1 % BSA TBST	0 nM OPG 36 nM RANKL Universal buffer	0 nM OPG 8 nM RANKL Universal buffer	0 nM OPG 2.4 nM RANKL Universal buffer	0.0 nM OPG 0 nM RANKL Universal buffer	Blank
E	36 nM OPG 36 nM RANKL HiBlock buffer	36 nM OPG 8 nM RANKL HiBlock buffer	36 nM OPG 2.4 nM RANKL HiBlock buffer	36 nM OPG 0 nM RANKL HiBlock buffer	36 nM OPG 36 nM RANKL Immunoassay buffer	36 nM OPG 8 nM RANKL Immunoassay buffer	36 nM OPG 2.4 nM RANKL Immunoassay buffer	36 nM OPG 0 nM RANKL Immunoassay buffer	Blank
F	8 nM OPG 36 nM RANKL HiBlock buffer	8 nM OPG 8 nM RANKL HiBlock buffer	8 nM OPG 2.4 nM RANKL HiBlock buffer	8 nM OPG 0 nM RANKL HiBlock buffer	8 nM OPG 36 nM RANKL Immunoassay buffer	8 nM OPG 8 nM RANKL Immunoassay buffer	8 nM OPG 2.4 nM RANKL Immunoassay buffer	8 nM OPG 0 nM RANKL Immunoassay buffer	Blank
G	2.4 nM OPG 36 nM RANKL HiBlock buffer	2.4 nM OPG 8 nM RANKL HiBlock buffer	2.4 nM OPG 2.4 nM RANKL HiBlock buffer	2.4 nM OPG 0 nM RANKL HiBlock buffer	2.4 nM OPG 36 nM RANKL Immunoassay buffer	2.4 nM OPG 8 nM RANKL Immunoassay buffer	2.4 nM OPG 2.4 nM RANKL Immunoassay buffer	2.4 nM OPG 0 nM RANKL Immunoassay buffer	Blank
H	0 nM OPG 36 nM RANKL HiBlock buffer	0 nM OPG 8 nM RANKL HiBlock buffer	0 nM OPG 2.4 nM RANKL HiBlock buffer	0 nM OPG 0 nM RANKL HiBlock buffer	0 nM OPG 36 nM RANKL Immunoassay buffer	0 nM OPG 8 nM RANKL Immunoassay buffer	0 nM OPG 2.4 nM RANKL Immunoassay buffer	0.0 nM OPG 0 nM RANKL Immunoassay buffer	Blank
I - P	Blank	Blank	Blank	Blank	Blank	Blank	Blank	Blank	Blank

Table A4.1 Results of AlphaLISA assay

AlphaScreen Protocol - raw

	OPG Concentration							
	1 % BSA TBST					Universal Buffer		
RANKL Conc.	0.0 nM	2.4 nM	8.0 nM	36 nM		0.0 nM	2.4 nM	8.0 nM	36 nM
0.0 nM	1,299	1,549	1,718	1,686		1,855	2,086	2,311	2,394
2.4 nM	1,334	1,619	1,764	1,638		1,929	2,140	2,025	2,553
8.0 nM	1,510	1,854	1,732	1,841		1,979	2,531	2,200	2,701
36 nM	1,580	1,741	2,169	1,946		2,006	2,117	2,549	2,449
RANKL Conc.	HiBlock Buffer					Immunoassay Buffer		
	0.0 nM	2.4 nM	8.0 nM	36 nM		0.0 nM	2.4 nM	8.0 nM	36 nM
0.0 nM	732	730	822	714		852	840	854	954
2.4 nM	671	732	776	738		764	836	952	1022
8.0 nM	810	794	847	788		902	994	958	922
36 nM	805	811	909	975		921	1,019	1,011	979

AlphaScreen Protocol- corrected

	OPG Concentration							
	1 % BSA TBST					Universal Buffer		
RANKL Conc.	0.0 nM	2.4 nM	8.0 nM	36 nM		0.0 nM	2.4 nM	8.0 nM	36 nM
0.0 nM	1,386	1,652	1,831	1,739		1,917	2,155	2,390	2,391
2.4 nM	1,426	1,730	1,885	1,750		2,063	2,286	2,162	2,730
8.0 nM	1,612	1,980	1,847	1,903		2,112	2,704	2,345	2,792
36 nM	1,690	1,861	2,320	2,080		2,146	2,261	2,724	2,617
RANKL Conc.	HiBlock Buffer					Immunoassay Buffer		
	0.0 nM	2.4 nM	8.0 nM	36 nM		0.0 nM	2.4 nM	8.0 nM	36 nM
0.0 nM	782	779	878	760		881	868	882	983
2.4 nM	693	781	828	788		789	892	1,017	1,091
8.0 nM	866	848	904	839		964	1,062	1,023	981
36 nM	832	866	971	1,042		952	1,087	1,079	1,045

A4.3 TRAP assay

RAW 264.7 cells were maintained in 75ml flasks containing supplemented D-MEM (with 1% penicillin/streptomycin, 1% L-Glutamine and 10 % FCS) with media refreshed every 2 days. Cells split by trypsinisation prior to assay (4ml trypsin added to flask then cells liberated by shaking). Pooled cells were counted in a modified Neubauer cell counter.

Cells were made up to a final concentration of 200,000 cells/ml by adding the appropriate volume of supplemented D-MEM to the cells.

Either 100µl of the 200,000 cell/ml suspension (20,000 cells/well) or 50µl of 200,000 cell/ml suspension (10,000 cells/well) were added to 3 x 96 well micro-titre plates as shown below. To wells with 50µl of cells, a further 50µl of supplemented media was added to give a final volume of 100µl.

Plates and flask were incubated at 37^{o}C overnight.

	1	2	3	4	5	6	7	8	9	10	11	12
A	-	-	-	-	-	-	-	-	-	-	-	-
B	-	10,000	10,000	10,000	10,000	10,000	20,000	20,000	20,000	20,000	20,000	-
C	-	10,000	10,000	10,000	10,000	10,000	20,000	20,000	20,000	20,000	20,000	-
D	-	10,000	10,000	10,000	10,000	10,000	20,000	20,000	20,000	20,000	20,000	-
E	-	10,000	10,000	10,000	10,000	10,000	20,000	20,000	20,000	20,000	20,000	-
F	-	10,000	10,000	10,000	10,000	10,000	20,000	20,000	20,000	20,000	20,000	-
G	-	10,000	10,000	10,000	10,000	10,000	20,000	20,000	20,000	20,000	20,000	-
H	-	-	-	-	-	-	-	-	-	-	-	-

The following 10X samples were prepared and incubated at 37 ^{o}C with shaking:

Control = 140µl supplemented D-MEM
500ng/ml RANKL = 0.7µl of 100µg/ml RANKL + 139.3µl sup D-MEM
1000ng/ml RANKL = 1.4µl of 100µg/ml RANKL + 138.6µl sup D-MEM x 2
2000ng/ml RANKL = 2.8µl of 100µg/ml RANKL + 137.2µl sup D-MEM

To one 140µl aliquot of the 1000ng/ml RANKL, 1.4µl of 100,000 ng/ml (100ng/µl) OPG (R&D systems, 185-OS-025 CF) was added to give a solution of 1000 ng/ml RANKL and 1000 ng/ml OPG.

To each well of the 3 seeded microtitre plates 90µl of supplemented D-MEM was added. Then, to the appropriate wells, 10µl of the corresponding treatment was added, thus giving the treatment plan shown below (R = RANKL):

	1	2	3	4	5	6	7	8	9	10	11	12
A	-	-	-	-	-	-	-	-	-	-	-	-
B	-	Ctrl	50 ng/ml R	100 ng/ml R	200 ng/ml R	100 ng/ml R + 100 ng/ml OPG	Ctrl	50 ng/ml R	100 ng/ml R	200 ng/ml R	100 ng/ml R + 100 ng/ml OPG	-
C	-											-
D	-											-
E	-											-
F	-											-
G	-											-
H	-	-	-	-	-	-	-	-	-	-	-	-

One plate was incubated for 24 hours, the second for 48 hours and the third for 72 hours.

From the 24 hour plate, two 20µl aliquots of supernatant were drawn off without disturbing the cells and transferred to two fresh 96-well plates. These were stored at -20^{o}C until required. The remaining cells were rinsed twice with PBS and then fixed with 4% Formaldehyde for 10 minutes. Finally, cells were rinsed twice in PBS and stored at 4^{o}C until required.

The remaining two plates were treated in the same fashion at 48 and 72 hours respectively.

TRAP supernatant reaction buffer comprised:

1M acetate	- 29.5ml 100 % acetic acid
0.5% Triton X-100	- 2.5ml Triton X-100
1M NaCl	- 29g NaCl
10mM EDTA	- 1.86g EDTA

The above reagents were added to 350ml of dH20 and then the pH adjusted to 5.5 with 6M NaOH (6 g in 25ml). The solution was made up to a final volume of 500ml with dH20. Note: Buffer was cooled down to dissolve completely.

To treat the supernatants from one plate for each of the time points, the following solutions were prepared fresh:

8.8mg/ml L-Ascorbic acid in dH20 (0.044g in 5ml dH20)
46mg/ml Di-sodium tartrate in dH20 (0.23g in 5ml dH20)
18mg/ml 4-Nitrophenylphosphate in dH20 (0.09g in 5ml dH20)

1ml of each of these solutions was used to prepare 8ml TRAP solution (made up with 2ml reaction buffer and 3ml dH20) per plate, ie for 3 plates use 3ml each solution, 6ml reaction buffer and 9ml dH20.

To the 20µl supernatant aliquots, 80µl of the TRAP solution was added. The plate was covered with foil to protect from light and evaporation and incubated on a shaker (300-400 rpm) at 37^{o}C for 1 hour.
The reaction was then stopped by the addition of 0.3 M NaOH (6g in 500ml dH20). The absorbance at 650nm was measured subtracting the OD405nm values as background values.

The plates of fixed cells from each time point were also stained as below:

A 10mg/ml Naphtol-AS-BI-phosphate solution was prepared in Dimethylformamide (0.005g in 500µl)

Staining solution A was prepared by mixing the following in a clean GLASS test tube:
450µl of Naphtol-AS-BI-phosphate
2,250µl of Veronal buffer (see below)
2,700µl of Acetate buffer
2,700µl of Acetate buffer with 100 mM Tartrate

Staining solution B was prepared by mixing (NOT vigorously) the following in a clean GLASS test tube:
360µl of Pararosanilin
360µl of Sodium Nitrite (4 %) (Toxic cabinet)

TRAP staining solution was prepared by mixing solutions A and B and 0.45 µM filter sterilised into a further clean glass test tube.
Cells were covered in 80µl TRAP staining solution and incubated for 50-60 minutes at 37^{o}C. Cells were then rinsed twice with PBS and then covered with 200µl of 70 % ethanol (per well). Plate was then wrapped in cling film and stored at 4 ^{o}C.

Experiment was unsuccessful; no staining of the cells or supernatant was achieved. Presumption made was that the stored RAW cells used had deteriorated.

Stock solutions for cell staining :
Veronal buffer: dissolve the following in 100ml of dH20:
1.17g sodium acetate anhydrous
2.94g veronal (sodium barbiturate)
Acetate buffer: Adjust the pH of (a) to a pH of 5.2 with (b)

a. 0.82g sodium acetate anhydrous (dissolve in 100ml of dH20)
b. 600µl glacial acetic acid (make up to 100ml with dH20)

Pararosanilin:
Add 1g to 20ml of dH20, add 5ml of concentrated HCl and heat carefully in a water bath while stirring. Filter once cooled.

A4.4 Secreted alkaline phosphatase (SEAP) assay

A4.4.1 SEAP Protocol

A RAW 264.7 cell line expressing the SEAP reporter gene under the transcriptional control of a NF-kB response element (IML-120 Imgenex) was investigated for use in a functional model of OPG inhibition. SEAP catalyses the hydrolysis of pNitrophenyl phosphate (PNPP) producing a yellow product that can be read in a spectrophotometer or ELISA reader at 405nm.

A vial of prepared frozen cells was thawed quickly and mixed with 9ml freshly prepared pre-warmed media (dMEM). This was then centrifuged at 1,000rpm for 10 minutes to pellet the cells. The supernatant was discarded and the cells re-suspended in a further 9ml of fresh, pre-warmed media (dMEM containing 10% FCS, 2mM L-glutamine, 4.5g/l glucose, 100u/ml penicillin, 100ug/ml streptomycin and 100ug/ml normocin) and transferred to a small tissue culture flask. The flask was incubated at 37^{o}C and split when approaching confluence (~90–95% confluence).

For the assay, cells from 3 confluent tissue flasks were liberated with a cell scraper in warm PBS. Cells were centrifuged at 1,000rpm for 10 minutes to pellet the cells. The supernatant was discarded and the cell pellet re-suspended in 10ml warmed test medium (dMEM as above with heat inactivated FCS). Cells were counted in a modified Neubauer cell counter and resuspended at a concentration of 550,000 cells/ml. 100µl cells (ie 55,000 cells/well) were added to a black 96-well plate (to minimise transference of signal). The outer wells had 100µl of media alone added to minimise effects of evaporation. The plate was incubated at 37 ^{o}C for 16 hours (± 2 hours).

Commercial LPS solution (IMG-2204, 1mg/ml) was diluted to a 100 µg/ml working stock solution by adding 10µl to 90µl of culture media to provide a positive control.

Treatments with RANKL and OPG were prepared at 10X concentration and incubated at 37^{o}C for 20 min before use. To make up each treatment

Treatment Sample (10 x concentrated) 100 µl	Volume of stock solution required (µl)			Volume of media required (µl) DMEM + pen/strep/glut/ sodium pyru/Geneticin
	RANKL (100µg/ml)	OPG (100µg/ml)	LPS (100µg/ml)	
-ve	0	0	0	500
R100	2	0	0	98
R200	4	0	0	96
R400	6	0	0	94
R800	8	0	0	92
R1,600	16	0	0	84
R200, O200	4	4	0	92
L200	0	0	2	98
L400	0	0	4	96
L5,000	0	0	50	50

e.g. R200 = 200 ng/ml final concentration per well of RANKL and
L200 = 200 ng/ml final concentration per well of LPS
0200 = 200 ng/ml final concentration per well of OPG

From each well, using a multichannel pipette, 10µl of cell supernatant (or media only) was discarded. Then, 10µl of the 10X concentrated samples was added to the remaining 90µl of D-MEM in which the cells had been incubated overnight (or media only). Each treatment sample was added to all eight wells in a column

Secreted alkaline phosphatase was measured using the provided buffers and standards (Alkaline Phosphatase assay - Imgenex Cat. No.10055K). The 10X sample dilution buffer and 10 x PNPP buffer provided were diluted to 1X with sterile dH20 (eg 1ml of 10X buffer + 9ml of sterile dH20). SEAP standards were prepared with serial doubling dilutions of the 400ng/ml SEAP standard stock solution to a final volume of 100µlin dilution buffer. After stimulation, 5µl of supernatant from each well of cells was transferred to a fresh 96 well plate and diluted 1:2 by the addition of 5µl of dilution buffer. Standards were arranged in duplicate with 10µl per well. The plate was sealed

with a plate sealer and incubated at 65ºC for 30 minutes to inactivate any endogenous alkaline phosphatase and allow for precise quantification of SEAP.

During this incubation, to the remaining 95µl of media containing stimulated 9.5µl Alamar Blue (10X ready-to-use solution) was added and cells were incubated at 37ºC for a further 3 hours. Also during this incubation period, the PNPP substrate was prepared. This was done by dissolving two 5mg PNPP substrate tablets in 10ml of 1X PNPP buffer (to give a final concentration of 1 mg/ml).

After incubation the plate was spun briefly to return all liquid to the bottom of the well and then the plate sealer was removed. To each well, 100µl of the freshly prepared 1 mg/ml PNPP substrate solution was added and the plate incubated at room temperature. Absorbance readings at 405nm were recorded after 2 hours, 4 hours and approximately 24 hours using a plate reader. Cell viability of the cultures cells after 3 hours was determined by measuring absorbance at 570nm.

A4.3.2 SEAP Assay results

LPS induced RAW cell secretion of ALP robustly and at all time-points, confirming that the cells were viable, functioning as anticipated, and that the assay was performed correctly. Alamar blue staining confirmed cells were still viable for 3 hours after the supernatant samples had been removed for the SEAP assay, with similar levels of viability in all wells. Disappointingly there was no signal observed at any concentration of RANKL meaning that this line could not be used as hoped (Table A4.2). Even though this cell line is thought to be of monocyte/macrophage lineage these results would suggest that it no longer expresses a functional RANK receptor.

Table A4.2 Results of the Alkaline Phosphatase assay at 2, 4 and 24 hours.

Note: RANKL doses indicated by prefix R and LPS by prefix L.

2 hours											
Mean Conc. (ng/ml)	Sample	Neg	R100	R200	R400	R800	R1,600	R200, O200	L200	L400	L5,000
	Result	<0.0	<0.0	<0.0	<0.0	<0.0	<0.00	<0.00	43.3	40.7	63.8
	SD	N/A	N/A	N/A	N/A	N/A	N/A	N/A	6.94	5.467	9.917
	CV (%)	N/A	N/A	N/A	N/A	N/A	N/A	N/A	16.0	13.44	15.54

4 hours											
Mean Conc. (ng/ml)	Sample	Neg	R100	R200	R400	R800	R1,600	R200, O200	L200	L400	L5,000
	Result	<0.0	<0.0	<0.0	<0.0	<0.0	<0.0	<0.0	42.6	40.4	63.8
	SD	N/A	N/A	N/A	N/A	N/A	N/A	N/A	6.74	4.7	9.30
	CV (%)	N/A	N/A	N/A	N/A	N/A	N/A	N/A	15.8	11.7	14.5

24 hours											
Mean Conc. (ng/ml	Sample	Neg	R100	R200	R400	R800	R1,600	R200, O200	L200	L400	L5,000
	Result	<0.0	<0.0	<0.0	<0.0	<0.0	<0.0	<0.0	77.6	73.7	122
	SD	N/A	N/A	N/A	N/A	N/A	N/A	N/A	14.7	12.8	18.7
	CV (%)	N/A	N/A	N/A	N/A	N/A	N/A	N/A	18.9	17.4	15.3

A5 Questionnaire administered in Medical Physics department

BONE DENSITY QUESTIONNAIRE

Lothian Osteoporosis Service
Western General Hospital
Phone 0131-537-2155

We would be grateful if you could try and complete the following questionnaire. Don't worry if you can't answer all the questions, since any information you provide will be helpful and we will go over the questions with you when you come for your scan

Section 1. Personal Details	
Name	GP's Name
Address	Date of Birth
	Please tick √ the box if you are:
Postcode	Male ☐ Female ☐

Section 2. Fractures (broken bones)

Have you ever suffered a fracture? (broken bone) (please tick √ the box) **Yes** ☐ **No** ☐

If you ticked YES, please list the site of these fractures below, describe how they occurred and tell us what age you were when the fractures occurred.

Site of Fracture *(e.g. hip, wrist, shoulder, ankle, etc.)*	**Cause of Fracture** *(e.g. fell or tripped, car accident)*	**Age** (at time of fracture)

Section 3. Steroid Treatment

Are you taking steroid tablets at present? (for example, prednisolone or dexamethasone - please tick √ the box) **Yes** ☐ **No** ☐

If you answered YES, please write down the month and year you started the tablets and please bring them (or your prescription) with you when you come for your scan

(office use only, please leave blank)
Steroid name
Steroid/dose

Have you previously taken steroid tablets? (for example, prednisolone or dexamethasone - please tick √ the box) **Yes** ☐ **No** ☐

If you answered YES, please write down the month and year when you started and stopped the steroid tablets
(e.g. January 2004 – February 2005)

Section 4. Medication and Medical Conditions

Do you suffer from any of the following medical conditions?
(please tick √ the boxes for all those that apply)

Ankylosing Spondylitis	☐	Rheumatoid Arthritis	☐
Anorexia	☐	Thyroid overactive	☐
Crohn's Disease	☐	Thyroid underactive	☐
Coeliac Disease	☐	Ulcerative Colitis	☐
Gastrectomy	☐	Heartburn	☐
Hyperparathyroidism	☐	Dypepsia	☐
Kidney Failure	☐	Stomach Ulcer	☐
Malabsorption	☐		

Section 5. Medications

Are you being treated with any of the following medications for osteoporosis?
(please tick √ the boxes for all those that apply)

Calcium / Vitamin D	☐	Strontium (Protelos)	☐
Calcitonin	☐	Teriparatide	☐
Alendronate (Fosamax)	☐	Pamidronate (Aredia)	☐
Risedronate (Actonel)	☐	Didronel	☐
Ibandronate (Bonviva)	☐	Raloxifene	☐
		Other	☐

Are you being treated with any of the following medications for pain, heartburn or dyspepsia?
(please tick √ the boxes for all those that apply)

Anti-inflammatory tablets	☐
Antacid medication	☐

Section 6. Diet, Alcohol and Smoking

We would like to know about your diet. Please fill in the table below to tell us how many times per **week** on average you eat the following foods or drinks.

Food Item	Number per week
Cups of tea or coffee with milk	
Milk or milk drinks (e.g. hot chocolate)	
Cereal or porridge with milk	
Milk puddings (custard, ice cream, yoghurt etc.)	
Chocolate bars	
Slices of bread	
Portions of cheese	
Lasagne, macaroni cheese, mousaka, or pizza.	
Portions of cottage cheese	
Eggs	
Biscuits	
Portions of Cake	
Portions of green vegetables	
Portions of sardines/pilchards	
Portions of other fish	
Oranges	

(Calcium/day - office use only, please leave blank)	

	Yes	No
Do you smoke? (please tick √ the box)		
If you answered YES, please enter in this box how many cigarettes or cigars per day.		
Did you smoke previously (please tick √ the box)		
Do you drink alcohol regularly? (please tick √ the box)		
If you answered YES, please estimate how many units of alcohol you take per week. (1 unit equals 1 glass of wine, ½ pint of beer or 1 nip)		

Section 7. Falls

	Yes	No
Have you fallen in the past 12 months? (please tick √ the box)		
If you answered YES, how many falls have you had in the past 12 months		

(office use only, please leave blank)
Get up and go test *Passed / Failed*
Falls referral *Yes / No*

Section 8. Physical Activity and Sports

	Yes	No
Are your on your feet for more than 4 hours a day? (please tick √ the box)		
Do you take part in impact sports regularly? (e.g. football, rugby, hockey, squash, running; please tick √ the box)		
Do you take part in non impact sports regularly? (e.g. swimming, cycling, golf, walking, riding; please tick √ the box)		

Section 9. Family History of Osteoporosis

	Yes	No
Has your father suffered a hip fracture? (please tick √ the box)		
Has your mother suffered a hip fracture? (please tick √ the box)		
Has your brother or sister suffered a hip fracture? (please tick √ the box)		
Has your father been diagnosed with osteoporosis? (please tick √ the box)**?**		
Has your mother been diagnosed with osteoporosis? (please tick √ the box)**?**		
Have any of your brothers been diagnosed with osteoporosis? (please tick √ the box)		
Have any of your sisters been diagnosed with osteoporosis? (please tick √ the box)		

Section 10. Your Ethnic Background

How would you describe yourself with regard to your ethnic background?
(please tick √ boxes that apply; you can tick more than one box if you are of mixed ethnic background)

White Scottish	☐	Pakistani	☐
White other British	☐	Asian any other	☐
White Irish	☐	Black Caribbean	☐
White any other	☐	Black African	☐
Asian Indian	☐	Black any other	☐
Asian Pakistani	☐	Mixed	☐
Asian Bangladeshi	☐	Other	☐
Asian Chinese	☐		

Section 11. Periods and Menopause (Women only)

What age were you when your periods first started?
(please enter the age in the box) — **Age (yrs)** ☐

	Yes	No
Are you having periods regularly? (please tick √ the box)	☐	☐
Are your periods irregular? (please tick √ the box)	☐	☐
Have your periods stopped altogether? (please tick √ the box)	☐	☐

If your periods have **stopped** what age were you when this happened? ☐

Section 12. Hysterectomy and Hormones (Women only)

	Yes	No
Have you had a hysterectomy? (please tick √ the box)	☐	☐

If you answered YES what age were you when you had the hysterectomy? ☐

	Yes	No
Have you had your ovaries removed? (please tick √ the box)	☐	☐

If you answered YES what age were you when you had the ovariectomy? ☐

	Yes	No
Are you taking HRT at present? (please tick √ the box)	☐	☐

If you answered YES, please enter for how long you have taken HRT *(e.g. Jan 2002- present date)* ☐

	Yes	No
Did you ever take HRT in the past? (please tick √ the box)	☐	☐

If you answered YES, please write down the month and years when you started and stopped HRT *(e.g. Jan 2002-Feb 2004)* ☐

Yes **No**

Are you using PROVERA (the Jag) contraceptive
(please tick √ the box)

If you answered YES, please enter the month and year when you started the this

Thank you! Remember to bring the completed questionnaire with you when you come for the scan.

(For use of Osteoporosis Service Only)

(Office Use only)	Source of Referral (please tick √ one box
DADS	
FLS	
Hospital referral	
Other (please specify)	